Study the Performance of Channel Estimation Techniques for Massive MIMO Systems

By

Mubarek Abdulkadir

A Thesis Submitted to

The Department of Electronics and Communication Engineering
School of Electrical Engineering and Computing

Presented in Partial Fulfillment of the Requirement for the Degree of Master's in Electronics and Communication Engineering (Communication Engineering)

Office of Graduate Studies
Adama Science and Technology University

September, 2021
Adama, Ethiopia

Study the Performance of Channel Estimation Techniques for Massive MIMO Systems

Mubarek Abdulkadir

Advisor: Dr. Demissie Jobir (PhD)

Co-Advisor: Dr. Ellappan V.

A Thesis Submitted to

The Department of Electronics and Communication Engineering
School of Electrical Engineering and Computing

Presented in Partial Fulfillment of the Requirement for the Degree of Master's in Electronics and Communication Engineering (Communication Engineering)

Office of Graduate Studies
Adama Science and Technology University

September, 2021

Adama, Ethiopia

DECLARATION

I hereby declare that this Master Thesis entitled “Study the Performance of Channel Estimation Techniques for Massive MIMO Systems” is my original work. That is, it has not been submitted for the award of any academic degree, diploma or certificate in any other university. All sources of materials that are used for this thesis have been duly acknowledged through citations.

Name of the student	Signature	Date

RECOMMENDATION

We, the advisors of this thesis, hereby certify that we have read the revised version of the thesis entitled "Study the Performance of Channel Estimation Techniques for Massive MIMO Systems" prepared under our guidance by Mubarek Abdulkadir submitted in partial fulfillment of the requirements for the degree of Mater's of Science in Electronics and Communication Engineering (Communication Engineering). Therefore, we recommend the submission of revised version of the thesis to the department following the applicable procedures.

______________________	______________________	______________________
Major Advisor	Signature	Date
______________________	______________________	______________________
Co-advisor	Signature	Date

APPROVAL PAGE OF M.SC. THESIS

We, the advisors of the thesis entitled **"**Study the Performance of Channel Estimation Techniques for Massive MIMO Systems **''**and developed by Mubarek Abdulkadir, hereby certify that the recommendation and suggestions made by the board of examiners are appropriately incorporated into the final version of the thesis.

______________________	______________________	______________
Major Advisor	Signature	Date
______________________	______________________	______________
Co-advisor	Signature	Date

We, the undersigned, members of the Board of Examiners of the thesis by Mubaek Abdulkadir have read and evaluated the thesis entitled "Study the Performance of Channel Estimation Techniques for Massive MIMO Systems" and examined the candidate during open defense. Therefore this is to certify that the thesis is accepted for partial fulfillment of the requirement of the degree of Master of Science in Electronics and Communication engineering (Communication Engineering).

______________________	______________________	______________
Chairperson	Signature	Date
______________________	______________________	______________
Internal Examiner	Signature	Date
______________________	______________________	______________
Eternal Examiner	Signature	Date

Finally, approval and acceptance of the thesis is contingent upon submission of its final copy to the Office of Postgraduate Studies (OPGS) through the Department Graduate Council (DGC) and School Graduate Committee (SGC).

______________________	______________________	______________
Department Head	Signature	Date
______________________	______________________	______________
School Dean	Signature	Date
______________________	______________________	______________
Postgraduate Dean	Signature	Date

ACKNOWLEDGEMENT

First and foremost, I would like to thank the Almighty God for providing me with the knowledge and strength to accomplish this thesis study.

I would want to convey my heartfelt appreciation to my mentor, Dr. Demissie Jobir, for his unwavering support, patience, motivation, and vast knowledge. His advice was incredibly useful throughout the research and writing of this thesis. I couldn't have asked for a better adviser for my thesis research. I am particularly grateful to my second supervisor, Dr. Ellappan V, for his encouragement and sacrifice of his important time in encouraging me to work in my own style, as well as for allowing me the flexibility to properly investigate this subject deeply.

I would want to thank everyone in the School of Electrical and Computer Engineering (SoECE), especially the division of electronics and communication engineering, for creating such a wonderful educational and research environment. I am grateful to all of the students in the Communication Engineering division who have provided me with all of the information. Last but not least, I'd want to my fiancé Seble Deme for her endless support, as well as for providing the required assistance throughout this thesis study. I am also grateful to my friends and my board of examiners for their encouragement and assistance in giving me with the essential needs and comments.

TABLE OF CONTENTS

DECLARATION i

RECOMMENDATION ii

APPROVAL PAGE OF M.SC. THESIS iii

ACKNOWLEDGEMENT iv

LIST OF TABLES viii

LIST OF FIGURES ix

LIST OF ABBREVIATIONS xi

ABSTRACT xiii

CHAPTER ONE 1

1 INTRODUCTION 1

1.1 Background 1

1.2 Statement of the Problem 5

1.3 Objectives 5

1.3.1 General Objective 5

1.3.2 Specific Objective 5

1.4 Significance of the Study 6

1.5 Scope of the Study 6

1.6 Thesis organization 6

1.7 Contributions of the Thesis 7

CHAPTER TWO 8

2 Literature Review 8

2.1 MIMO Systems 10

2.2 Advancements from MIMO to Massive MIMO 11

2.3 Massive MIMO Systems 13

2.3.1 Massive MIMO and 5G 16

2.3.2 Channel Estimation 17

2.3.3 Channel Estimation in TDD Systems 17

2.3.4 Channel Estimation in FDD Systems 20

2.4 Properties and Advantageous of Massive MIMO 23

2. 5 Pilot Contamination: The Limiting Factors of Massive MIMO 25

CHAPTER THREE 27

3 System Model for Massive MIMO 27

3.1 Channel Model 29

3.1.1 Additive White Gaussian Noise (AWGN) 30

3.1.2 Perfect Channel 31

3.1.3 Rayleigh Fading 32

3.1.4 Rican Fading 32

3.2 Mathematical Model for the UL Transmission 33

3.2.1 Uplink Transmission 34

3.2.2 Downlink Transmission 35

3.3 Channel Estimation Techniques in Massive MIMO Systems 36

3.4 The Minimum Mean Square Error Algorithm 38

3.5 The Least Square Algorithm 41

3.6 Element wise Minimum Mean Square Error Algorithm (EW MMSE) 43

CHAPTER FOUR 46

4 RESULT AND DISCUSSION 46

4.1 Simulation Results 46

4.1.1 Steps Followed to Reach to Results 48

4.2 Uplink Spectral Efficiency for Rayleigh and Rician fading for (M=50, 100) 48

4.3 Down Link Spectral Efficiency for Rayleigh and Rician fading 54

For (M=100) 54

4.4 Estimation Quality of MMSE, EW-MMSE, and LS Estimators 56

4.5 Number of Complex Multiplications per coherence for (50 ≤M ≤150) 57

4.6 Number of Complex Multiplications per coherence when (100 ≤k ≤200) 59

CHAPTER FIVE 63

5 CONCLUSIONS AND FUTURE WORKS 63

5.1 CONCLUSION 63

5.2 FUTURE WORKS 64

REFERENCES 65

APPENDEIX 68

LIST OF TABLES

TABLE 4. 1: SIMULATION PARAMETERS 49
TABLE 4. 2 : UPLINK SPECTRAL EFFICENCY FOR M=50,100 USING RICAN AND RAYLEIGH FADING 53
TABLE 4. 3 : DOWN LINK SPECTRAL EFFICIENCY FOR M=50,100 USING RICAN AND RAYLEIGH FADING 55
TABLE 4. 4: NUMBER OF COMPLEX MULTIPLICATIONS PER COHERENCE WHEN ($100 \leq K \leq 200$) 62

LIST OF FIGURES

Figure 1.1 : Illustration of Downlink Transmission in a MU-MIMO System, Where the BS is Equipped With M Antennas and Serves K User Terminals Simultaneously 1
Figure 1. 2 : Illustration of Uplink Transmission in a MU-MIMO System, Where the BS is Equipped With M Antennas and Serves K User Terminals Simultaneously 2
Figure 1. 3 : Number of Connected Devices... 3
Figure 1. 4: Growth In Mobile Data Traffic 4
Figure 2. 1: Basics of SISO, SIMO, MISO and MIMO Systems…...……………….…………..11
Figure 2. 2 : Line Of Sight (Los) Antenna Setup of a MIMO System. 12
Figure 2. 3: Comparing SIMO/MISO Systems With MIMO Systems. 13
Figure 2. 4: Cell Centric and User Centric Cellular Networks. 14
Figure 2. 5 : Particular Massive Mimo System in the Uplink Transmission 15
Figure 2. 6: Antenna Configurations and Deployment Scenarios for a Massive Mimo Base Station 16
Figure 2. 7: Tdd And Fdd Topologies 18
Figure 2. 8 : Slot Structure and Channel Estimation in Tdd Systems 19
Figure 2. 9: Time Division Duplex Scenario..….........20
Figure 2. 10 : Frequency Division Duplex Scenario ………………………………………..21
Figure 2. 11 : Slot Structure and Channel Estimation In Fdd Systems 22
Figure 2. 12 : The Regions Of Possible (M, K) in Tdd and Fdd Systems, For a Coherence Interval of 200 Symbols.. 22
Figure 2. 13 :Transmission Protocol of Tdd Massive Mimo. 23
Figure 3. 1: A Typical Multi-Cell Multi-User Massive Mimo Systems ………………………..27
Figure 3. 2 : Time Division Duplex Multi-Carrier Modulation Scheme of a Canonical Massive Mimo Network 29
Figure 3. 3: Uplink Samples For UL Pilots, UL Data, and DL Data.. 29
Figure 3. 4 : A Diagram of Massive Mimo Systems With The Channel 30
Figure 3. 5 : Block Diagram of Awgn Channel Model 31
Figure 3. 6: Block Diagram of Rayleigh Channel Model 32
Figure 3. 7: Block Diagram of Rician Channel Model 33

Figure 3. 8: Illustration of The UL Massive Mimo Transmission in Cell *J* And Cell *L*. 34
Figure 3. 9: Illustration of The DL Massive Mimo Transmission in Cell *J* And Cell *L* 35
Figure 3. 10 : Block-Type Pilot Channel Estimation Arrangement. the Black Dots Represent the Pilot While the White Dots Represent the Actual Data 37
Figure 3. 11 : Comb-Type Pilot Channel Estimation Arrangement. The Black Dots Represent the Pilot While The White Dots Represent The Actual Data. 38
Figure 4. 1 : Uplink Spectral Efficiency For 50 Number of Antennas (M) With Rayleigh Fading…………………………………………………………………………………50
Figure 4. 2 : Uplink Spectral Efficiency For 50 Number of Antennas (M) With Rayleigh Fading 50
Figure 4. 3 : Uplink Spectral Efficiency For 50 Number of Antennas (M) With Rician Fading . 51
Figure 4. 4 : Uplink Spectral Efficiency For 100 Number of Antennas (M) With Rician Fading 52
Figure 4. 5 : Downlink Link Spectral Efficiency For 100 Number of Antennas (M) With Rican Fading Fading 54
Figure 4. 6 : Downlink Link Spectral Efficiency For 100 Number of Antennas (M) Rayleigh Fading 54
Figure 4. 7 : Different Estimators, The NMSE In The Estimation of A Spatially Coupled Channel Based on The Local Scattering Model With Gaussian Angular Distribution 56
Figure 4. 8 :Number of Complex Multiplications Per Coherence Block With 10 Ues, When Using Different Channel Estimation Schemes, When M=50 57
Figure 4. 9 :Number of Complex Multiplications Per Coherence Block With 10 Ues, When Using Different Channel Estimation Schemes, When M= 100 58
Figure 4. 10 :Number of Complex Multiplications Per Coherence Block With 10 Ues, When Using Different Channel Estimation Schemes, When M=150 59
Figure 4.11: Number of Complex Multiplications Per Coherence Block With, When Number of Users(*K*)= 100 When Using Different Channel Estimation Schemes 60
Figure 4. 12: Number of Complex Multiplications Per Coherence Block With, When Number of Users(*K*)= 150 When Using Different Channel Estimation Schemes. 61
Figure 4. 13: Number of Complex Multiplications Per Coherence Block With , When Number of Users(*K*)= 200 When Using Different Channel Estimation Schemes. 61

LIST OF ABBREVIATIONS

1G	**1**st **G**eneration
2G	**2**nd **G**eneration
3G	**3**rd **G**eneration
4G	**4**th **G**eneration
5G	**5**th **G**eneration
Aka	**a**lso **k**nown **a**s
AWGN	**A**dditive**W**hite **G**iassian **N**oise
BS	**B**ase **S**tation
CSI	**C**hannel **S**tate **I**nformation
DL	**D**own **L**ink
EW MMSE	**E**lement **W**ise **M**ean **M**inimum **S**quare **E**rror
FDD	**F**requency **D**ivision **D**uplex
gNB	next **g**eneration **N**ode **B**
IEEE	**I**nstitute of **E**lectrical and **E**lectronics **E**ngineers
IMT	**I**nternational**M**obile **T**elecommunications
IoT	**I**nternet **o**f **T**hings
ISI	**I**nter **S**ymbol **I**nterference
LAN	**L**ocal **A**rea **N**etwork
LoS	**L**ine **o**f **S**ight
LS	**L**east **S**quare
LTE	**L**ong **T**erm **E**volution
MAP	**M**aximum **A** **P**osteriori
MATLAB	**MAT**trix **LAB**oratry
MIMO	**M**ultiple **I**nput**M**ultiple **O**utput
MISO	**M**ultiple **I**nput **S**ingle **O**utput
ML	**M**aximum **L**ikelihood
MMSE	**M**inimum**M**ean **S**quare **E**rror
MR	**M**aximal **R**atio
MSE	**M**ean **S**quare **E**rror

MU	**M**ulti **U**ser
MWC	**M**obile**W**orld **C**onference
NB	**N**ode **B**
NLoS	**N**one **L**ine **o**f **S**ight
NMSE	**N**ormalized **M**ean **S**quare **E**rror
NR	**N**ew **R**adio
OFDM	**O**rthogonal **F**requency **D**ivision**M**ultiplexing
PA	**P**ower **A**mplifier
PC	**P**ersonal **C**omputer
PRB	**P**hyscal **R**esource **B**lock
QAM	**Q**adrature **A**mplitude**M**odulation
RF	**R**adio **F**requency**SE** **S**pectral **E**fficiency
SIMO	**S**ingle **I**nput**M**ultiple **O**utput
SINR	**S**ignal to **I**nterference and **N**oise **R**atio
SISO	**S**ingle **I**nput **S**ingle **O**utput
SU	**S**ingle **U**ser
TDD	**T**ime **D**ivision **D**uplex
UE	**U**ser **E**quipment
UL	**Up** **L**ink
UMa	**U**rban **Ma**crocell
UMi	**U**rban **Mi**crocell
WLAN	**W**ireless **L**ocal **A**rea **N**etwork
ZF	**Z**ero **F**orcing

ABSTRACT

The number of wirelessly connected gadgets has increased dramatically during the past ten years. Wireless networks connect and manage billions of devices. . At the same time, each device needs a high performance connection for applications like as voice, real-time video, movies and games. The demand is always strong for wireless throughput and the quantity of wireless devices. Massive MIMO, coupled with 5G and other technologies, can satisfy this need with more capacity and efficiency. An important part of Massive MIMO system is channel estimation which is essential to optimize link performance. Acquiring channel state information (CSI) is particularly challenging for Massive MIMO systems because of the massive number of antennas, the complex architecture of the Transceiver and the large exploited bandwidth. But which one of the channel estimators should be used for a specific situation is another problem. This thesis will analyze the performance of channel estimation techniques specifically the least square (LS) and minimum mean square error channel (MMSE) Element-wise MMSE Channel Estimator ,(EW MMSE) estimation methods for massive MIMO systems and based on the analysis results, different discussions and conclusions are made. Furthermore, comparison among their characteristics is simulated in MATLAB and useful conclusions are given. To achieve this goal different algorithms and MATLAB simulation results will be used. When the performance of the channel estimators was tested using the maximum ratio (MR) detection algorithms, the result showed that the MMSE estimator performed better In terms of spectral efficiency. While EM MMSE and LS estimators less Computational complexity. Different comparison techniques were also run and they showed that the MMSE estimator to be shown more complex than the LS and EW MMSE estimator by the increase in the number of users and the number of antennas array used.

Keywords: C*hannel Estimation, Massive MIMO, Least Square (LS), Minimum Mean Square Error (MMSE), Element Wise Minimum Mean Square(EW MMSE), and Maximum Ratio*

CHAPTER ONE

1 INTRODUCTION

1.1 Background

Massive MIMO refers to MU-MIMO (Multi-user Multiple input Multiple output) systems with a large number of BS (base station) antennas and users. Hundreds or thousands of BS antennas serve tens or hundreds of users in the same frequency resource at the same time in Massive MIMO[1]. The increase in the number of antennas is the key to the increase in the capacity of the Massive MIMO systems. This feature makes the 5G network requirements possible. Figures 1.1 and 1.2 show downlink and uplink transmission in a MUMIMO system in which the BS is equipped with M antennas and serves K user terminals at the same time. Beam-forming is used to service the users in this downlink and uplink transmission. Uplink (or reverse link) transmission occurs when the K users send signals to the BS. The uplink data transmission uses a portion of the coherence interval. During the uplink, all K users send data to the BS using the same time-frequency resource. The BS then employs the channel estimates and combining algorithms to detect signals transmitted by all users.

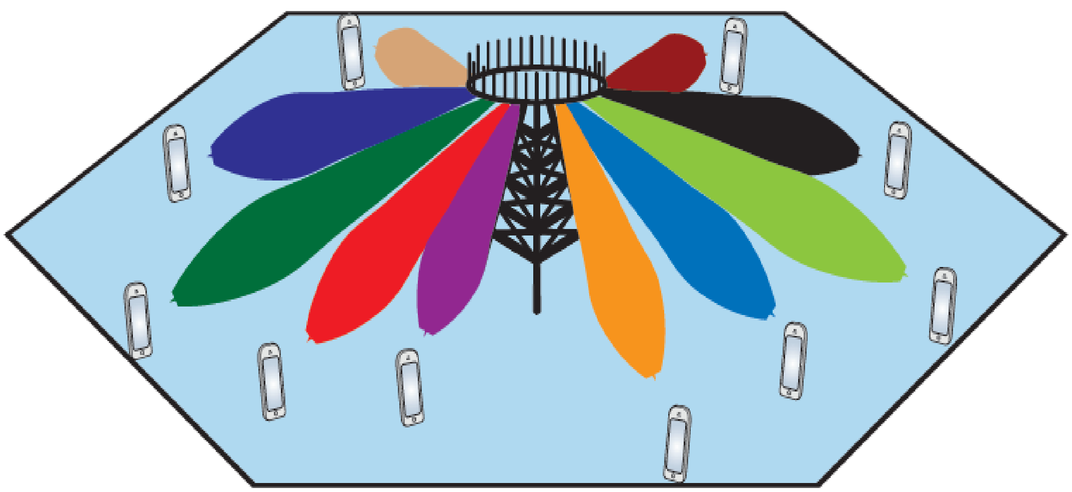

Figure 1.1 : Illustration of downlink transmission in a MU-MIMO system, where the BS is equipped with M antennas and serves K user terminals simultaneously [1].

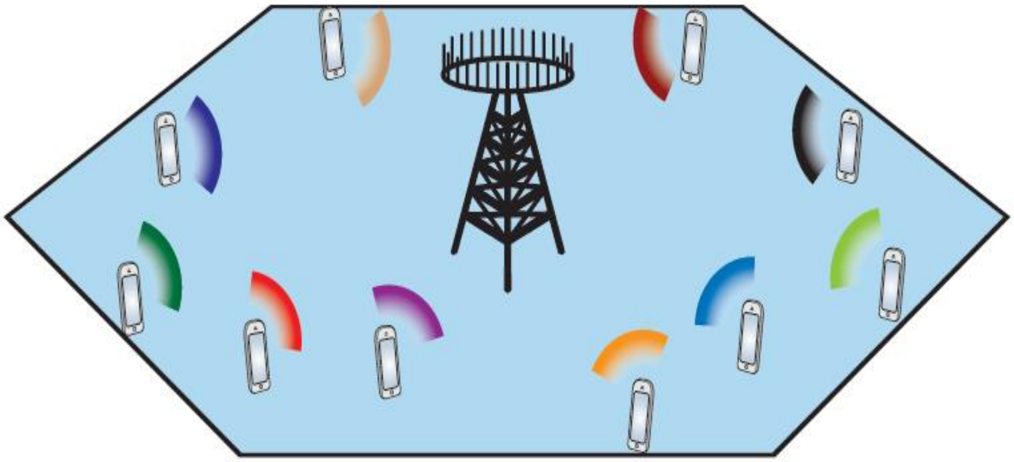

Figure 1. 2 : Illustration of uplink transmission in a MU-MIMO system, where the BS is equipped with M antennas and serves K user terminals simultaneously [1].

When the BS broadcasts signals to all K users, this is referred to as the downlink (or forward link) scenario. Using the same time-frequency resource, the BS transmits signals to all K users in the downlink. In greater detail, the BS generates M precoded signals using its channel estimates and the symbols intended for the K users, which are then transmitted to M antennas.

A fundamental aspect of massive MIMO is that channel estimation is essential for massive MIMO systems to operate optimally. The BS requires CSI (channel status information) to detect and precode signals sent by users in the uplink. The uplink training yielded this CSI. Each user is given an orthogonal pilot sequence that they must broadcast to the BS. The BS is aware of all users' pilot sequences and estimates the channels based on the pilot signals received.

In addition, each user may require only a portion of the CSI information to detect the signals provided by the BS in a coherent manner. This data can be obtained using the downlink training procedure. Because the BS beamforms the signals To detect the desired signals when utilizing linear precoding techniques, the user only needs the effective channel gain (which is a scalar constant). As a result, the BS can spend a limited amount of time in the downlink to beamform pilots for CSI acquisition at users [1]. Commonly, channel estimation is done with the help of pilot symbols[2]. Chapter 3 will go over different pilot based channel estimation techniques.Data traffic (both mobile and fixed networks) has increased tremendously as a result of the rapid proliferation of smart phones, Tablets, laptops, and other wireless data consumers According to the study [3]. We can expect a surge in connected devices such as phones, tablets, wearable gadgets, sensors, internet of things (IoT), connected cars, and so on in the near future.

As illustrated in Figure 1.3, about 21.2 billion connected devices are predicted by 2020, with phones, tablets, laptops, and PCs accounting for 11.3 billion of those (Non-IoT). This demonstrates the increasing trend and a forecast of the number of linked devices from 2015 to 2020. High-quality video streaming, cloud computing, and IoT all necessitate far faster data rates than today's 4G networks. We may also predict that by the end of 2025, there will be 34.2 billion active devices linked globally[4]. This is a significant amount, and it will continue to rise.

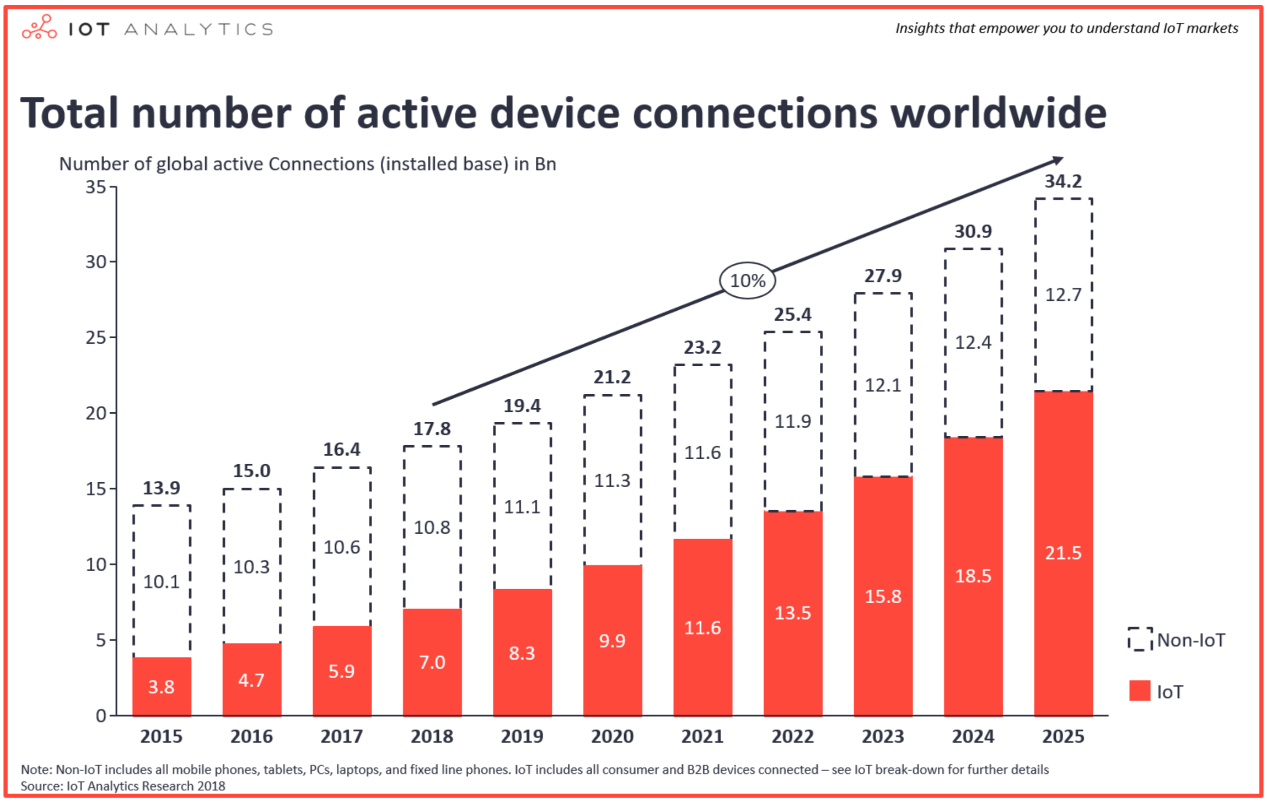

Figure 1. 3 : Number of connected devices[4].

According to Figure 1.4, video accounted for around 45 percent of mobile data traffic in 2014. By 2020, video is predicted to account for 60% of all mobile data usage. As a result, the quantity of mobile data traffic due to video streaming is expected to be 13 times higher by 2020 [3]. As a result, as the demand for video streaming develops, so does the demand for a high data rate internet connection increase exponentially.

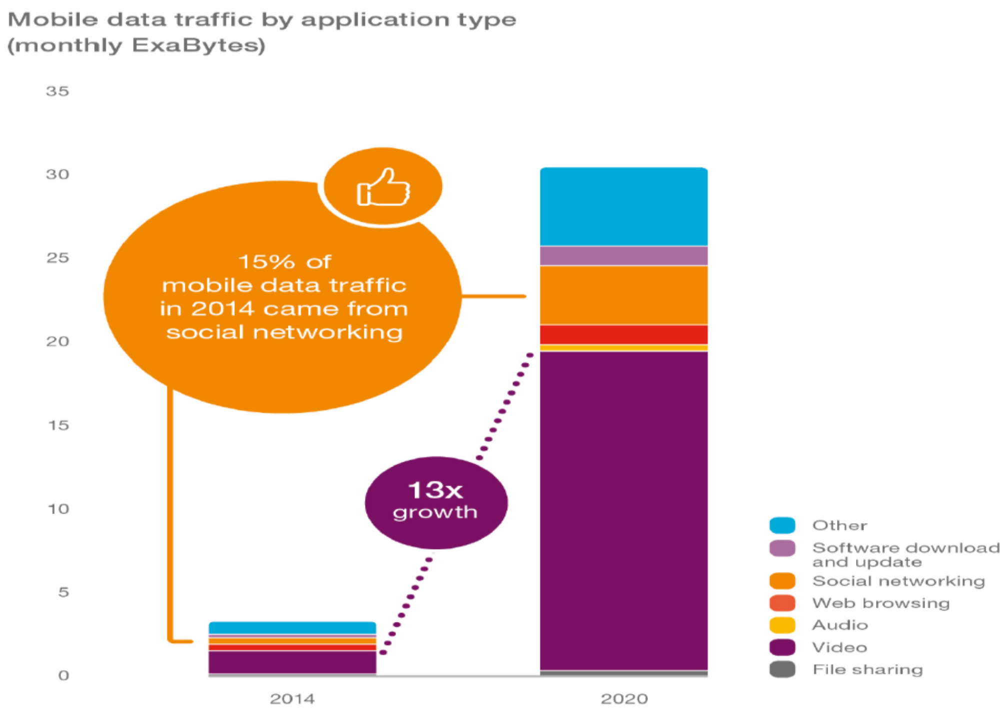

Figure 1. 4: Growth in mobile data traffic [3].

Massive MIMO may be able to satisfy these future demands. So, because data demand is always increasing, we must discover a method to enhance the capacity of cellular networks in unprecedented ways, because data traffic is increasing in unprecedented ways. The main parameter that measures the capacity of a network is the throughput. The expression for throughput is given as:-

Throughput (bit/s/km2) = Cell Density [Cell/km2] *Bandwidth (Hz)*Spectral efficiency (bits/s/Hz/cell) (1.1)

As we can see from Equation 1.1, if we want to increase the throughput of a given communication system, we can increase the bandwidth, the cell density and/or the spectral efficiency (SE). The method of increasing the cell density and the bandwidth has been used to much till now. We need a different way of increasing the throughput. The best way to increase the throughput is by increasing the spectral efficiency of the cellular network. Increasing the number of antennas in the BS and/or UE is one technique to improve spectral efficiency (user equipment). When the number of antennas increases, it is almost as if the Shannon capacity is doubled by the BS or UE's minimum number of antennas. Here, we are constructing many single antenna to single antenna communication for all users, which considerably enhances the network's capacity, even to the extent of several tens of times that of typical single antenna to single antenna communication.

1.2 Statement of the Problem

Massive MIMO systems are also efficient in energy usage. The usage of multiple antennas, on the other hand, at the transceivers requires the estimation of the channel characteristics very difficult. An important part of Massive MIMO system is channel estimation which is essential to optimize link performance. Acquiring channel state information (CSI) is particularly challenging for Massive MIMO systems because of the massive number of antennas, the complex architecture of the Transceiver and the large exploited bandwidth. This thesis will analyze the performance of channel estimation techniques specifically the Least square (LS), Minimum Mean Square Error (MMSE) and Element-wise MMSE (EW MMSE) estimation methods for massive .

1.3 Objectives

1.3.1 General Objective

The general objectives of this thesis is to study and evaluate the performance of the LS and MMSE and EW MMSE channel estimation techniques for massive MIMO system to determine the best possible channel estimation technique.

1.3.2 Specific Objective

The specific objectives of this thesis are:-

1. To compare the performance the LS, EW MMSE and MMSE channel estimation techniques for massive MIMO systems.

2. Study the mathematics of LS and MMSE, EW MMSE channel estimation techniques when implemented to a massive MIMO cellular system.

3. to evaluate and analysis of spectral efficiency of LS and MMSE EW MMSE estimators.

4. Study the effect of computational complexity on LS and MMSE EW MMSE.

5. Study the effect of increasing the number antennas on LS, EW MMSE and MMSE.

1.4 Significance of the Study

This thesis work improves the overall performance of Massive MIMO systems, by appropriately estimating its channel state information.in this thesis we analyze, examine and compare channel estimation techniques (least square, minimum mean square error and Element wise minimum mean square error) with respect to their Spectral efficiency, computational complexity and Signal noise to ratio. By doing so we can predict and assign which technique must be used in order to improve the system performance. We also try study the effect of Number of antennas and Number of users in our estimation techniques.

1.5 Scope of the Study

This thesis focuses to study the effect of channel estimation techniques for massive MIMO systems under different parameters. Acquiring channel state information (CSI) is particularly challenging for Massive MIMO systems because of the massive number of antennas, the complex architecture of the Transceiver and the large exploited bandwidth. But which one of the channel estimators should be used for a specific situation is another problem. This thesis will analyze the performance of channel estimation techniques specifically the least square (LS) and minimum mean square error channel (MMSE) Element-wise MMSE Channel Estimator ,(EW MMSE) estimation methods. Different channel estimation comparison methods are proposed by different researchers.in thesis we only compare the effects of the Spectral efficiency, the Number of users and the Number of antennas in Massive MIMO systems. The thesis do not include the effect of pilot contamination and other limiting factors of estimation and only focus on the objective.

1.6 Thesis organization

The rest of this thesis is organized as follows.

Chapter 2 studies Literature Review and massive MIMO systems deeply. Section 2.1 discuss MIMO systems generally. Then in Section 2.2 the steps in advancing from MIMO to massive MIMO are discussed. Section 2.3 studies massive MIMO systems. Then the sections following this section will discuss the operation, properties and advantageous of massive MIMO and limiting factors in massive MIMO are also studied in their respected sections.

Chapter 3 is devoted for the discussion of the system model for massive MIMO systems. In section 3.1 system model, channel model and mathematical model for the system will be discussed. In

Section 3.2 the system model for massive MIMO is developed. Based on the system model, Section 3.3 discusses channel estimation techniques. Then from Section 3.4-3.6 studies about channel estimation techniques specially the LS, MMSE and EW MMSE algorithms.

Chapter 4 is devoted for the discussion of the simulation results and discussion of these channel estimators. All these will be discussed from Section 4.2 to 4.6. Here in this chapter different simulation results will be presented and explained.

Finally, Chapter 5 is for the conclusion and future work. Section 5.1 is for discussing the conclusion of the paper. Section 5.2 gives indications for possible future works related to this work. This is what the organization of the paper looks like.

1.7 Contributions of the Thesis

A lot of papers have been written on this topic, the topic of pilot based channel estimation in massive MIMO systems. One may ask "What would be the contribution of this particular thesis?" Well, there will be contribution from this paper. Some of the contributions of this paper would be:-

- The thesis study analyze and compare between different channel estimation techniques in a way that is different from other scientific papers (using spectral efficiency(SE, number of antenna(M), computational complexity and effective SNR (signal noise to ratio).
- The thesis will predict the effect of the number of antennas on the LS EW- MMSE and MMSE channel estimators. It will also predict which of these estimators is affected more than the other by SE, SNR, and number of antennas (M).

CHAPTER TWO

2 Literature Review

Since the focus of this thesis is on channel estimation methods in massive MIMO systems, in this section, we will review important papers that are written in the topic related to channel estimation in Massive MIMO systems. Many papers have been written on different channel estimation techniques. For this thesis I have reviewed many papers some of these are:-

The first paper [5] is written by one of the pioneers of this field. This paper discusses massive MIMO systems under pilot contamination and favorable propagation conditions. The objective of the paper was to analyze in massive MIMO systems terms of SE and energy efficiency and Effects of pilot contamination in massive MIMO systems. The paper does not use other comparisons methods to compare between the channel estimation techniques. It does not also estimate the effect of the increase in the number of users on the estimation algorithms.

The second paper [6]assumes cellular time-division duplexing systems with a large number of antennas at each base station. The paper wanted to challenge the idea that blind channel estimation is always better than the other two channel estimation techniques. The objective of the paper was to compare and contrast between pilot based, blind, and semi-blind channel estimation techniques. The paper concluded that semi-blind channel estimation techniques are the best for the current technologies. It also stated that blind channel estimations have unsatisfactory results for typical massive MIMO systems. One of the short coming of the paper was that the paper only considers MAP estimator to compare these channel estimation techniques and does not consider the performance difference of different algorithms within a given channel estimation techniques.

The third paper is [7] is written by the same author as the second paper. The objective of the paper is to study Massive MIMO with Spatially Correlated Rician Fading Channels using LS and MMSE channel estimation algorithms. The SE is used as a comparison method between the channel estimation techniques. This paper as the previous paper does not use other comparisons methods to compare between the channel estimation techniques. It does not also estimate the effect of the increase in the number of users on the estimation algorithms. This paper does not incorporate the recommended antenna spacing between the antennas.

The paper [8]is one of the significant papers written in this field. This paper addresses on how channel estimation techniques are done. The objective of the paper is on how to reduce pilot contamination. The paper concluded that covariance-aided channel estimation methods are good methods in order to decrease the pilot contamination. It also stated that blind and semi-blind channel estimation have a good estimate but are complex. This paper compares between the estimators based on SE and mean square error (MSE). It does not consider other comparison merits. This paper does not compare different channel estimation algorithms with in the pilot based channel estimation category.

Another important paper [9] written in Massive MIMO. It starts from the problem of studying massive MIMO systems deeply. Its objective is to study communication theory behind the Massive MIMO technology, and provides implementation related design guidelines. The paper concluded that Massive MIMO can theoretically provide ten-fold or even 50-fold improvements in SE over IMT-Advanced (International Mobile Telecommunications-Advanced). It does not consider comparison between different channel estimation techniques.

The paper [10] states that it is crucial to define techniques for channel estimation that together with pilot contamination mitigation allow best system performance and at same time low complexity. This paper concluded that a channel estimation technique with Zadoff-Chu sequences was introduced in order to replace channel estimation based on matrix inversions, such as the MMSE estimator. The paper uses BER (bit error rate) and MSE to compare between different channel estimation techniques. The paper does not consider other merits of comparison.

2.1 MIMO Systems

Technologies are constantly evolving. The first communication system was a point-to-point communication system known as a single input single output communication system (SISO). Then followed by SIMO (single input multiple output) and MISO (multiple input single output) communication systems, and eventually to MIMO systems. Figure 2.1 shows the fundamentals of SISO, SIMO, MISO, and MIMO systems.

MIMO technology is a wireless technology that uses many transmitters and receivers to transfer more data at the same time. MIMO technology takes advantage of a radio wave phenomena known as multipath, in which transmitted data bounces off walls, ceilings, and other objects several times, reaching the receiving antenna at slightly different angles and times. MIMO channel technology aims to increase wireless network capacity. MIMO gained popularity in the field after its invention. After the invention of MIMO, it gained the popularity in the field. It was used in commercial wireless devices and networks including broadband wireless access systems, wireless local area networks (WLAN), 3G networks, and 4G networks. Figure 2.2 displays a MIMO system's line of sight (LoS) antenna configuration, with each *h's* representing path (channel) characteristics.

MIMO systems have several times the capacity of SISO systems. As an example, consider a system with a communication channel frequency of 20MHz. If we assume a certain SNR value for the connection speed of 8 Mbps. Using Shannon's equation, we can show that the new system's capacity is 16 Mbps if we utilize a 2x2 MIMO system. Using the same logic, if a 4x4 MIMO system is used, the new system's capacity would be 32 Mbps. By doubling the antennae on both sides of the communication system, the system's capacity was doubled. This is a very promising technology for communication systems. That is why it is popular in the technology industry. This is also the reason behind why the current communication system are looking forward for massive MIMO systems. Figure 2.3 shows a comparison between SIMO/MISO systems and MIMO systems. It is clear from the figure that MIMO systems have very high capacity because of the increase in the number of antennas.

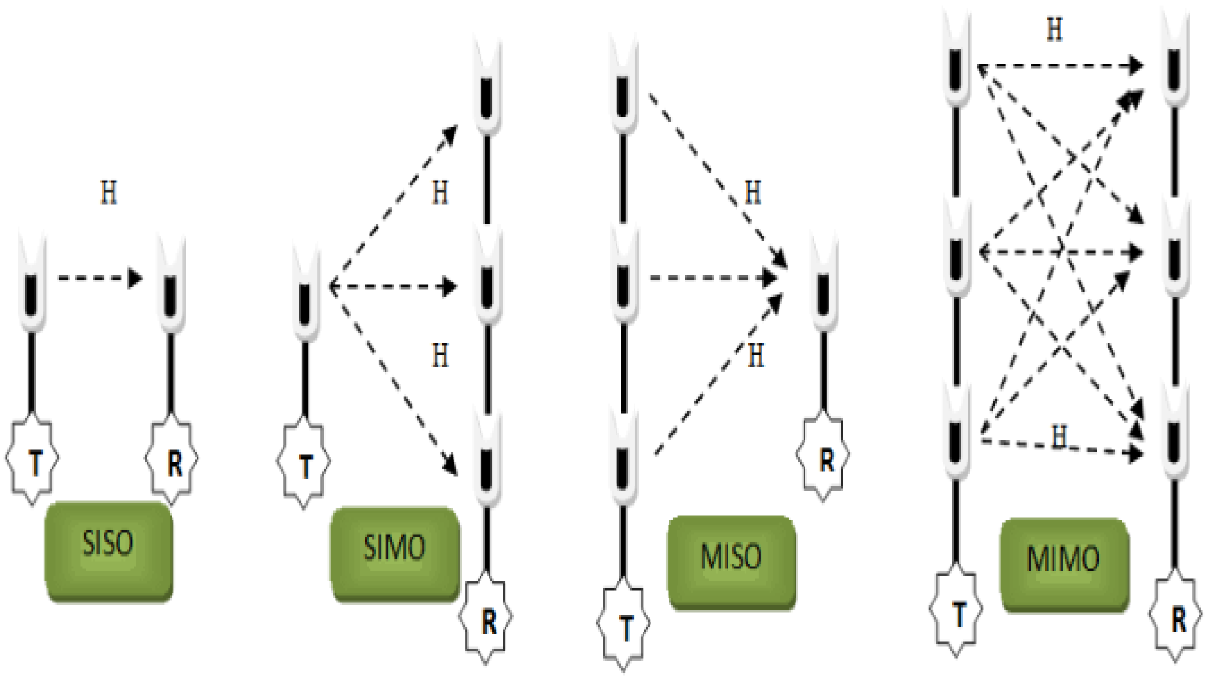

Figure 2. 1: Basics of SISO, SIMO, MISO and MIMO systems[10].

MIMO wireless technology can significantly enhance the capacity of a particular channel because of the use of several antennas. The throughput of the channel can be raised linearly by increasing the number of receive and transmit antennas in the system for each pair of antennas added. As a result, MIMO wireless technology has evolved into one of the most important wireless techniques in recent years. As spectral bandwidth becomes a more important commodity for radio communications systems, methods for making greater use of the existing bandwidth are necessary[10]. One of these ways is MIMO wireless technology.

2.2 Advancements from MIMO to Massive MIMO

According to the research[11] , MIMO antennas of today typically employ two broadcast and two receive antenna elements, twice the capacity of a basic antenna.. However, nowadays, 4 to 8 antenna elements are employed. Massive MIMO, developed by Nokia's Bell Labs, takes things a step further by employing many antenna elements to concurrently broadcast and receive streams of signals handled by complicated software, resulting in significantly improved network capacity. [11]. The capacity increases from MIMO systems were so significant that many scientists began to investigate the effect of increasing the number of antennas beyond the usual MIMO systems. As a result, massive MIMO technology was developed. The high data rate needed by consumers is the major reason for increasing the capacity of our communication systems. This demand is increasing all the time.

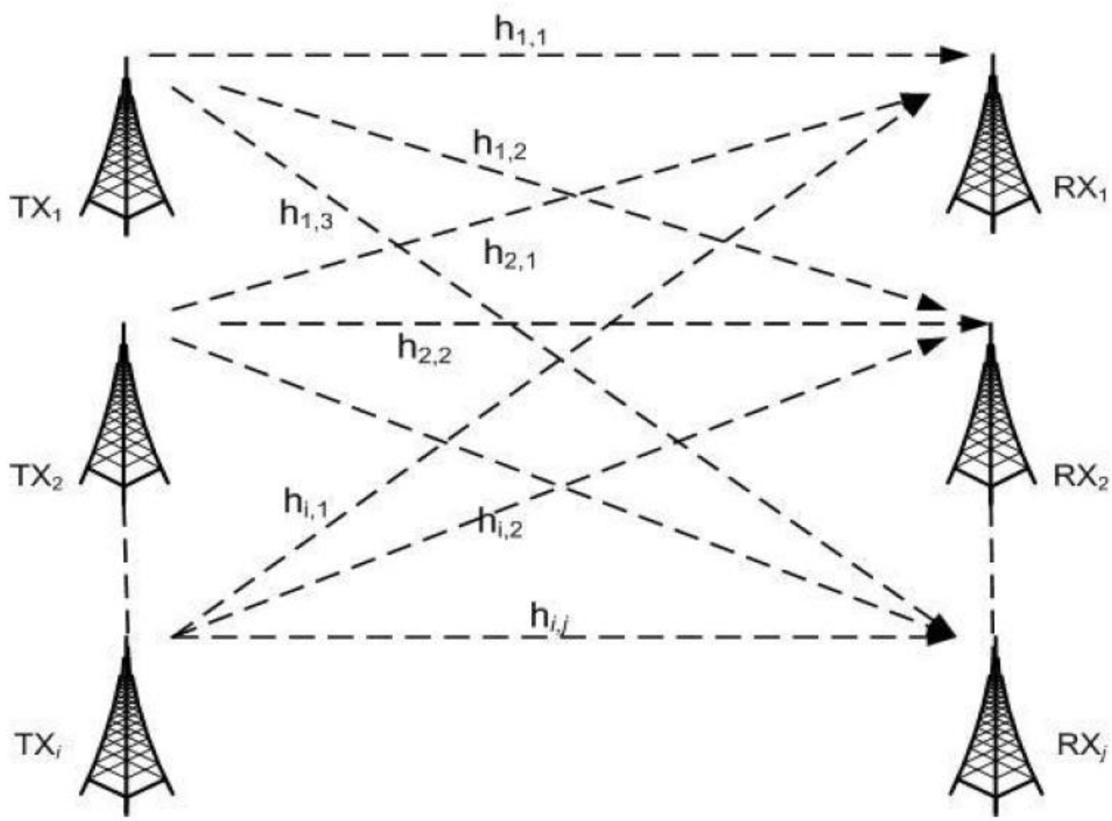

Figure 2. 2 : Line of sight (LoS) antenna setup of a MIMO system [10].

The main changes that were applied when advancing from MIMO to massive MIMO

- The antennas used in MIMO systems were 2,4,8,..., but the antennas used in massive MIMO systems are hundreds or even thousands of antennas [11].
- Massive MIMO systems are characterized by [11],

Number (BS antennas) >> Number (users)

Currently, cellular technologies are cell-centric, which is not ideal if we want a really high-speed connection. As a result, we must transition from cell-centric to user centric cellular networks by employing beamforming technology (described in Section 2.4). Massive MIMO with beam formation improves the end-user experience significantly by increasing network capacity and coverage while lowering latency.

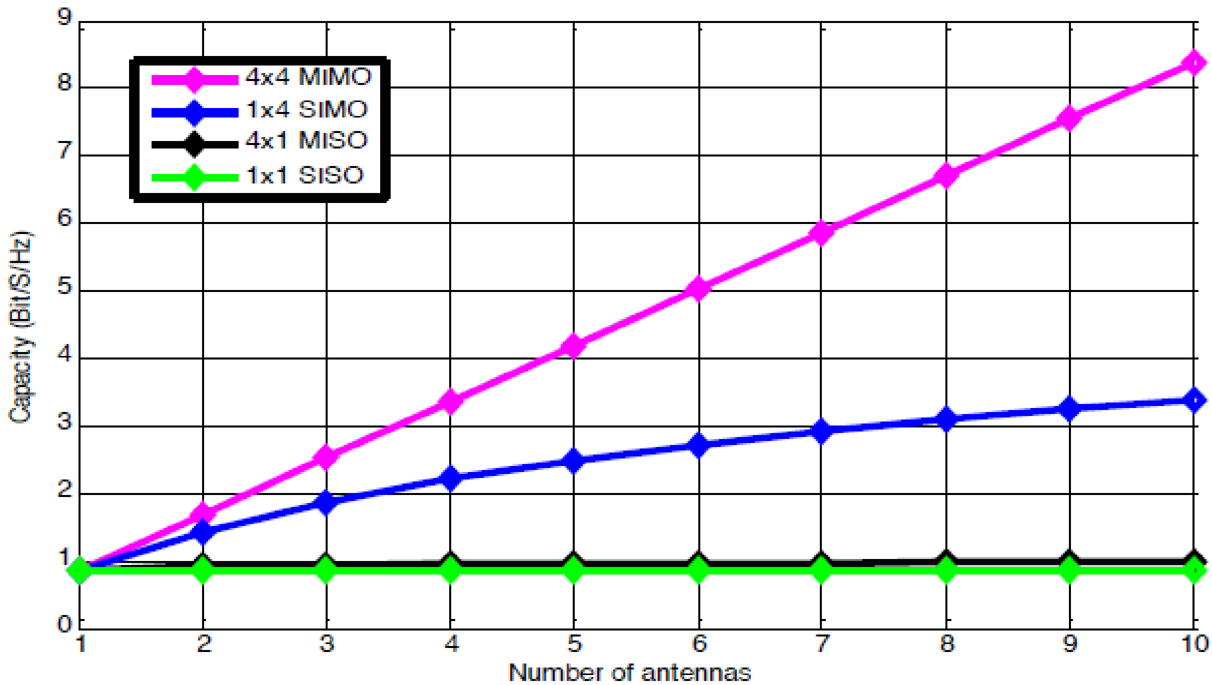

Figure 2. 3: Comparing SIMO/MISO systems with MIMO systems[10].

This is performed by increasing the efficiency of the transmission. The employment of highly focused radio waves leads in a stronger radio signal and higher data throughput across longer distances. This is also an effective method for improving capacity in congested areas, especially when adding another frequency band is not an option. The Massive MIMO antenna array with a huge number of steerable ports enables beam forming, which means radio signals and information are sent directly to the device rather than being broadcast throughout the entire cell. This has the added benefit of reducing radio interference across the cell, resulting in a more satisfying user experience[12].

2.3 Massive MIMO Systems

Massive MIMO is a viable solution for future high-capacity connectivity requirements. Massive MIMO is the most attractive wireless physical layer technology at the moment, and it is a critical component of 5G systems[13] . We shall create a system model for huge MIMO communication systems in this thesis. We will also run various simulations to evaluate the performance of various channel estimation strategies. This thesis will not take into account pilot contamination. Massive MIMO is a massive system that consists of numerous infrastructures and equipment. The antenna is a critical component in massive MIMO.

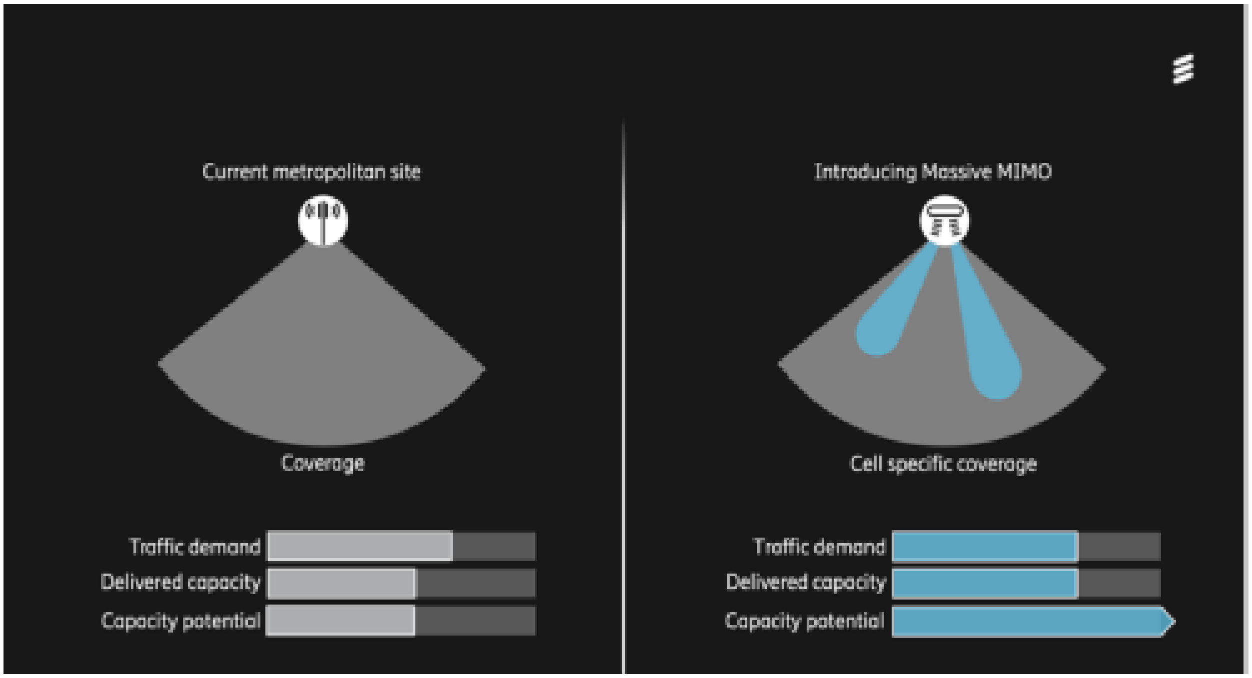

Figure 2. 4: Cell Centric and User Centric Cellular Networks[14].

since there is large number of antennas, the antennas need to be configured in some way for the best results. Figure 2.6 shows possible antenna configuration for massive MIMO.

A typical huge MIMO system is shown in Figure 2.5. Whereas the figure depicts massive MIMO systems that use antenna arrays with hundreds of antennas to support tens of terminals in the same time-frequency resource. The primary purpose of massive MIMO is to gain all of the benefits of conventional MIMO on a much greater scale. Overall, massive MIMO is a critical enabler for future broadband (fixed and mobile) networks that are energy-efficient, secure, and robust, as well as efficient spectrum users. As such, it is a facilitator for future digital society infrastructure that will connect the Internet of people, the Internet of things, clouds, and other networks infrastructure. Massive MIMO provides operators with a strong new tool for increasing capacity while utilizing existing airwaves[14]. As the demand for mobile broadband services develops, operators must maximize the efficiency of their pricey spectrum resources in order to boost network capacity. This leads in massive MIMO being a viable technology for the telecoms sector. This is something that massive MIMO techniques and technology have the ability to perform. Massive MIMO is based on spatial multiplexing, which requires the base station to have sufficient channel information on both the uplink and the downlink. On the uplink, this is simply accomplished by having the terminals provide pilots, which the base station uses to estimate the channel replies to each of the terminals. The downlink is more difficult to establish. In typical MIMO systems, such as the LTE (long term evolution) technology, the base station sends out pilot waveforms from which the terminals estimate channel responses, quantize them, and broadcast them back to the base station.

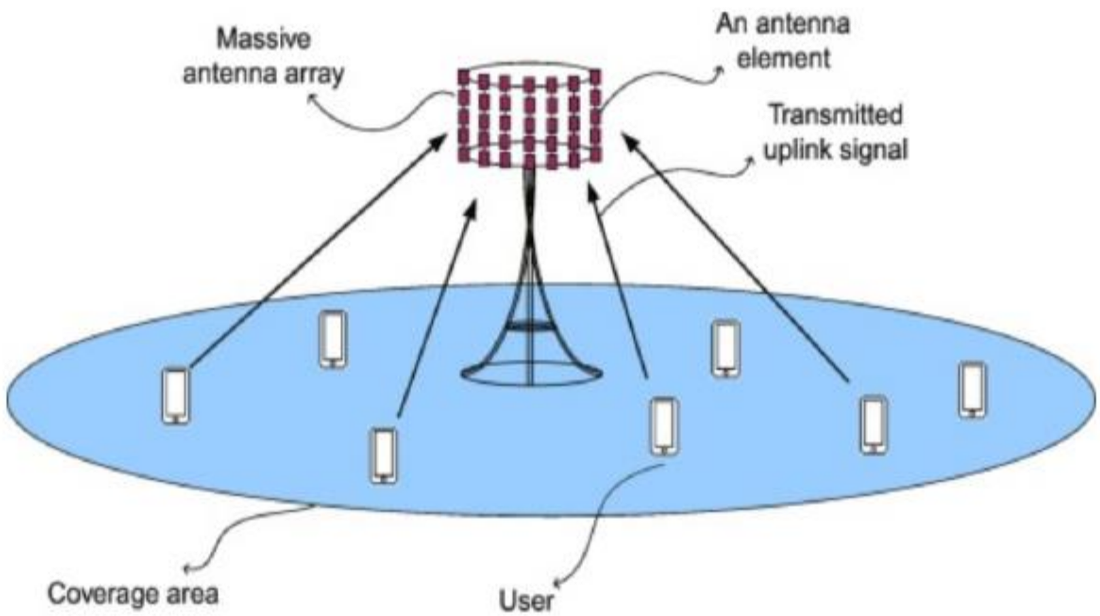

Figure 2. 5 : Particular massive MIMO system in the uplink transmission [14].

This will not be achievable in massive MIMO systems, at least not in a high-mobility environment, for two reasons. To begin, the best downlink pilots should be orthogonal to the antennas. This means that as the number of antennas increases, the amount of time frequency resources required for downlink pilots increases, therefore a massive MIMO system may require up to a hundred times the amount of such resources as a conventional system. Second, the number of channel responses required by each terminal is directly proportional to the number of base station antennas. As a result, the uplink resources required to inform the base station about channel responses would be hundreds of times greater than in existing method [15]. In general, the approach is to use TDD mode and rely on channel reciprocity between the uplink and downlink channels, while FDD operation may be achievable in exceptional circumstances[15]. Because the training burden is independent of the number of base station antennas, TDD operation is ideal for Massive MIMO.

2.3.1 Massive MIMO and 5G

While traditional MIMO concepts are already used in a number of Wi-Fi and 4G protocols, Massive MIMO will play an important role in 5G. Massive MIMO is widely anticipated to be a critical enabler and key component of 5G [16]. Indeed, as we have seen recently, huge MIMO is the primary component of the 5G network. One of the most critical functions of any 5G network will be to handle the tremendous increase in data demand that is coming. Cisco predicts that by 2020, when 5G is generally accessible, there will be 5.5 billion mobile users worldwide, with everyone consuming 20 GB of data each month. That doesn't even take into account the massive impact the Internet of Things is expected to have on our mobile networks [16]. The ability of Massive MIMO to serve multiple people and various devices concurrently within a condensed area while maintaining fast data rates and consistent performance makes it the ideal technology for meeting the needs of the approaching 5G era.

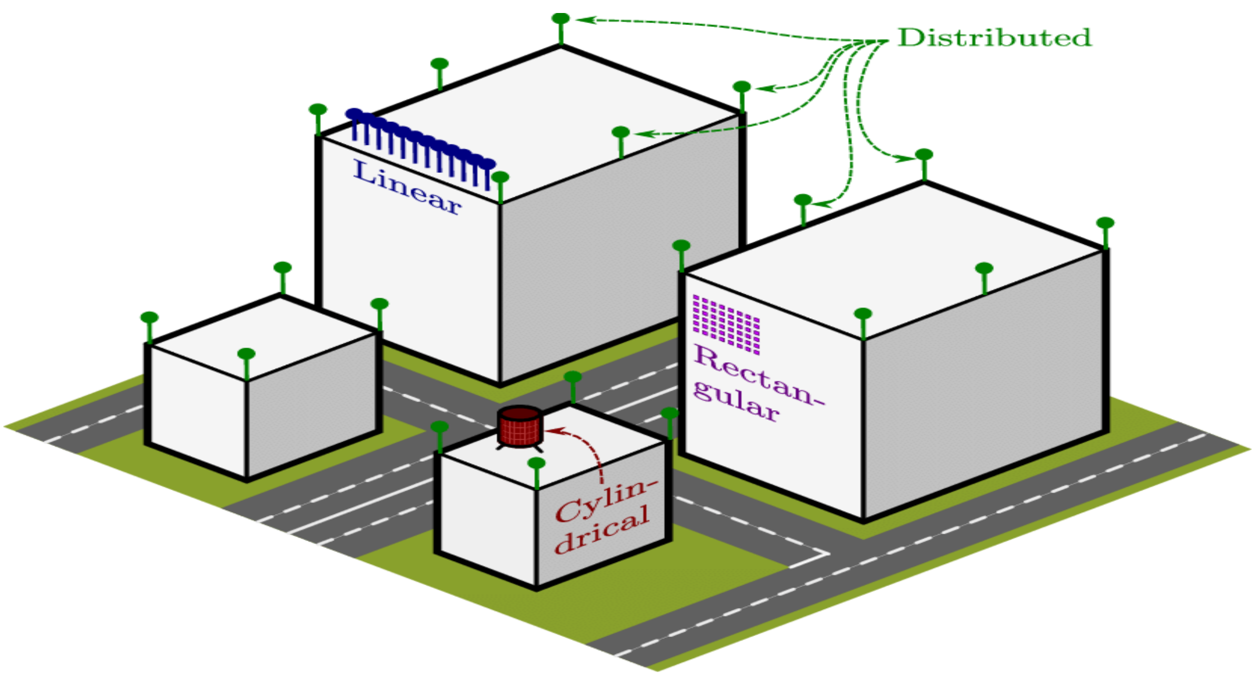

Figure 2. 6: Antenna configurations and deployment scenarios for a massive MIMO base station [15].

In practice, 5G will use more radio spectrum than 2G/3G/4G, including centimeter and millimeter waves at 3.5 GHz and 28 GHz, respectively. It has a substantially higher radio propagation loss than prior sub-1GHz and about 2 GHz models. Furthermore, the surrounding environment can have a significant impact on 5G radio propagation, Building shadowing, reflection from walls, human bodies, and rain attenuation are just a few examples. This sensitivity would highlight the potential of massive MIMO to improve coverage [17]. As explained previously, beamforming and MU-MIMO can both enhance single-user performance and total network capacity per base station. At higher frequencies, like as those proposed for MU, massive MIMO becomes significantly more realistic such as those planned for many 5G deployment [17].

Mr. Yang Chaobin, head of Huawei's 5G product line, emphasized on the premise that Massive MIMO is the key to simpler 5G networks during the debate session on "5G Deployments in High-Frequency Bands are Uneconomic" on February 26 at the Mobile World Conference (MWC) 2019. Using thorough theoretical analysis as well as intensive testing As a result, he responded favorably to the hotly disputed question of the economics of 5G network construction. Mr. Yang underlined that when deployed on the same sites as LTE in 1:1 mode, 5G with 3.5 GHz Massive MIMO provides superior coverage and capacity than LTE. Furthermore, operators will experience much lower cost per bit and overall deployment costs [18]. Massive MIMO, in general, appears to be quite promising for the future of 5G. In the long term, service providers are quite likely to discover huge MIMO to be the only way to meet IMT-2020 [17].

2.3.2 Channel Estimation

Based on the way of sharing the available spectrum in massive MIMO systems source. There are two massive MIMO systems. Time division duplex and Frequency division duplex are two topologies that share critical resources such as time and frequency among mobile customers or terminals. LTE makes advantage of both of these categories to allow mobile consumers or UEs to efficiently use scarce resources based on their demands.

2.3.3 Channel Estimation in TDD Systems

Massive MIMO is an original concept that assumes TDD and uses reciprocity to acquire CSI at the BS. On the uplink (UL), UEs send pilots; all UE-to-BS channels are estimated, and each antenna has its own RF electronics. Since its introduction a decade ago, the concept has progressed significantly: robust information-theoretic studies are accessible, field trials have proved its performance in high-mobility circumstances, and circuit prototypes have demonstrated the genuine practicability of implementations[19].

In a TDD system, uplink and downlink transmissions use the same frequency spectrum but separate time slots. The uplink and downlink channels are mutually exclusive [14]. As shown in Figure 2.7, the same carrier frequency Fc is used for uplink and downlink transmission at distinct time instants t1 and t2. As a result, the CSI can be obtained using the following scheme (see Figure 2.8):

- The BS requires CSI to detect the signals sent by *K* users during uplink transmission. This CSI is assessed at the BS. On the uplink, the *K* users deliver the BS *K* orthogonal pilot sequences. The BS then estimates the channels based on the received pilot signals. At least *K* channels are required for this operation [14].
- The BS requires CSI to precode the downlink signals, whereas each user requires effective channel gain to identify the needed signals. Because of channel reciprocity, the channel determined at the BS in the uplink can be used to precode the transmit symbols. To learn about the effective channel gain, the BS can beamform pilots, and each user can estimate
- the effective channel gains based on the received pilot signals. This requires the use of at least K channels [14].

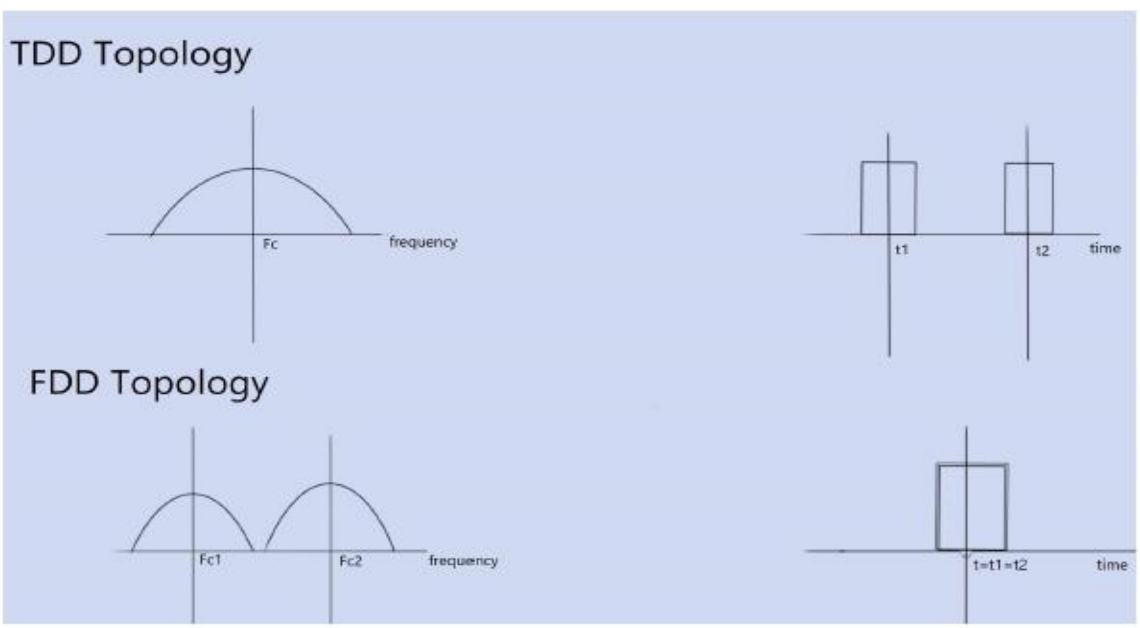

Figure 2. 7: TDD and FDD topologies [34].

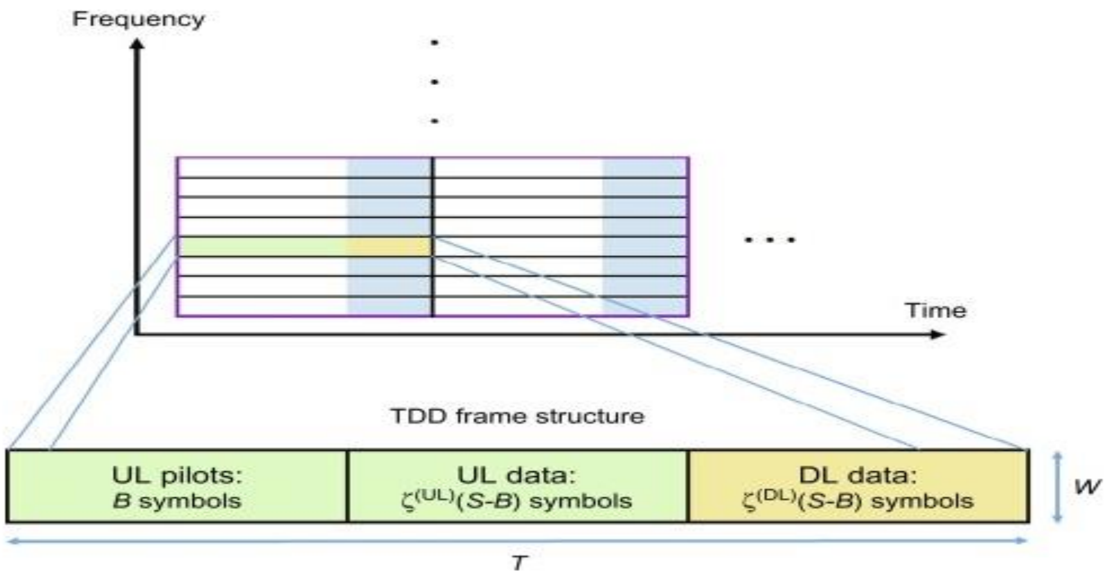

Figure 2. 8 :Slot structure and channel estimation in TDD systems [14].

The BS can beamform pilots to gather knowledge of the effective channel gain, and each user can estimate the effective channel gains based on the received pilot signals. This requires the employment of at least K channels [14]. As illustrated in Figure 2.9, both the uplink and the downlink have the same frequency f1 = f2, but they employ separate time slots to map their information packets. As a result, the entire radio frame is divided into subframes that are used for both the uplink and downlink directions. A total of 2K channel usage are required for the training process. We suppose that the channel remains constant over the course of T symbols. As a result, 2K T [14] is required. Figure 2.8 shows an implementation of channel estimation in Time Division Duplex systems.

2.3.4 Channel Estimation in FDD Systems

Because the uplink and downlink transmissions in an FDD system employ different frequency spectrums, the uplink and downlink channels are not reciprocal[14]. The following training scheme can be used to obtain channel knowledge at the BS and users:

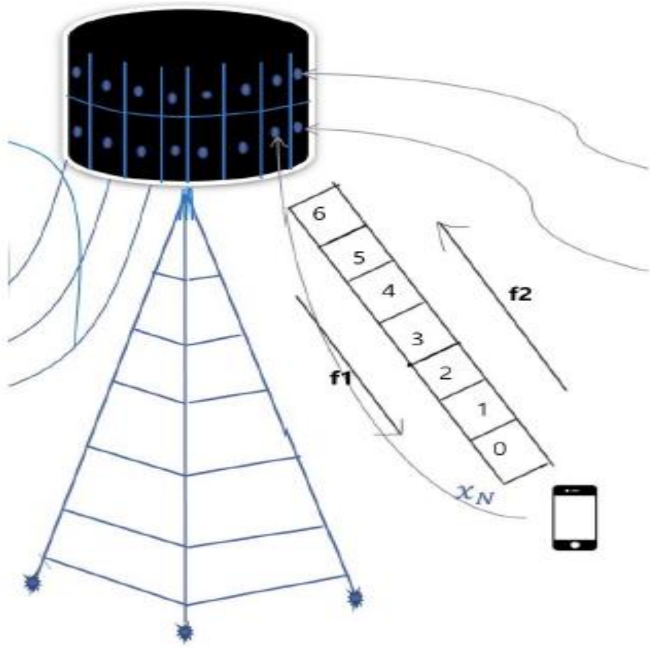

Figure 2. 9: Time Division Duplex scenario [6].

As we can see from Figure 2.7, at the same time t1, two separate carrier frequencies, Fc1 and Fc2, are used for uplink and downlink, respectively. Downlink is associated with the upper part of the spectrum, whereas uplink is associated with the lower part of the spectrum via the guard band. (i.e. duplex gap) between these parts.

As shown in the Figure 2.10, f1 and f2 are two frequencies that are allocated individually for the uplink and downlink directions. As a result, f1 is assigned to the downlink frequency band and f2 is assigned to the uplink frequency band. The complete radio frame is used in both the downlink and uplink directions at the same time. The BS requires CSI to precode the symbols before transferring them to the K users for the downlink transmission. M orthogonal pilot sequences are transmitted to K users by the M BS antennas. Based on the pilots received, each user will estimate the channel. Then, via the uplink, it sends its channel estimations (M channel estimates) back to the BS. This method requires the employment of at least M channels for the downlink and M channels for the uplink [14].

- For uplink transmission, the BS requires CSI to decode the signals sent by the K users. One simple method is for the K users to send K orthogonal pilot sequences to the BS. The BS will then estimate the channels based on the pilot signals received. This procedure necessitates the utilization of at least K channels for the uplink. [14].

As a result, the complete the channel estimation process needs at least M + K uplink channel uses and M downlink channel uses. Assume that the lengths of the coherence intervals for the uplink and downlink are equal to T. Then there are the constraints: M T and M+ K T. As a result, the constraint for FDD systems is M+ K T. Figure 2.11 illustrates an example of channel estimation in Frequency Division Duplex systems.

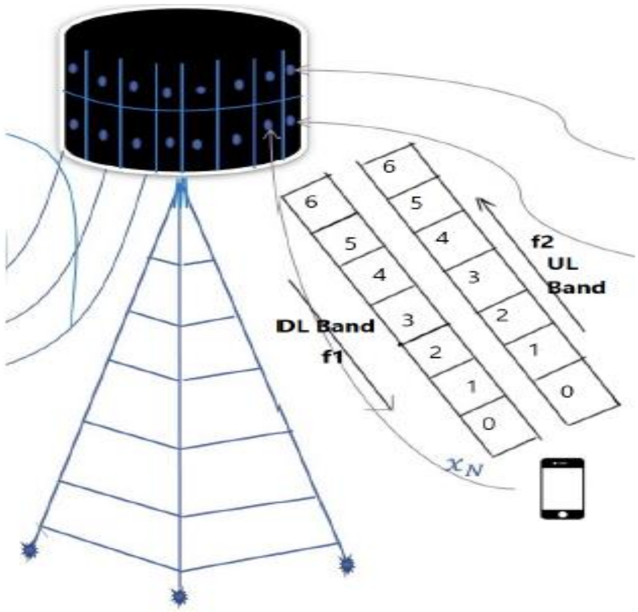

Figure 2. 10 : Frequency Division Duplex scenario [6].

Because system constraint is one parameter for comparison, it is possible to perform system constraint between TDD and FDD in order to select the optimal system. The publication [14] provides an excellent comparison of the two systems based on system constraints. The overhead for channel estimation with FDD is proportional to the number of BS antennas, M. TDD, on the other hand, has a channel estimation overhead that is independent of M. Because M is huge in Massive MIMO, TDD operation is ideal. Assume that the coherence interval is T = 200 symbols (corresponding to a coherence bandwidth of 200kHz and a coherence time of 1ms). Then, in FDD systems, the number of BS antennas and the number of users are constrained by M + K < 200, while in TDD systems, the constraint on M and K is 2K < 200. Figure 2.12 shows the regions of feasible (M, K) in FDD and TDD systems. The FDD region is clearly smaller than the TDD zone. When using TDD, adding extra antennas has no effect on the resources required for channel estimate.

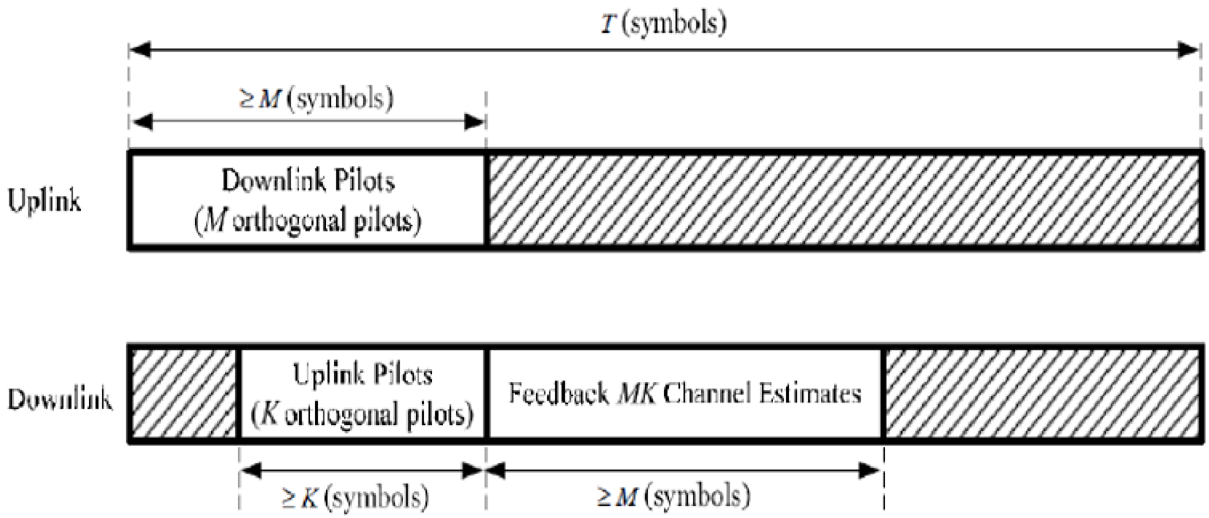

Figure 2. 11 : Slot structure and channel estimation in FDD systems [14].

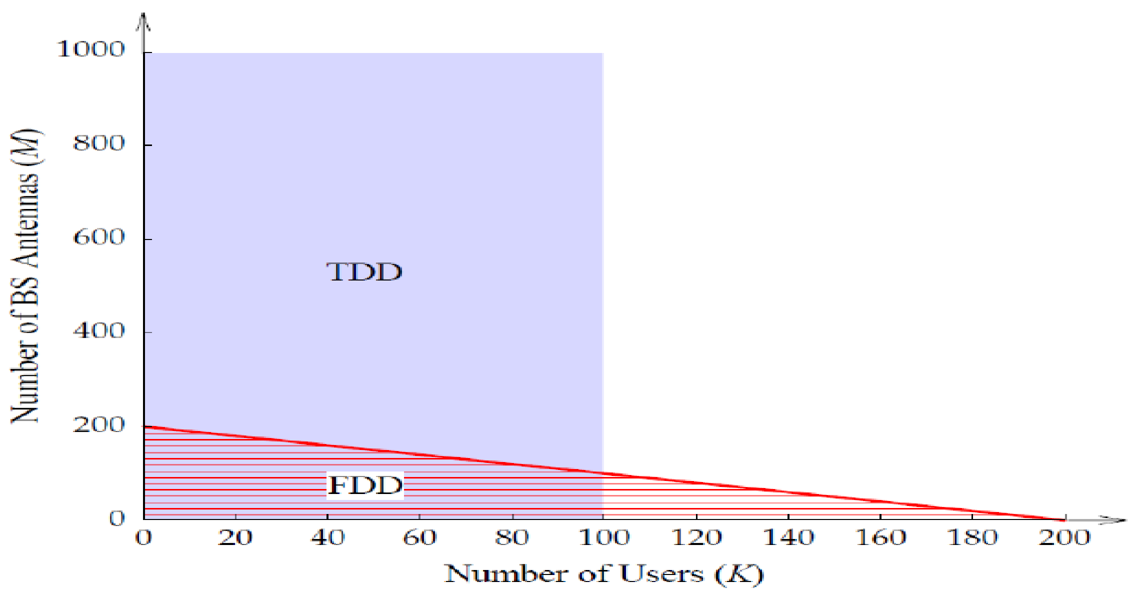

Figure 2. 12 : The regions of possible (M, K) in TDD and FDD systems, for a coherence interval of 200 symbols

It is not that much difficult to switch between TDD and FDD systems because Now a days, many chip-set Companies such as Ericsson, Altair semiconductor, and Qualcomm support both TDD and FDD versions of LTE on a single chip, and telecommunication operators can take advantage of this adaptability traffic volume and other considerations.

2.4 Properties and Advantageous of Massive MIMO

Massive MIMO is a type of MU-MIMO system in which the number of BS antennas and users are both large. Hundreds or even thousands of BS antennas simultaneously serve tens or hundreds of users in the same frequency resource in Massive MIMO. The following are some of the most important aspects of Massive MIMO:

TDD operation: As described in Section 2.3.2, the channel estimate overhead with FDD is equivalent to the number of BS antennas, M. TDD, on the other hand, there is an overhead channel estimate independent of M. Because M is massive in Massive MIMO, TDD operation is ideal. Figure 2.17 depicts the TDD Massive MIMO transmission protocol.

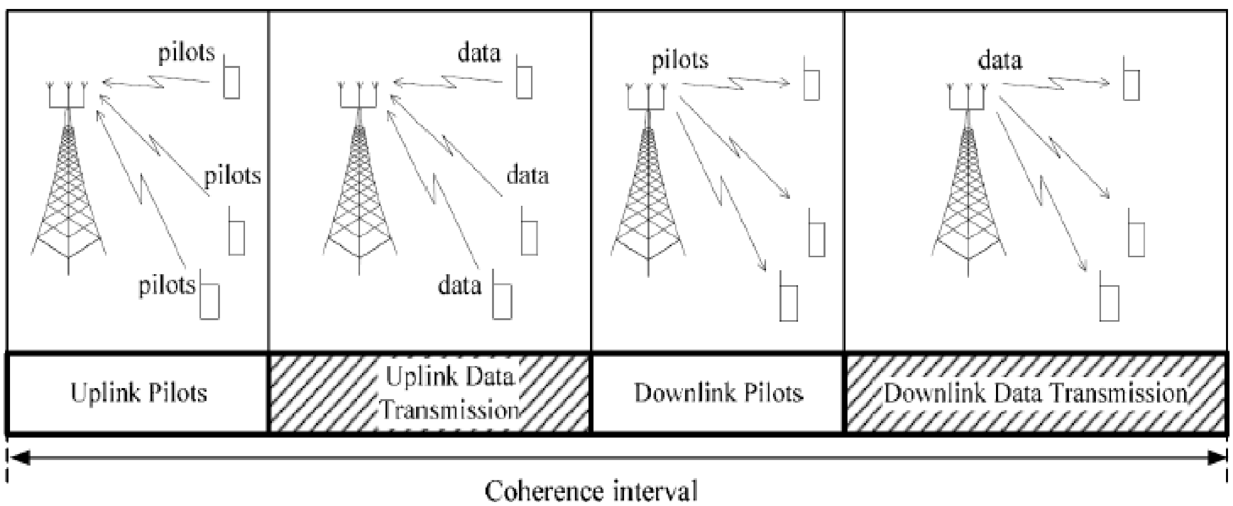

Figure 2. 13 :Transmission protocol of TDD Massive MIMO[14].

Linear processing: Because of the large number of BS antennas and users, Signal processing at the endpoints must deal with high-dimensional matrices/vectors. As a result, basic signal processing is preferred. Linear processing (linear combing techniques in the uplink and linear precoding schemes in the downlink) is approximately ideal in Massive MIMO[14].

Favorable propagation: When the channel matrix between the BS antenna array and the users has been properly conditioned, it is also said to be favorable propagation. Due to the law of large numbers, the advantageous propagation property holds in Massive MIMO under certain conditions.

Massive MIMO is scalable: The BS in Massive MIMO learns the channels through uplink training while running in TDD mode. Furthermore, signal processing is relatively simple at each user and does not rely on the presence of other users, i.e., no multiplexing or de-multiplexing signal processing occurs at the users. Adding or removing users from the service has no effect on the activity of other users. It is not essential for a massive BS antenna array to be physically large. Consider a cylindrical array of 128 antennas made up of four rings of 16 dualpolarized antenna pieces. At 2.6GHz, the spacing between neighboring antennas is around 6cm, which is half a wavelength, hence this array is only 28cm -29cm in size [14].

Massive MIMO systems offer numerous advantages that make them superior than earlier technologies. One of these advantages is that it can increase capacity by 10 times or more while also increasing radiated energy efficiency by 100 times [15]. The increased capacity is due to the huge number of antennas utilized in massive MIMO. The energy-efficiency is due to the large beamforming capacity. The underlying premise that enables the massive increase in energy efficiency is that energy may be concentrated with extraordinary precision into small regions of space employing a large number of antennas. By appropriately organizing the signals sent out by the antennas, the base station may ensure that all wave fronts collectively radiated by all antennas sum up constructively at the locations of the intended terminals, but destructively (randomly) almost everywhere else. Interference between terminals can be reduced even more by employing various combining techniques and algorithms.

The second advantage is that it may be constructed with low-cost, low-power components [15]. Massive MIMO technology is the finest option in terms of theory, systems, and execution. Massive MIMO replaces expensive non-linear technology utilized in conventional systems with low-cost linear equipment. Several costly and bulky elements, such as big coaxial cables, can be completely eliminated. Today's coaxial cables for tower-mounted base stations are more than four centimeters in diameter. Massive MIMO minimizes the accuracy and linearity restrictions of each individual amplifier and RF chain. All that matters is their joint action.

Massive MIMO, in some ways, relies on the law of large numbers to ensure that noise, fading, and hardware flaws average out when signals from a large number of antennas are joined in the air. The same property that makes Massive MIMO immune to fading also makes the system extremely resistant to the failure of one or more of its antenna unit components. A massive MIMO system has an abundance of degrees of freedom. With 200 antennas covering 20 terminals, for example, 180 degrees of freedom are useless. These degrees of freedom can be employed for signal filtering that is hardware-friendly. Each antenna, in instance, may transmit signals with very low peak-to-average ratios or even constant envelopes at a very low cost in terms of increased overall radiated power [15].

The third advantage is that it allows for large reductions in latency on the air interface. Normally, fading limits the performance of wireless communications systems. Fading might cause the received signal strength to be very low at times. This happens when a signal sent from a base station travels via several paths before arriving at the terminal, and the waves created by these multiple paths interfere destructively. Because of this fading, it is challenging to build low-latency wireless networks. If the terminal is caught in a fading dip, it must wait until the propagation channel has sufficiently modified before receiving any data. Massive MIMO employs the law of large numbers of antennas and beamforming to overcome fading dips, allowing fading to no longer limit latency [15].

Massive MIMO makes the multiple-access layer easier to understand. Because of the law of big numbers antenna the channel hardens to the point where frequency-domain scheduling is no longer profitable. Each subcarrier in a Massive MIMO system will have roughly the same channel gain when using OFDM. Because each terminal can be assigned the entire bandwidth, much physical layer control signaling is made redundant. Another advantage of Massive MIMO is that it increases resistance to both unintentional man-made interference and purposeful jamming. Intentional jamming of civilian wireless systems is a developing worry and a serious cyber security danger that the general public appears to be unaware of [15].

2. 5 Pilot Contamination: The Limiting Factors of Massive MIMO

In a perfect scenario, each terminal in a Massive MIMO system would be assigned an orthogonal uplink pilot sequence. The maximum number of orthogonal pilot sequences that can occur, on the other hand, is limited by the coherence interval time divided by the channel delay spread. In [14], For a typical operational state, the maximum number of orthogonal pilot sequences in a one millisecond coherence period is anticipated to be around 200. The available supply of orthogonal pilot sequences in a multicellular system is quickly depleted.

The process of reusing pilots from one cell to another, as well as the negative consequences, is known as "pilot contamination." When the service-array correlates its received pilot signal with the pilot sequence associated with a particular terminal, it obtains a channel estimate that is contaminated by a linear combination of channels to other terminals that share the same pilot sequence. Downlink beamforming dependent on the contaminated channel estimate results in interference directed towards terminals with the same pilot sequence. Uplink data streams are subject to similar interference. This directed interference builds at the same rate as the desired signal as the number of service antennas increases [14]. Direct interference occurs even with imperfectly correlated pilot sequences. Pilot contamination as a fundamental phenomenon is not unique to massive MIMO, although its impact on massive MIMO looks to be far greater than in conventional MIMO[14].

CHAPTER THREE

3 System Model for Massive MIMO

The massive MIMO system model will be built in this chapter. We will choose models for our channel and observe the mathematical model for our system as we create the model for massive MIMO systems. The simulation results for the modeled system will then be produced in Chapter 4.We consider a massive MIMO system with many cells and multiple users. The system is made up of B cells, each having one base station (BS). As shown in Figures 3.1 shows MU Massive MIMO each BS contains a large number of fixed transmit antennas N that serve K single antenna user terminals (UT). It is assumed that N>> K>> 1 exists.

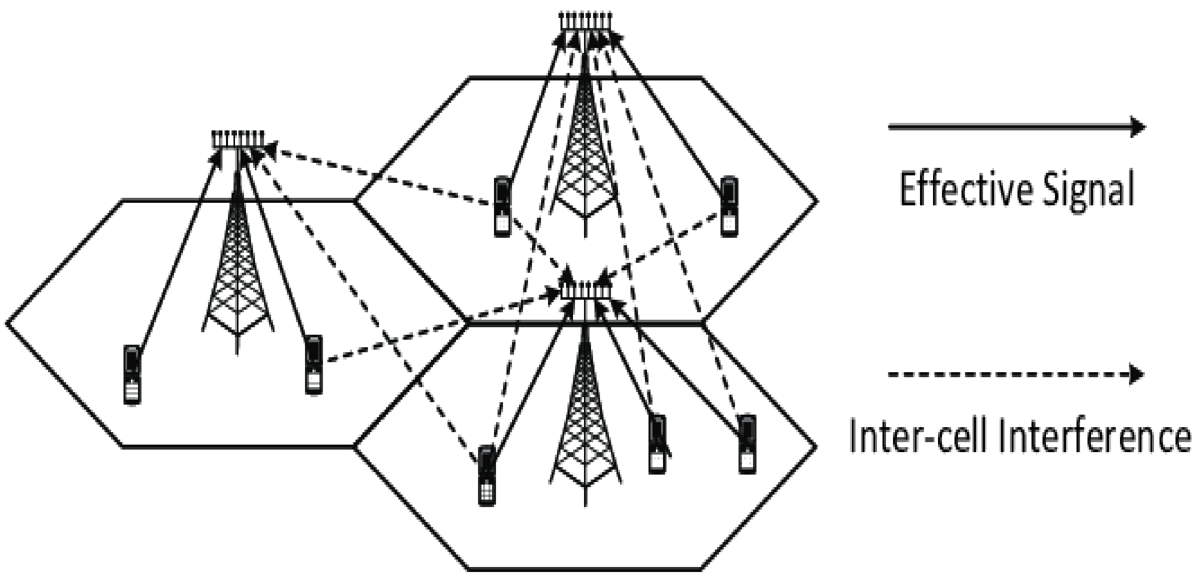

Figure 3. 1: A typical multi-cell multi-user massive MIMO systems [20].

The system works in TDD mode, which maintains constant channel replies throughout a coherence block of τ_c samples. The channel between the UE and BS is rician (i.e. the presence of LoS component is assumed).Furthermore, we assume that channel realizations are independent of any pair of coherence blocks. Furthermore, we assume that channel realizations are independent of any pair of coherence blocks. A coherence block is made up of a number of subcarriers and time samples that can be used to approximate the channel response as steady and flat-fading. If the coherence bandwidth is Bc and the coherence time is Tc, then each coherence block contains τ_c = $\mathbf{B}_c * \mathrm{T}_c$ complex-valued samples[5]. Regardless of time and/or frequency separation, the random channel answers in one coherence block are statistically similar to those in any other coherence block. As a result, channel fading is described by a stationary random process.

As a result, the performance analysis is carried out by examining a single statistically representative coherence block. We make the assumption that channel realizations are independent of any pair of blocks, which is known as the block fading assumption. Each coherence block is operated in TDD mode. Figures 3.2 and 3.3 illustrate how the τ_c samples are located in the time and frequency plane. The samples are used for three

Different things:

- τ_u UL data signals;
- τ_p UL pilot signals;
- τ_d DL data signals;

As we can see, we need $\tau_p + \tau_d + \tau_u = \tau_c$. The percentage of UL and DL data can be chosen based on network traffic statistics, but the number of pilots per coherence block is a design parameter. Many user applications (e.g., video streaming and web browsing) mainly generate DL traffic, which can be dealt with by selecting $\tau_d + \tau_u$. The size of a coherence block is impacted by numerous parameters. Among the parameters are the propagation environment, UE mobility, and carrier frequency. Individual coherence bandwidth and coherence time are assigned to each UE, but dynamically adapting the network to these values is problematic because the same protocol should apply to all UEs. A reasonable solution is to dimension the coherence block for the network's worst-case propagation scenario. If a UE has a substantially larger coherence time/bandwidth, it is not required to send pilots in every block. The samples are used for three different tasks: τ_p samples for uplink (UL) pilot signals, τ_u samples for UL data transmission and τ_d samples for downlink (DL) data transmission where $\tau_c = \tau_p + \tau_u + \tau_d$ Both UL and DL channels are estimated by uplink pilot signals by exploiting channel reciprocity in the TDD protocol.

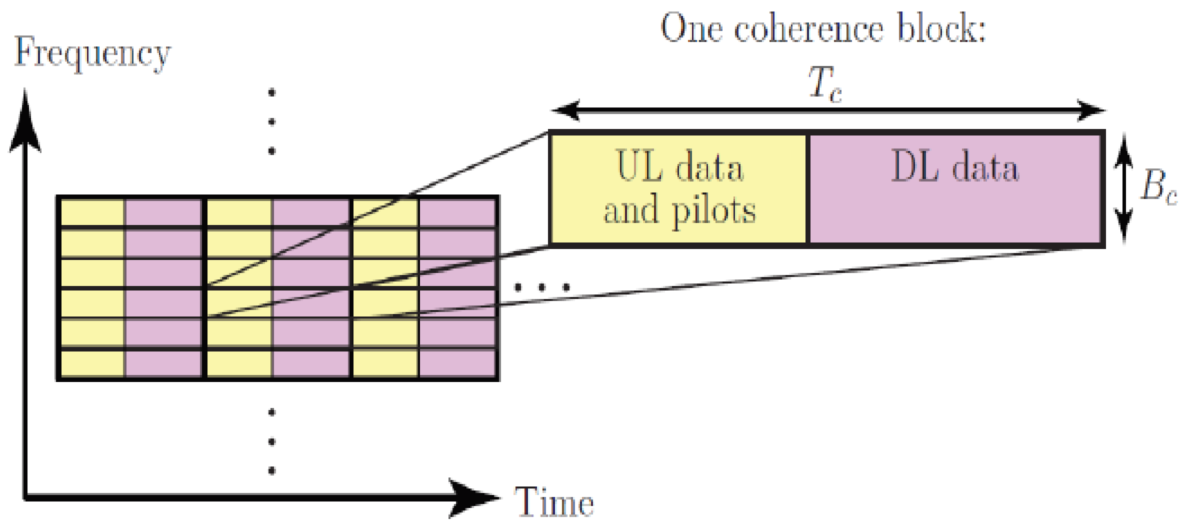

Figure 3. 2 : Time Division Duplex multi-carrier modulation scheme of a canonical Massive MIMO network [5].

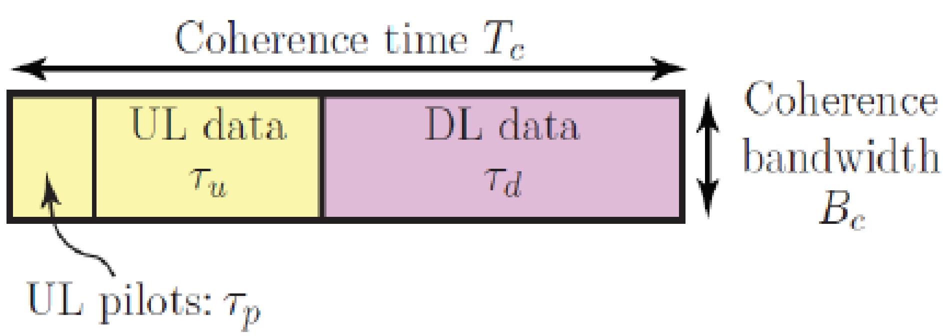

Figure 3. 3: Uplink samples for UL pilots, UL data, and DL data..

3.1 Channel Model

In general, the channel creates a path between the UE and the BS. There are other channel models that have already been examined. To be able to design and develop a wireless communication system, you must first grasp several types of channel models and their properties. When modeling networks, channel models are used to see how the system design functions in different settings and under different conditions. Fading, for example, shows the variable attenuation that a signal experiences in different propagation settings. Some of these models are as follows:

1, Additive White Gaussian Noise (AWGN)

2, Perfect Channel

3, Rayleigh fading

4, Rician Channel

Each of these channel models will be discussed in the following sections;

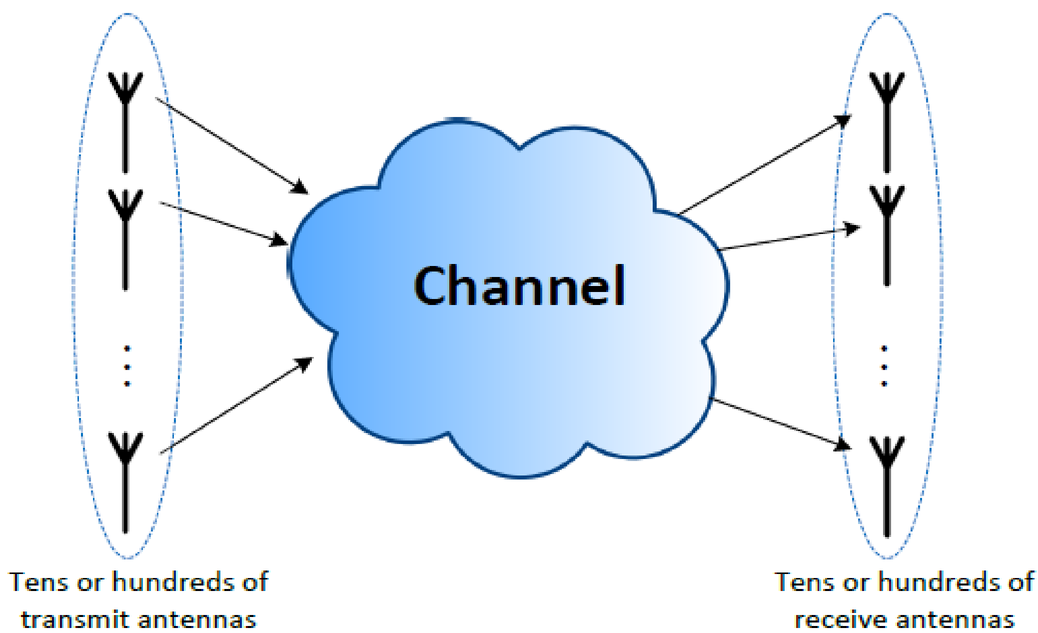

Figure 3. 4 : A diagram of massive MIMO systems with the channel [21].

3.1.1 Additive White Gaussian Noise (AWGN)

The Additive White Gaussian Noise (AWGN) channel model is a popular communication channel model in which the primary degradation is a linear introduction of wideband or white noise. It is a fundamental and widely accepted model for thermal noise in communication systems.

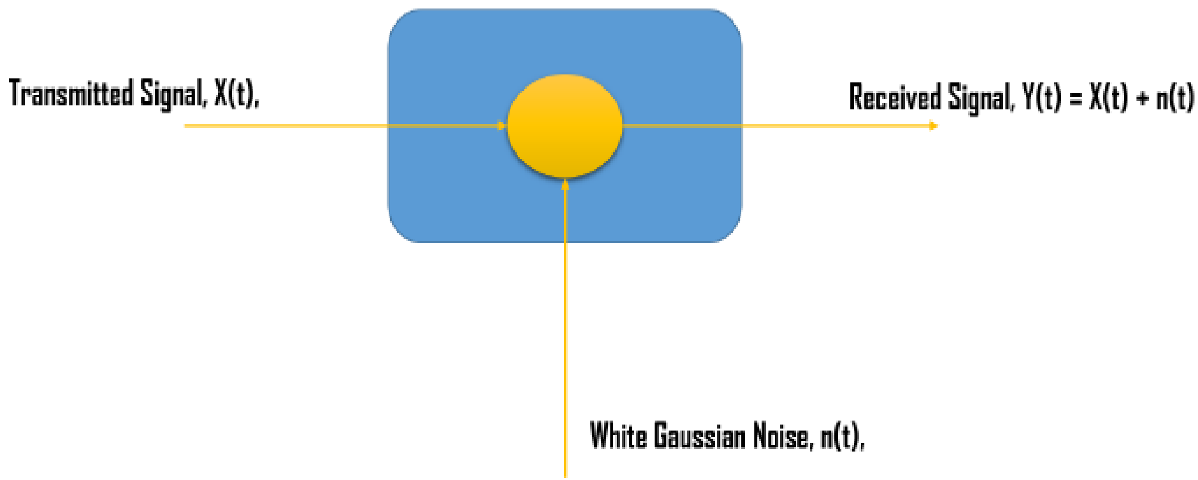

Figure 3. 5 : Block diagram of AWGN channel model [20].

The AWGN model is a statistical model that predicts the distribution of noise in a communication system. A multitude of reasons, including thermal noise in the receiver circuitry and external noise sources picked up by the antenna, can generate AWGN. Because it is added to the received signal, it is additive. It is white because the power of the noise is frequency independent and thus the same throughout the entire spectrum. It is Gaussian because of its Gaussian distribution [21].

3.1.2 Perfect Channel

The ideal channel is a form of channel in which all environmental noises, interferences, and fading effects are disregarded. It is expected that the channel can be perfectly estimated and measured in this case. Most previous studies assume perfect channel reciprocity by demanding that the time delay between UL channel estimation and DL transmission be less than the coherence time of the channel. This assumption ignores two critical facts:

- UL and DL radio-frequency (RF) chains are independent circuits with random effects on broadcast and received signals.
- The interference profile on the BS and UE sides may be drastically different. The former is known as RF mismatch. RF mismatches can produce random differences in the estimated values of the UL channel from the actual values of the DL channel during the channel's coherent time. Such deviations are called as reciprocity [21].

3.1.3 Rayleigh Fading

Rayleigh fading models assume that the magnitude of a signal flowing over a transmission medium (also known as a communication channel) would change randomly, or fade, according to a Rayleigh distribution. The radial element of the sum of two uncorrelated Gaussian random variables.

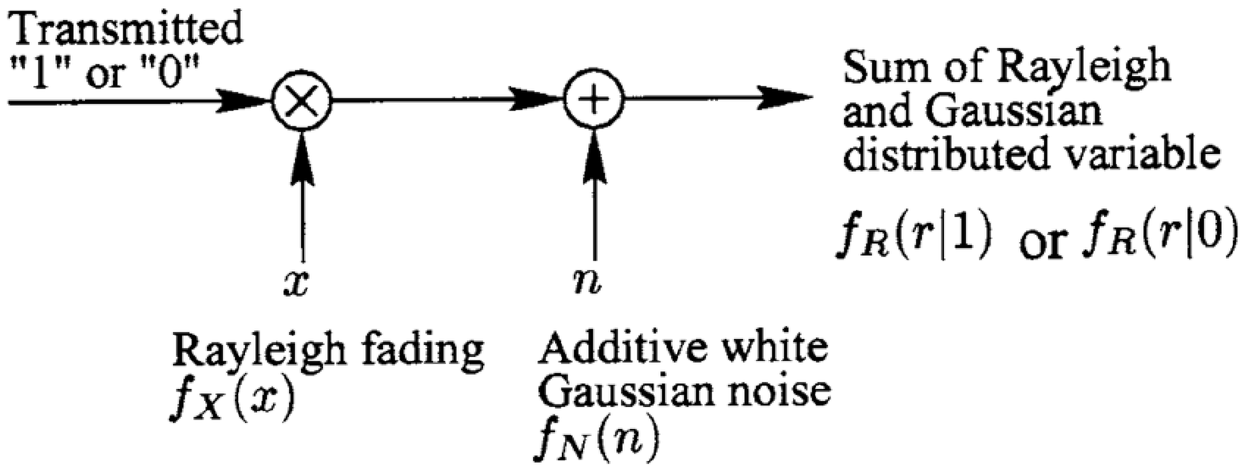

Figure 3. 6: Block diagram of rayleigh channel model [22].

Rayleigh fading is a statistical model for a small-scale fading channel with no line of sight (LOS), which is frequent in urban areas. The amplitude variations of two uncorrelated orthogonal Gaussian random variables are described by a Rayleigh distribution [22]. Figure 3.5 shows a possible signal representation of a communication medium involving a Rayleigh fading channel where both the Rayleigh fading and AWG noise are considered in the system. Where:

- *fX(x)* represents the distribution of the Rayleigh fading
- *fN(n)* represents the distribution of the noise in the channel and
- *fR(rj1) and fR(r/0)* represent the effect of both the Rayleigh fading and AWGN.

3.1.4 Rican Fading

The Rican fading channel block simulates a Rican fading propagation channel in baseband. When the sent signal may go to the receiver over a dominant line-of-sight or direct path, this block is useful for modeling mobile wireless communication systems. If the signal can travel through a line-of-sight path as well as other fading paths, this block can be used in conjunction with the Multipath Rayleigh Fading Channel block.

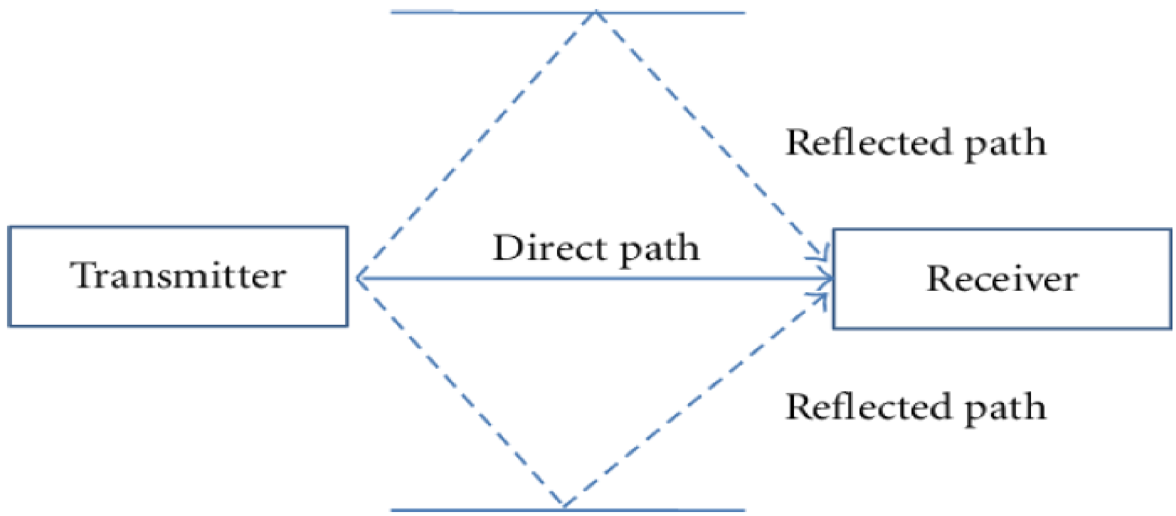

Figure 3. 7: Block diagram of rician channel model [23].

The Rician fading channel is a statistical model for a small-scale fading channel that includes a line of sight (LOS) component as well as a non-LOS component. As described in previous sections, we will select the Rician channel model from the list above. This model is preferable to the Rayleigh model, which was previously used for cellular networks, because the cell radius in large MIMO systems is tiny in comparison to other cellular networks. So, the assumption of the presence of line of sight between the BS and the UE is reasonable which leads to choice of Rician channel model. Now, we will define mathematical symbols and parameters that will be used for discussing the channel model for massive MIMO. The channel response between UE k in cell l and the BS in cell j is denoted by h_{ik}^{j} Each element of h_{ik}^{j} corresponds to the propagation channel from the UE to one of the BS's M_j antennas The superscript h_{ik}^{j} indicates the BS index and the subscript identifies the index of the cell and the UE. The channel responses are the same in the UL and DL of a coherence block. In this thesis, we consider spatially correlated Rican fading channels.

3.2 Mathematical Model for the UL Transmission

After defining the Massive MIMO channel model, we shall define the UL and DL system models used in this thesis:

3.2.1 Uplink Transmission

Figure 3.8 shows the UL transmission in Massive MIMO. The UL signal received $Y_j \in \mathbb{C}^{M_j}$ at BS j is modeled as $Y_j = \sum_{l=1}^{L} \sum_{k=1}^{K_l} h_{lk}^{\ j} + n_j$

$$= \sum_{K=1}^{k_j} h_{jk}^{j} s_{jk} + \sum_{\substack{l=1 \\ l \neq j}}^{L} \sum_{i=1}^{kl} h_{li}^{j} s_{li} + n_j \qquad (3.1)$$

Where $n_j \sim N\mathbb{C}(0_{M_j}, \sigma^2_{UL} \mathbf{I}_{M_j})$ is independent additive receiver noise With zero mean and variance σ^2_{UL} .The UL signal from UE k in cell l is denoted by $S_{lk} \in \mathbb{C}$ has power $p_{lk} = E\{|S_{lk}|^2\}$ irrespective of whether it is a random payload data signal $S_{lk} \sim N_c(0, p_{lk})$ or a deterministic pilot signal with $p_{lk}^{pliot} = |S_{lk}|^2$ The channels are constant within a coherence block, while the signals and noise take new realization at every sample. During data transmission, the BS in cell j selects the receive combining vector $v_{jk} \in| \mathbb{C}^{M_j}$ to separate the signal from its kth desired UE from the interference as

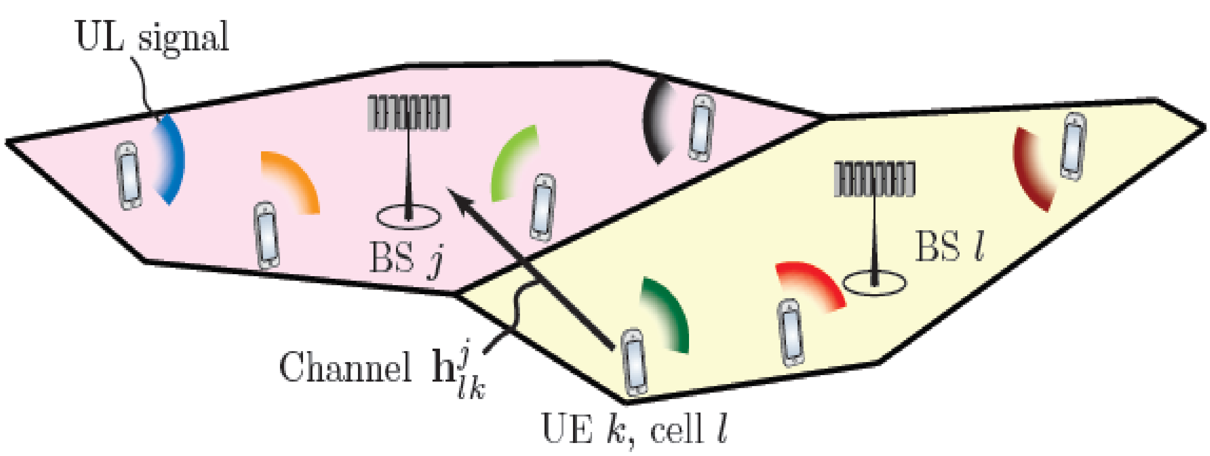

Figure 3. 8: Illustration of the UL Massive MIMO transmission in cell j and cell l.[5]

The channel vector between BS *j* and UE *k* in cell *l* is called h_{lk}^{j}

$$v_{jk}^{H} y_{j} = v_{jk}^{H} s_{jk} + \sum_{\substack{i=1 \\ i \neq k}}^{k_j} v_{jk}^{H} h_{ji}^{j} s_{ji} + \sum_{\substack{l=1 \\ l \neq j}}^{L} \sum_{i=1}^{K_t} v_{jk}^{H} h_{li}^{j} s_{li} + v_{jk}^{H} n_{j} \tag{3.2}$$

3.2.2 Downlink Transmission

The DL transmission in Massive MIMO is illustrated in Figure 3.8. The BS in cell *l* transmits the DL signal

$$x_l = \sum_{i=1}^{k_l} w_{li} \varsigma_{li} \tag{3.3}$$

Where $\varsigma_{li} \sim N_{\mathbb{C}}(0, \rho_{lk})$ is the DL data signal intended for UE *k* cell and ρ_{lk} .This signal is assigned to a transmit precoding vector $| w_{lk} \in \mathbb{C}^{M_l} |$ that determines the spatial directivity of the transmission. The precoding vector satisfies $E\{|| w_{lk} ||^2\} = 1$, such that $E\{|| w_{lk} \varsigma_{lk} ||^2\} = \rho_{lk}$

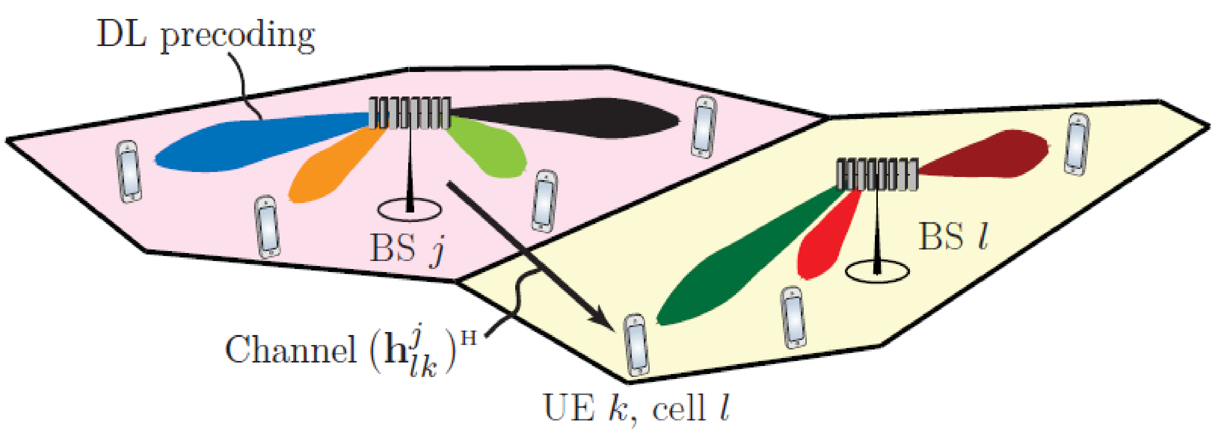

Figure 3. 9: Illustration of the DL Massive MIMO transmission in cell *j* and cell *l* [5]

The received signal $y_{jk} \in \mathbb{C}$ at UE *k* in cell *j* is modeled as

$$y_{jk} = \sum_{l=1}^{L} (h_{jk}^{l})^{H} x_l + n_{jk}$$

$$=\sum_{l=1}^{L}\sum_{i=1}^{k_l}(h^l{}_{jk})^H w_{li}\varsigma_{li}+n_{jk}$$

$$=\left|(h^j{}_{jk})^H w_{jk}\varsigma_{jk}+\sum_{\substack{i=1\\i\neq k}}^{k_j}(h^j{}_{jk})^H w_{li}\varsigma_{ji}+\sum_{l=1}^{L}\sum_{i=1}^{k_l}(h^l{}_{jk})^H w_{li}\varsigma_{li}+n_{jk}\right. \quad (3.4)$$

Where $n_{jk}\sim N\mathbb{C}(0,\sigma_{DL}{}^2)$ is independent additive receiver noise with variance $\sigma_{DL}{}^2$.

The channels are constant within a coherence block, while the signals and noise take new realization at every sample.

3.3 Channel Estimation Techniques in Massive MIMO Systems

As described in Chapter 2, channel estimation approaches in massive MIMO systems are examined in this thesis. We've also highlighted how FDD-based channel estimate necessitates orthogonal pilots equal in number to the number of antennae, whereas TDD based channel estimation necessitates orthogonal pilots equal in number to the number of users, which is substantially fewer than the number of antennas. As a result, our huge MIMO system employs TDD-based channel estimation.

Based on a normal MIMO system, a Massive MIMO system is designed in which the base station is equipped with a high number of antennas [24]. Massive MIMO benefits from a large number of antennas at each base station. It should be highlighted that these advantages are contingent on the BS obtaining accurate estimates of each user's CSI [5]. Denotes the deterministic pilot sequence of UE k in the supplied cell.

$$\phi_k\in\mathbb{C}^{\tau_p} \text{ and } ||\phi_k||^2=\tau_p$$

Then the received pilot signal would be, as discussed in Chapter 3:-

$$y^{pilot}=\sum_{k=1}^{k}h_k\sqrt{p_k\phi_k}+n \quad (3.5)$$

Where $n\in\mathbb{C}_M$ which is zero-mean circularly symmetric complex Gaussian distributed

With variance σ^2_{UL} ;that is $n \sim N\mathbb{C}(0_M, \sigma^2_{UL}\mathbf{I}_M)$. Now, the task of the channel estimation is to estimate the channel vector, h_k from pre known pilot vectors, ϕ_k .This is what is called pilot based channel estimation. Depending on the methodologies utilized, pilot-based channel estimation might employ a variety of algorithms. This paper presents three of the most prominent channel estimation methodologies. The methodologies of least squares (LS), mean minimum square error (MMSE), and element wise mean minimum square error (EW MMSE) will be covered. The pilot sequence or symbols are placed into specific locations of the sent signals based on the pilot symbols that are delivered together with the information signal to keep track of the altering radio channel statistics. Because the receiver is fully aware of the pilot sequence as well as the fixed pilot positions, it estimate the channel based on the received pilot sequence.

Depending on the arrangement of pilots, three different types of pilot structures are considered: block type, comb type, and lattice type. These three types are explained as:-

1. **Block-type pilot:** Because covering all frequencies is useful against selective frequency fading but more sensitive to the impact of fast fading channels, it is accomplished by incorporating pilot tones into all. As a result, the blocktype pilot is built around the idea of a gradually diminishing channel. When there are the same number of pilots, the channel change rate, also known as coherent time, determines performance [25].

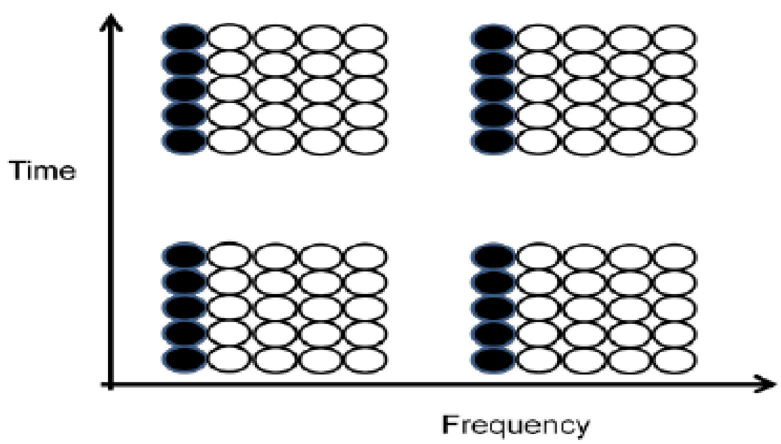

Figure 3. 10 : Block-type pilot channel estimation arrangement. The black dots represent the pilot while the white dots represent the actual data [25].

2. Comb-type pilot*:* This is performed by inserting pilot tones into certain subcarriers of each OFDM symbol, where interpolation is necessary to approximate the circumstances of date subcarriers. Because pilot symbols are inserted in subcarriers with the same spacing as in block-type pilot, comb-type pilot channel estimation is added to meet the requirement for equalizing when the channel changes even from one OFDM block to the next. When there are the same number of pilots, the channel multipath time delay, also known as coherent bandwidth, determines performance[25].

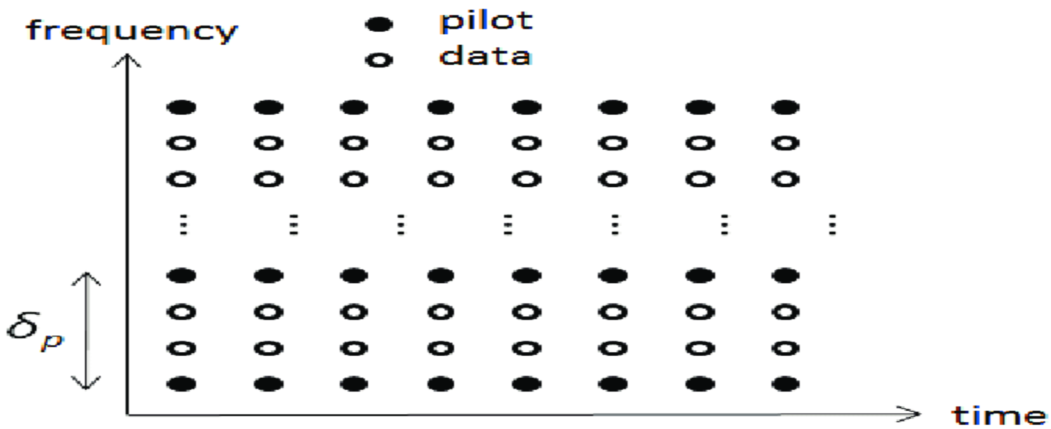

Figure 3. 11 : Comb-type pilot channel estimation arrangement. The black dots represent the pilot while the white dots represent the actual data[25].

3. **Lattice-type pilot*:*** is a pilot configuration in which pilots are placed along both the time and frequency axes to estimate the channel. A frequency-domain and a time-domain interpolation along the frequency axis Pilots are used to calculate the channel length along the time axis. To keep track of the frequency-selective and time-varying channel characteristics, the pilot subcarrier spacing must be less than the coherence bandwidth, and the pilot symbol period must be less than the coherence time.[25]

3.4 The Minimum Mean Square Error Algorithm

The MMSE channel estimation is an estimation technique with very high computational. It requires prior knowledge of the second order channel statistics[26]. MMSE channel estimation is a more accurate version of the LS channel estimation. The MMSE channel estimator minimizes the MSE between the true channel **H**, and the MMSE estimated channel, ˆH MMSE, by finding a good linear estimate in terms of M and the value of LS estimate. The MMSE channel estimator is designed to minimize the mean square error (MSE) of the estimation.

The correlation matrix of the error of the the given channel estimations given by[26].

$$R_{ee} = [H - \hat{H}] \times [H - \hat{H}]^H \tag{3.6}$$

As mentioned above, the task of MMSE is to minimize MSE of the LS estimator. i.e.

$$\text{MSEE } = Min[Argument[MSE]] \tag{3.7}$$

$$\text{MMSE} = | Min \| [H - \hat{H}] \times [H - \hat{H}]^H] \| \tag{3.8}$$

$$\text{MMSE} \rightarrow solve \frac{d}{d\hat{H}} \| [H - \hat{H}] \times [H - \hat{H}]^H] \| \tag{3.9}$$

$$H_{MMSE} \rightarrow \frac{d}{d\hat{H}} \| HH^H - H\hat{H} - H^H H^H + \hat{H}^H \hat{H} \| = 0 \tag{3.10}$$

$$H_{MMSE} \rightarrow \frac{d}{d\hat{H}} \| HH^H - H\hat{H}_H - H^H H^H + \hat{H}^H \hat{H} \| = 0 \tag{3.11}$$

To solve the above equation, we will differentiate the above equation with respect to $\hat{H}$, set the resulting equation to zero and after all this solve for $\hat{H}$ After solving the above

Equation for $\hat{H}$ we will get the following result, bear in mind that $\hat{H}$ here is the H_{MMSE} ;

$$H_{MMSE} = [R_{hy}] \times [R^{-1}{}_{yy}] * [R_{yh}] \tag{3.12}$$

Substituting the values for R_{hy} and R_{yy} we get the following result.

$$= H_{MMSE} = \sigma_h{}^2 x^H [\sigma^2 x x^H + \sigma^2 I_{M*M}]^{-1} * [R_{hy}] \tag{3.13}$$

$$H_{MMSE} = \sigma_h{}^2 x^H [\sigma^2 x^H x + \sigma^2 I_{M*M}]^{-1} X^H * [R_{hy}] \tag{3.14}$$

Equation 3.10 is for Rayleigh channel. In order to modify it for Rican channel, we will just add LOS component, *h*. So, by doing this we get the expression for the Rican channel:-

Where *h* is the LOS component, and is given as:-

$$h^{-} = R_{hh} \tag{3.15}$$

Going back to the original equation, we can write the above equation as:-

$$H_{MMSE} = h^{-} + [R_{hy}] \times [R^{-1}{}_{yy}] * [R_{yh}] \tag{3.16}$$

$$H_{MMSE=R_{hh}} + [R_{hy}] * [R_{yh}] \tag{3.17}$$

Where:

- $R_{hy} = E[h * y^H] = \sigma^2{}_h x^H,$
- $R_{yh} = E[h * y^H] = \sigma^2{}_h x \ ,$
- $R_{yy} | = E[y * y^H] = \sigma^2{}_h xx^H + \sigma^2 I_{M \times M},$
- $R_h | = E[h \times h * H \ ] = \sigma^2{}_h I,$

The above equation be more simplified by substituting R_{hy}, R_{yh} , R_{yy} , R_h by doing so we will achieve the following equation:-

$$H_{MMSE=} \sigma_h{}^2 + \sigma_h{}^2 I_{M \times M} [\sigma_n{}^2 (X^H X)^{-1} + \sigma^2 I_{M \times M}]^{-1} X^H * \sigma_h{}^2 X \tag{3.18}$$

Collecting like terms and rearranging the above equation we get a more simplified expression, given as:-

$$H_{MMSE} = \sigma^2 \sigma_h{}^2 [\sigma_h{}^2 X^H + \sigma^2 I_{M \times M}]^{-1} \tag{3.19}$$

$$H_{MMSE} = [\frac{X^H X}{\sigma^2} \sigma_h{}^2 + \frac{I_{M*M}}{\sigma_h{}^2}]_{-1} \tag{3.20}$$

Now, substituting by $\hat{X}$ the pilot vector and substituting the other vectors by their values, we can get the following expression for MMSE algorithm [5]:-

$$H_{MMSE} = h^{-} + \sqrt{P_k} R_k \psi_k (y_k{}^{pilot} - \hat{y}_k{}^{pilot}) \tag{3.21}$$

Where:

- h^{-} is the LOS component.
- R_k is the covariance matrix describing the spatial correlation of the NLoS components.
- $\psi_k = \tau_p Cov\{y_k^{pilot}\}^{-1}$

- $\hat{y}_k^{pilot} = \sum_{k=1}^{k} \hat{H}_k \sqrt{P_k}$

The MMSE typically has a higher complexity than the LS estimator, while the LS estimator has a higher MSE than the MMSE estimator. When N becomes a large amount, the MMSE estimator must calculate a N * N matrix, which results in a high level of complexity. Remember that both of these estimators are based on the assumption of known channel correlation and noise. variance, σ_n^2 [27]. The situation differs when the channel correlation and the noise variance are not known. We define the effective SNR during pilot signaling from UE k in cell j to its serving BS j as $SNR_{jk}^{p} = \frac{P_{jk}^{k} \tau_p \beta_{jk}^{j}}{\sigma^2 UL}$ and To compare the estimation quality obtained with different estimation schemes in different scenarios, the normalized MSE (NMSE) $NMSE_{ji}^{i} = \frac{t_r(\mathbb{C}_{li}^{j})}{t_r(R_{li}^{j})}$ (3.22) a suitable metric, since it measures the relative estimation error per antenna. This is a value between 0 (perfect estimation) and 1 (achieved by using the mean value of the variable $E\{\hat{h}_{li}^{j}\}$, as the estimate).

3.5 The Least Square Algorithm

The LS channel estimation method is a straightforward estimation methodology with a low level of complexity. It is not necessary to have prior knowledge of channel statistics. It is widely used because to its simplicity. However, it has a significant mean square error. [28]. The LS estimation approach makes no assumptions about the channel and bases its estimations exclusively on the received matrices. As a result, this approach is resistant to a lack of knowledge about the CSI. [7].

The channel should ideally be totally known (i.e. there is no noise or channel imperfection). The fact that the channel state is perfectly known is referred to as perfect channel state information. In this scenario, the system equation is (in vector form), and we will use X to represent both the data and the pilots delivered from the user equipment to the BS for the purposes of this analysis:

$$Y = H * X \tag{3.23}$$

From this, we can calculate the channel estimation as:-

$$H = Y * X^{-1} \tag{3.24}$$

$$H = Y * X^{-1} \tag{3.25}$$

Here **N** is assumed to be 0. But, in reality because of Channel imperfectness $\mathbb{N} \neq 0$, so the equation for the system can be written as (in vector form):-

$$\hat{y} = \hat{H} * X \tag{3.26}$$

Only first order statistics are considered in the LS algorithm. This algorithm disregards second and higher order channel statistics. We may derive the LS channel estimation from this as follows:

Any estimator's job is to find the value of an unknown parameter H based on an observed variable.

$$E\{ h/\hat{y} \} \tag{3.27}$$

As mentioned in the above statement, the task of LS is to minimize $(Y - \hat{y})$, in the equation $(Y - \hat{y})$, Substitute for Y and $\hat{y}$ we get the following expression

$$\text{Minimize: } \|(Y - \hat{y})\|^2 \tag{3.27}$$

$$\| d \frac{(Y - \hat{y})}{d\hat{H}} \|^2 = 0 \tag{3.28}$$

$$d \| \frac{((H * X) - (\hat{H} * X))}{dH} \|^2 = 0 \tag{3.29}$$

Similarly, the above equation can be represented as:-

$$d \| \frac{((\hat{H} * X) - Y)}{d\hat{H}} \|^2 = 0 \tag{3.30}$$

$$d \| \frac{((\hat{H} * X) - Y)((\hat{H} * X) - Y}{d\hat{H}} \|^2 = 0 \tag{3.31}$$

$$d/dH \, ((\hat{H}X - Y)((\hat{H}X) - Y)^H = 0 \tag{3.32}$$

Using the above property, we manipulate Equation 3.31 to get the following equation,

$$\frac{d}{d\hat{H}}[(\hat{H}X)^H(\hat{H}X)-Y^H\hat{H}X-(\hat{H}X)^HY+Y^HY]=0 \tag{3.33}$$

By using the properties of matrix and the properties of derivatives, the above equation becomes:-

$$\frac{d}{d\hat{H}}[(X^H\hat{H}^H)\ (\hat{H}X)-Y^H\hat{H}X-(X^H\hat{H}^H)+Y^HY]=0 \tag{3.34}$$

After evaluating the above equation by solving the derivative, setting all second order and higher statistics to zero and lastly solving for $\hat{H}$ we get the following expression:-

$$2X^HXH-2X^HY=0 \tag{3.35}$$

lastly, solving $\hat{H}$ we get the following expression for $\hat{H}$ which is the equation for an LS algorithm.

$$\hat{H}=(X^H*X)^{-1}(X^H*Y) \tag{3.36}$$

Which in the same way can be implemented as follows (it is just the assumption assumed when we start our derivation of the equation. the difference comes from the assumption whether you assume

$$\hat{y}=H*\hat{x} \tag{3.37}$$

Now, substituting $\hat{x}^{-1}$ by the pilot vector and substituting the other vectors by their values, we can get the following expression for LS algorithm:-

$$\hat{h}_k=\frac{1}{\sqrt{\phi_k*\tau_p}}*y^{pilot} \tag{3.38}$$

3.6 Element wise Minimum Mean Square Error Algorithm (EW MMSE)

There are alternate estimate algorithms if BS j cannot handle the computational complexity of MMSE channel estimation schemes. An arbitrary linear estimator h_{li}^{j} can be written as $A_{li}^{j}y_{jli}^{p}$ for some deterministic matrix $A_{li}^{j}\in\mathbb{C}^{M_j\times M_j}$ that specifies the estimation scheme. The corresponding $E\{\|h_{li}^{j}-A_{li}^{j}y_{jli}^{p}\|^2\}$ can be computed

$$MSE(A_{lj}^{j})=tr(R_{lj}^{j})-2\sqrt{plj}\,\tau_p\Re(tr(R_{li}^{j}A_{li}^{j}))+\tau_p tr(A_{li}^{j}(\Psi_{li}^{j})^{-1}(A_{li}^{j})^H) \tag{3.39}$$

with Ψ_{li}^{j} given by equation 3.38 The MMSE estimator is obtained for $A_{li}^{j}=\sqrt{pli}R_{li}^{j}\Psi_{li}^{j}$ However, we have the option of selecting an alternative A_{li}^{j} This makes calculating the estimate simpler. Diagonal matrices are especially beneficial for reducing computational complexity because each element is independent of y^{p}_{jli} can then be multiplied with only one scalar instead of M_j non-zero scalars from A^{j}_{li} For any deterministic A^{j}_{li}, the estimate $A^{j}_{li} y^{p}_{jli}$ and estimation error $\tilde{h}^{j}_{li} = h^{j}_{li} - A^{j}_{li} y^{p}_{jli}$ are Gaussian distributed, but they are frequently correlated random variables—a significant departure from the MMSE estimation. We have, in particular, we have that $\mathrm{E}\{\hat{h}^{j}_{li}(\tilde{h}^{j}_{li})\} = \sqrt{pli}\,\tau_p A^{j}_{li}(\Psi^{j}_{li})^{-1}(A^{j}_{li})^{H}$ (3.40)

Based on the discussion in equation 3.33 $[h^{j}_{li}]_m$ separately and thereby ignore the correlation between the elements. More precisely, we can look at the processed received signal in equation 3.23. Based on the observation $[y^{p}_{jli}]_m$ BS *j* can compute the MMSE estimate of the *m*th element $[h^{j}_{li}]_m$ 0f the channel from UE *i* in cell *l* as

$$[\tilde{h}^{j}_{ji}] = \frac{\sqrt{pli}[R^{j}_{li}]_{mm}}{\sum_{(l^{l},i^{l})\in p_{li}} p_{l^{l}i^{l}}\tau_p[R^{j}_{l^{l}i^{l}}]_{mm} + \sigma^2_{UL}}[y^{p}_{jli}]_m \tag{3.41}$$

The estimation error variance of this element is

$$[R^{j}_{li}]_{mm} - \frac{\sqrt{pli}\tau_p([R^{j}_{li}]_{mm})^2}{\sum_{(l^{l},i^{l})\in p_{li}} p_{l^{l}i^{l}}\tau_p[R^{j}_{l^{l}i^{l}}]_{mm} + \sigma^2_{UL}} \tag{3.42}$$

The EW-MMSE estimator corresponds to letting A^{j}_{li} be diagonal with

$$A^{j}_{li} = \frac{\sqrt{pli}\tau_p([R^{j}_{li}]_{mm})^2}{\sum_{(l^{l},i^{l})\in p_{li}} p_{l^{l}i^{l}}\tau_p[R^{j}_{l^{l}i^{l}}]_{mm} + \sigma^2_{UL}} \tag{3.43}$$

When pre calculating the fractional expression in (3.31) (at the slow time scale of large-scale fading changes) and multiplying it with the processed received pilot signal once every coherence block, the computing cost per UE is proportional to Mj. Except in the uncommon case where all of the spatial correlation matrices are diagonal and each channel element can be estimated separately without performance loss, this is much less difficult than the original MMSE estimator. It is vital to highlight that the significant reduction in complexity is due to the fact that A^{j}_{li} is diagonal. The MSE achieved by the EW-MMSE estimator is obtained by summing up the estimation error variances from equation 3.43 which can be expressed as

$$MSE = tr(R_{li}^{j}) - \sum_{m=1}^{M} \frac{pli\tau_p([R_{li}^{j}]_{mm})^2}{\sum_{(l^l,i^l)\in p_{li}} p_{l^l i^l}\tau_p[R_{l^l i^l}^{j}]_{mm} + \sigma_{UL}^2} \tag{3.44}$$

Although each element is estimated using the MMSE principle, when utilizing the EW-MMSE estimator, the vector with estimates and the vector with estimation errors are correlated.

CHAPTER FOUR

4 RESULT AND DISCUSSION

Simulations are a fantastic tool to compare different algorithms. We will utilize the MATLAB(2020) simulation program to compare alternative channel estimation methods. According to Wikipedia, MATLAB (short for MATrix LABoratory) is a specialized computer program designed to conduct engineering and scientific computations. It began as a program designed to conduct matrix mathematics, but it has evolved into a versatile computing system capable of handling virtually any technological challenge.

4.1 Simulation Results

Before we begin the simulations, we will set up our environment. For our system, we will assume that humans walk at their typical speed, with no regard for traffic speed. It is assumed that the distribution of users within the cell is random. The BS is positioned in the cell's center. Because we are designing a 5G infrastructure, it is logical to presume an urban setting because high data rates are typically necessary for urban duelers. Cells are classified according to their size. We will presume that our cell is a UMa (Urban Macro-cell) because [29]states that UMa have a coverage of less than 2000m and our system has a coverage of 250m. As a result, it is fair to select UMa cell for our system.

Now, using the above-mentioned imagined environment, we will compute the length of a coherence block for our system. As indicated in previous chapters, our system is made up of numerous coherence blocks. We will assume that all coherence blocks are the same and will evaluate the system using only one coherence block.

Length of the Coherence Block $= T_c * B_c$ (4.1)

Then, we will chose our operating frequency for our system. According to the recommendation of the [30], we will choose 50 GHz for our operation. Massive MIMO operates at a frequency starting from 5GHz.

Choosing higher frequencies is recommended by different papers including the paper [31] and choosing higher frequencies is advantageous for a couple of reasons. Some of the advantageous of choosing higher frequencies are:-

- The higher the frequency, the smaller the antenna array size.
- The higher the frequency, the higher the data rate it can serve.

One of the significant disadvantageous of using higher frequency for telecommunication is it can't travel long distance and this is not a problem in massive MIMO because cell size in massive MIMO is designed to be small. For example, our particular system has a size of 250m.Now, from the frequency chosen, we can then calculate the T_C and B_C. From this frequency value we first calculate the λ. Using the equation $C = \lambda * f$, we get λ to be about 6.30mm. From this λ value, we can now calculate the T_C using the equation

$$T_c = \frac{\lambda}{8 * v} \tag{4.2}$$

Where V is the UE's speed, Then the regular walking speed of humans is employed as the speed of the UE in this thesis, and this speed is usually estimated to be around 1.4 m/s (averaged), as mentioned in the paper [31]. We can now compute the value of T c using Equation 4.2. After calculating, the value of should be around 0.60 ms.

According to the paper [32], the B_c can be calculated as;

$$B_c = \frac{1}{2\Pi * D_S} \tag{4.3}$$

The delay spread is represented by the Ds. Using the parameters mentioned above (UMa cell and 50 GHz operating frequency), we will select Ds for our system. According to the study[33] , we will set the Ds for our system to be 240 ns. We chose this value because the study [32] recommends the following delay spread values for the various systems indicated in Table 4.1. By plugging this number into Equation 4.3, we get the Bc value of 665 KHz. And this is a realistic outcome given that the value of the Bc can range from 1000 KHz to several MHz.

By plugging the values of Bc and Tc into Equation 4.1, we can calculate the length of the coherence block to be around 400 samples. So, we'll investigate communication over a 20MHz channel with a total receiver sensitivity of -94dB. Each coherence block is made up of τ_c = 400 samples, and the same τ_p = 10 pilots are assigned at random in the cell.

4.1.1 Steps Followed to Reach to Results

In this section, we will go over the steps that were taken to generate the simulation results. We'll start by making noise, and then we'll make the pilot signal, Ypilot. The values of the LS, EW MMSE and the MMSE channel estimator are then generated. We will use this estimation value for detection once we have determined the channel's estimation. The system's SINR value is then calculated based on the estimation value and the detection technique. Finally, the SE, Number of complex factor and other metrics are used to compare the LS, EW MMSE and MMSE channel estimator.

4.2 Uplink Spectral Efficiency for Rayleigh and Rician fading for (M=50, 100)

The SE expressions established in the previous parts are validated and assessed in this simulation section by modeling a Massive MIMO cellular network. We have a single cell set up that covers a square of 250m. There are K = 10 UEs per cell, which are deployed independently and randomly inside each cell at distances more than 35 m from the BS. Each UE is assigned to the BS that gives the highest channel gain when all UE and BS combinations in the system are considered. When computing the large-scale fading and nominal angle between the UE and the BS, the position of each UE is employed.

Here are all the Simulation parameter used in this thesis

Table 4. 1: simulation parameters

parameter	**Value**
Network layout	*Square pattern (wrap-around)*
Number of cells	*L=16*
Cell area	*0.25*0.25km*
Number of antennas per BS	*M*
Number of UEs per cell	*K*
Channel gain at 1 km	γ = *-148.1db*
Pathloss exponent	α=*3.76*
Shadow fading (standard deviation)	$\sigma_{sf} = 10$
Bandwidth	*20MHZ*
Receiver noise power	*-94 db*
UL transmit power	*20 db*
DL transmit power	*20 db*
Samples per coherence block	*Bc=200*
Pilot reuse factor	*f=1, 2 ,4*
Number of UL pilot sequences	*Tp=fk*

Here in this section, we will see the effect of the increase in the number of antennas in the LS, MMSE and EW-MMSE estimators (i.e. when the number of antennas increases, which one of the estimators is affected more ?) with respect to Rayleigh and Rican fading.

When using MR combining based on either the MMSE, LS and EW-MMSE estimators. As a reference, we also provide curves for Rayleigh fading with the same covariance matrices, representing the case when all the LoS components are blocked but the small scale fading remains (i.e., the average channel gain is smaller, as it would be the case in practice).

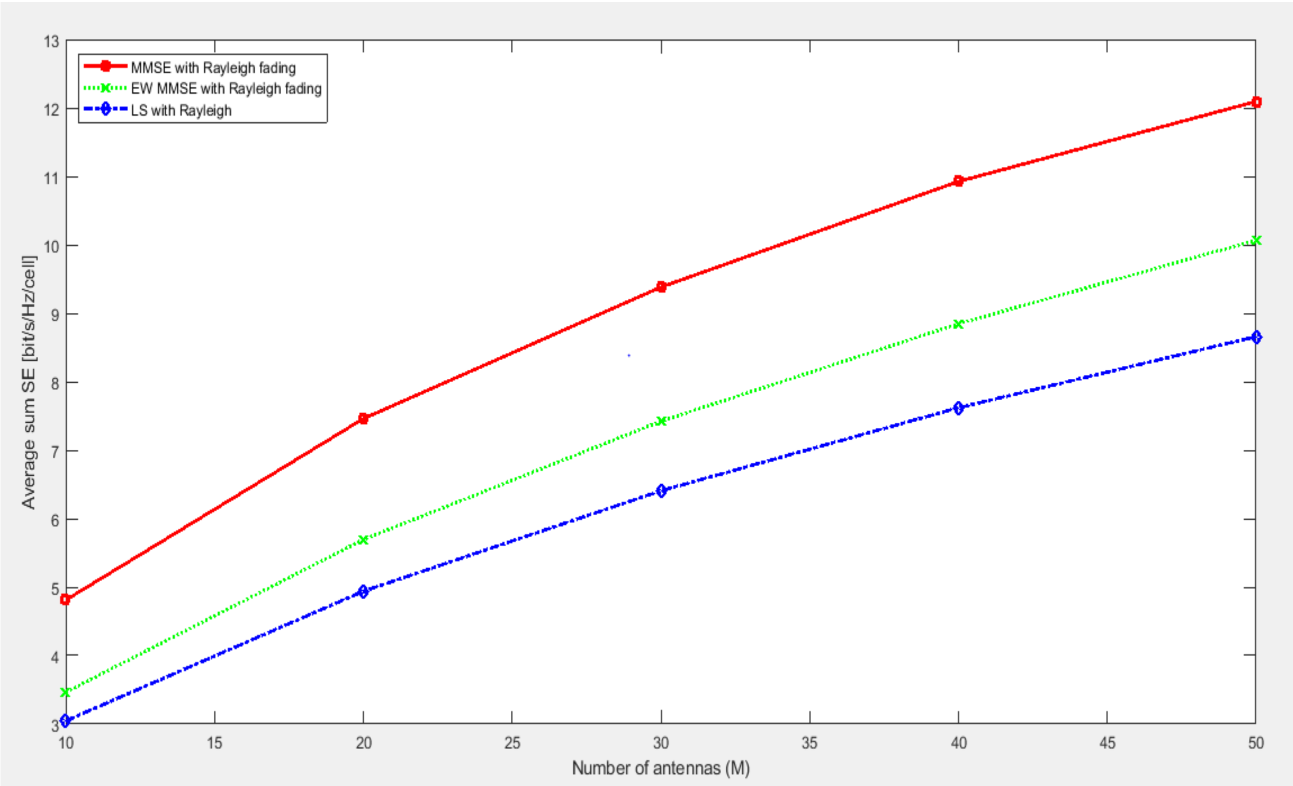

Figure 4. 1 : Uplink spectral efficiency for 50 number of antennas (M) with Rayleigh fading

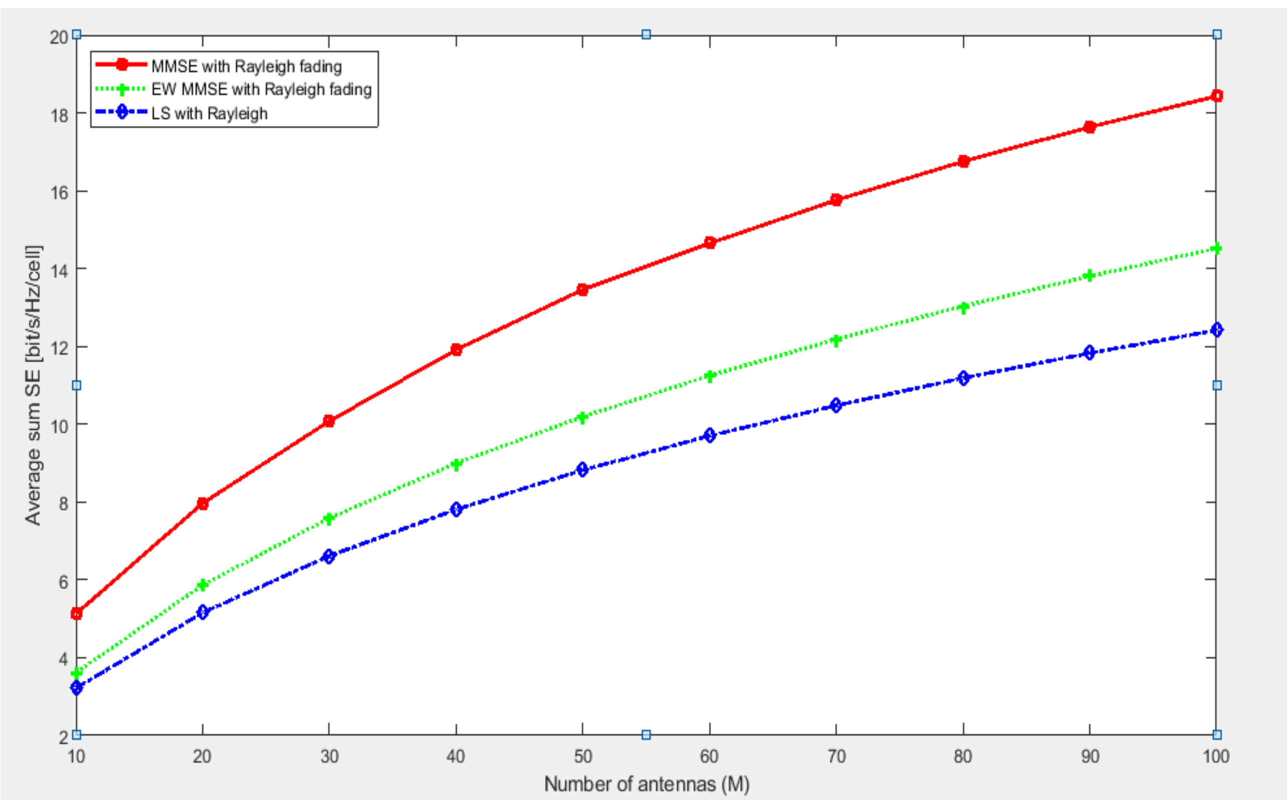

Figure 4. 2 : Uplink spectral efficiency for 50 number of antennas (M) with Rayleigh fading

Figure 4.1 shows the sum UL SE averaged over different UE locations and shadow fading realizations, when using MR detection and Rayleigh fading based on either the MMSE, EW MMSE and LS estimators. This result for uplink SE of the EW MMSE estimator at M = 50 is about 11.59 bits/s/Hz/cell and the SE of the MMSE estimator at M = 50 is about 14.17 bits/s/Hz/cell and the LS estimator is 9.863. In this case the MMSE performs better than the other two estimator.

Figure 4.2 shows the sum UL SE averaged over different UE locations and shadow fading realizations, when using MR detection and Rayleigh fading based on either the MMSE, EW MMSE and LS estimators. This result is for our specifically defined system. The uplink SE of the EW MMSE estimator at M = 100 is about 12.09 bits/s/Hz/cell and the SE of the MMSE estimator at M = 100 is about 16.65 bits/s/Hz/cell and the LS estimator is 10.63 for M=100. In this case the MMSE performs better than the other two estimator.

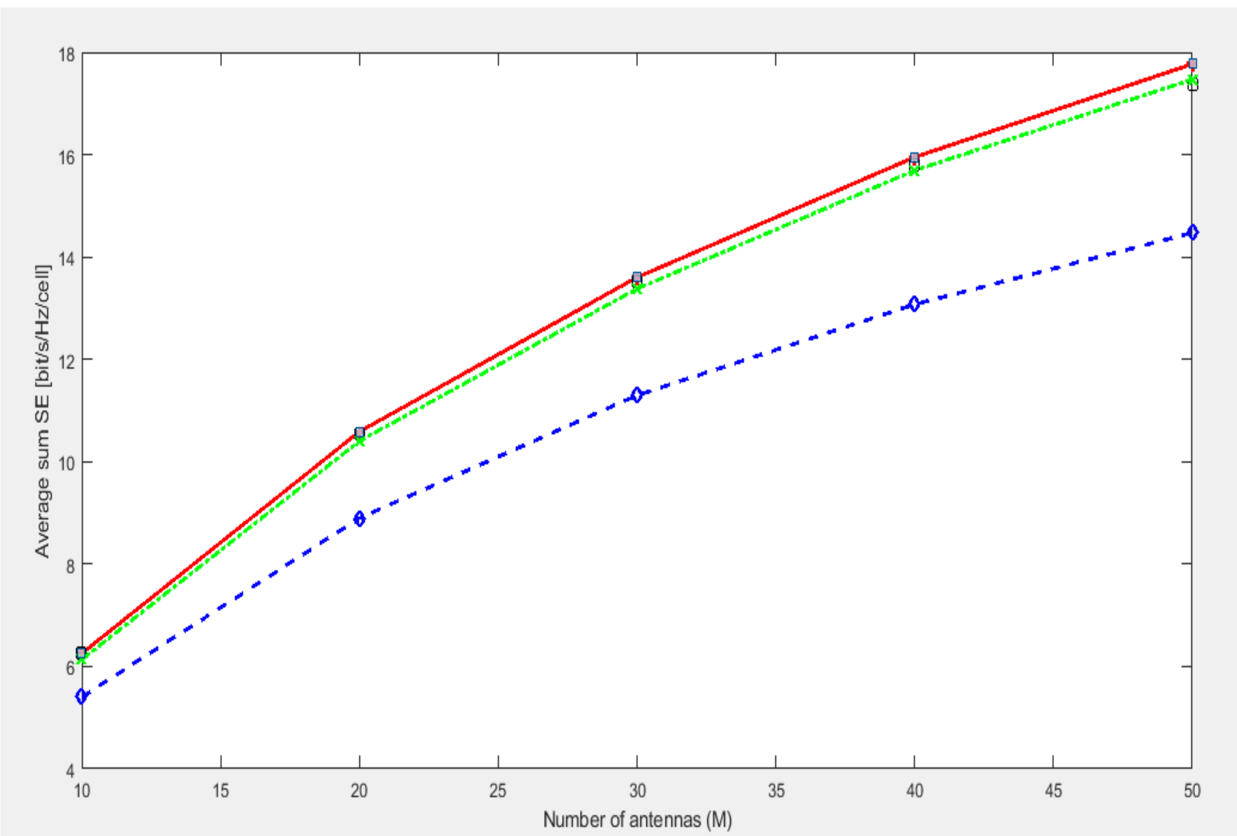

Figure 4. 3 : Uplink spectral efficiency for 50 number of antennas (M) with Rician fading

Figure 4.3 and figure 4.4 shows the sum UL SE averaged over different UE locations and shadow fading realizations, when using MR detection and Rican fading based on either the MMSE, EW MMSE or LS estimators. This result for uplink SE of the EW MMSE estimator at M = 50 is about 16.85 bits/s/Hz/cell and the SE of the MMSE estimator at M = 50 is about 17.87 bits/s/Hz/cell and the LS estimator is 14.3 bits/s/Hz/cell. Figure 4. 4: uplink spectral efficiency for 50 Number of Antennas (M) with Rican fading The uplink SE of the EW MMSE estimator at M = 100 is about 20.64 bits/s/Hz/cell and the SE of the MMSE estimator at M = 100 is about 20.79 bits/s/Hz/cell and the LS estimator is 15.7 for M=100.

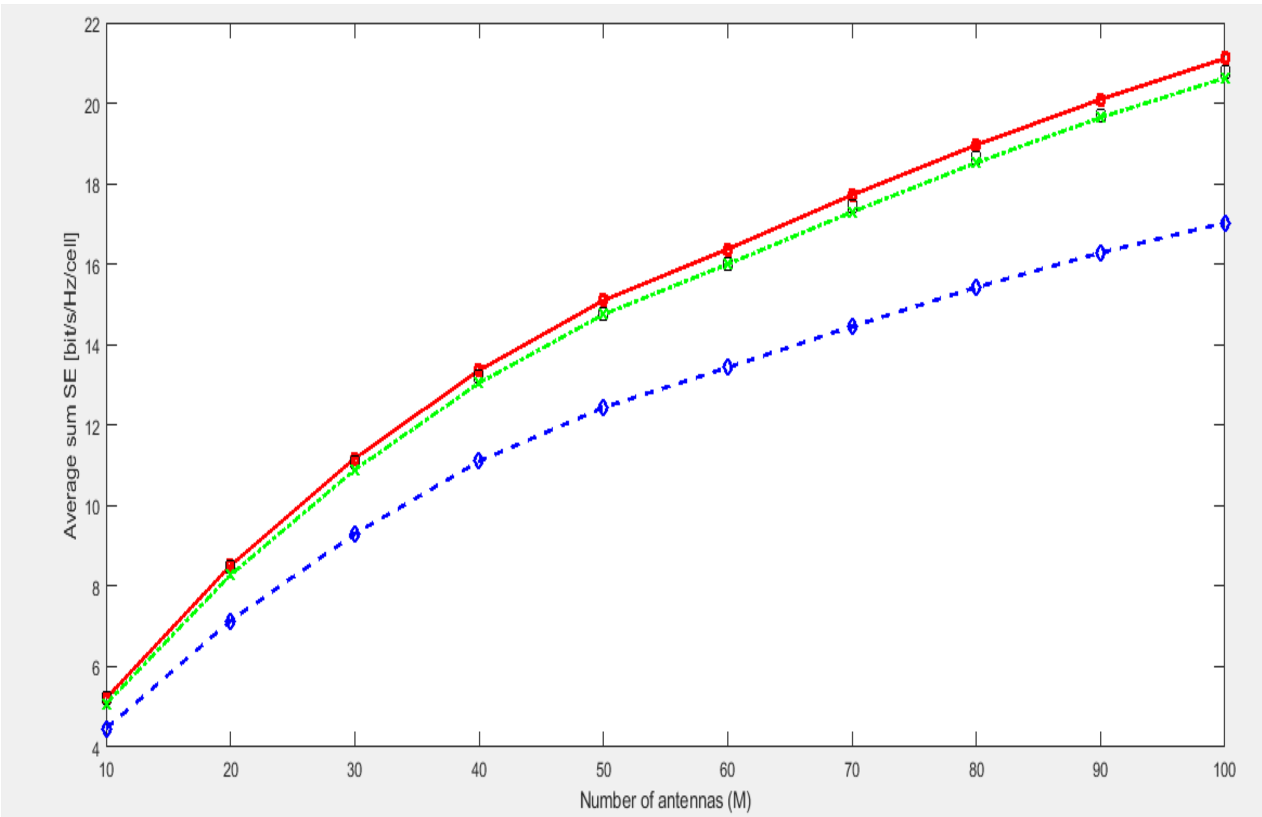

Figure 4. 4 : Uplink spectral efficiency for 100 number of antennas (M) with Rician fading

Table 4. 2 : Uplink Spectral Efficency for M=50,100 using Rican and Rayleigh fading

Uplink spectral efficiency(bits/s/Hz/cell)	**M =50 With rician fading**	**M =100 With rician fading**	**M =50 With rayleigh fading**	**M =100 With rayleigh fading**
MMSE	17.87 bits/s/Hz/cell	20.64 bits/s/Hz/cell	14.17 bits/s/Hz/cell	17.65 bits/s/Hz/cell
EW MMSE	16.85 bits/s/Hz/cell	20.79 bits/s/Hz/cell	11.59 bits/s/Hz/cell	12.89 bits/s/Hz/cell
LS	14.3 bits/s/Hz/cell	15.7 bits/s/Hz/cell	9.863 bits/s/Hz/cell	10.63 bits/s/Hz/cell

Table 1.2 shows the overall spectral efficiency of the system for both Rayleigh and Rician fading at 50 and 100 number of antennas. in case of Rayleigh fading In this case the MMSE performs better than the other two estimator as expected. When the number of antennas (M) increase from 50 to 100 the overall system capacity in increasing and all estimator shows in increase of spectral efficiency. The result we have is an expected result as stated in the states that the loss in SE incurred by using the LS estimator under Rican fading can be quite large depending on the dominance of LoS paths. The performance difference could be even large because the estimator improves the one link only but when the links between the BS and UE became many the performance is multiplied by the number of links.

4.3 Down Link Spectral Efficiency for Rayleigh and Rician fading For (M=100)

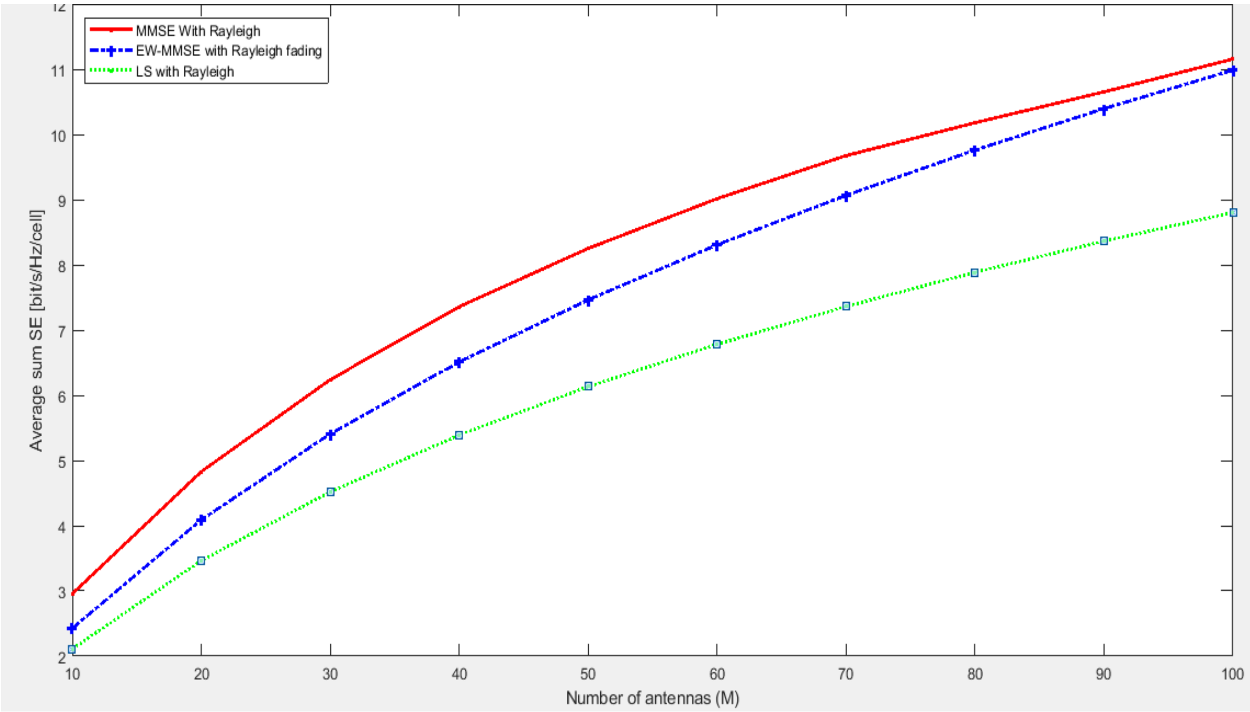

Figure 4. 6 : Downlink link spectral efficiency for 100 number of antennas (M) Rayleigh fading

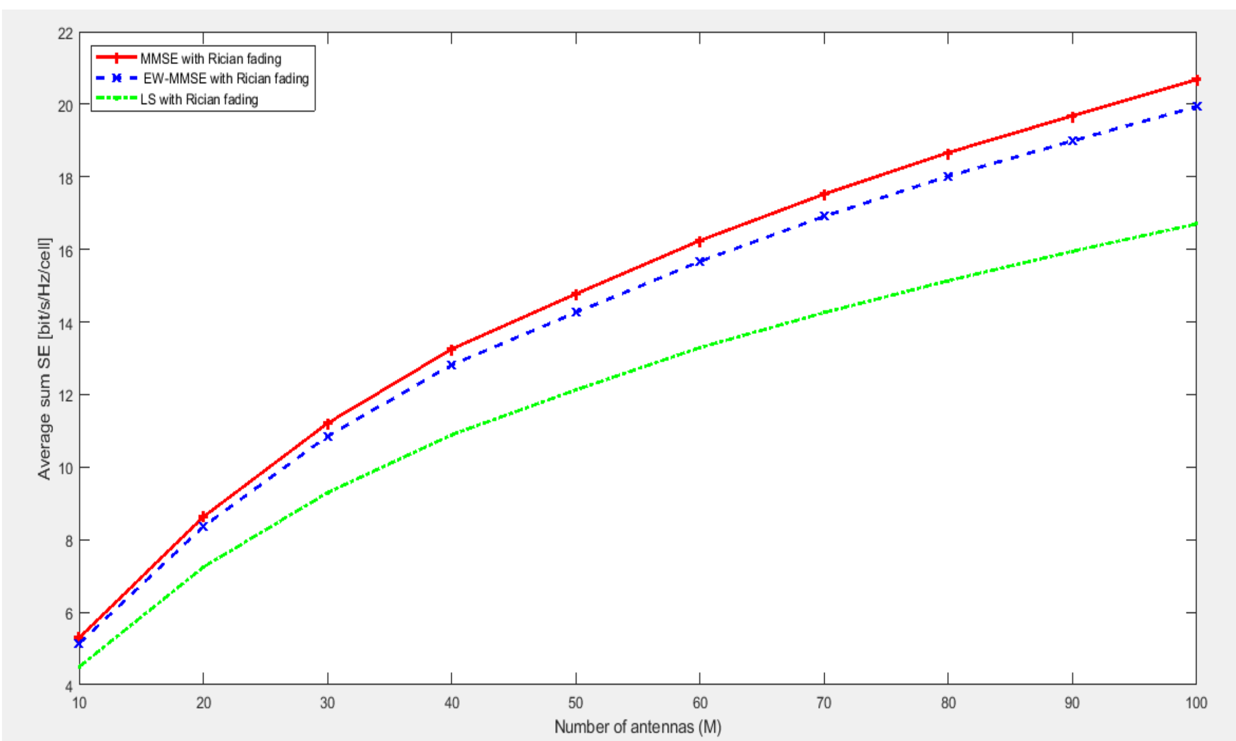

Figure 4. 5 : Downlink link spectral efficiency for 100 Number of Antennas (M) with Rican fading

Figure 4.5 and figure 4.6 shows the average sum DL SE over different UE locations and shadow fading realizations, with MR precoding based on the MMSE, LS and EW-MMSE estimators. The same behaviors are observed as in the UL. In this case, EW-MMSE and MMSE coincide since the spatial covariance matrices are diagonal. These estimators are better than LS when having Rician fading since the meanshows the average sum DL SE over different UE locations and shadow fading realizations, with MR precoding based on the MMSE, LS or EW-MMSE estimators. The same behaviors are observed as in the UL. Fig. 4.3 and 4.4 shows the average UL SE with uncorrelated fading as a function the number of antennas. In this case, EW-MMSE and MMSE coincide since the spatial covariance matrices are diagonal. These estimators are better than LS when having Rician fading.

Table 4. 3 : Down link Spectral Efficiency for M=50,100 using Rican and Rayleigh fading

Down link spectral efficiency(bits/s/Hz/cell)	**M =100 With rayleigh fading**	**M =100 With Rician fading**
MMSE	11.6 bits/s/Hz/cell	21.38 bits/s/Hz/cell
EW MMSE	10/99 bits/s/Hz/cell	19.72 bits/s/Hz/cell
LS	8.83 bits/s/Hz/cell	15.91 bits/s/Hz/cell

Table 4. 3 shows the Down link SE of channel estimator for Rician and Rayleigh fading for 100 numbers of antennas. The DL spectral efficiency of EW MMSE is about 10.99 bits/s/Hz/cell, the SE of the MMSE estimator is about 11.6 bits/s/Hz/cell and the LS estimator is 8.83 . The average sum DL SE having different UE locations and shadow fading realizations is shown in Fig. 4.5, with MR precoding based and Rayleigh fading on the MMSE, LS, and EW MMSE estimators. From our figure 4.5 we can understand that, the SE for the downlink system is somehow quite similar to that of the uplink spectral efficiency. Like in the uplink, the MMSE estimator have a

significant spectral efficiency than that of LS and EW MMSE estimator. Same behaviors as in the UL are observed. as we can see from the table that the MMSE and EW MMSE estimators have SE of 21.38 bits/s/Hz/cell and 19.72 bits/s/Hz/cell while the LS estimator is 15.41 bits/s/Hz/cell. This is because in case of Rican fading, the performance of MMSE and EW-MMSE is quite close, with EW-MMSE outperforming LS since it uses knowledge of the channel mean values. Here it's quite the same as of the uplink.

4.4 Estimation Quality of MMSE, EW-MMSE, and LS Estimators

Figure 4.7 compares the estimate quality of the MMSE, EW-MMSE, and LS estimators in terms of NMSE. Consider the following scenario: BS j estimates the channel of its UE k, while another UE in another cell sends the same pilot sequence. The desired UE's effective SNR is modified from 10 dB to 20 dB, while the interfering signal is always considered to be 10 dB weaker.

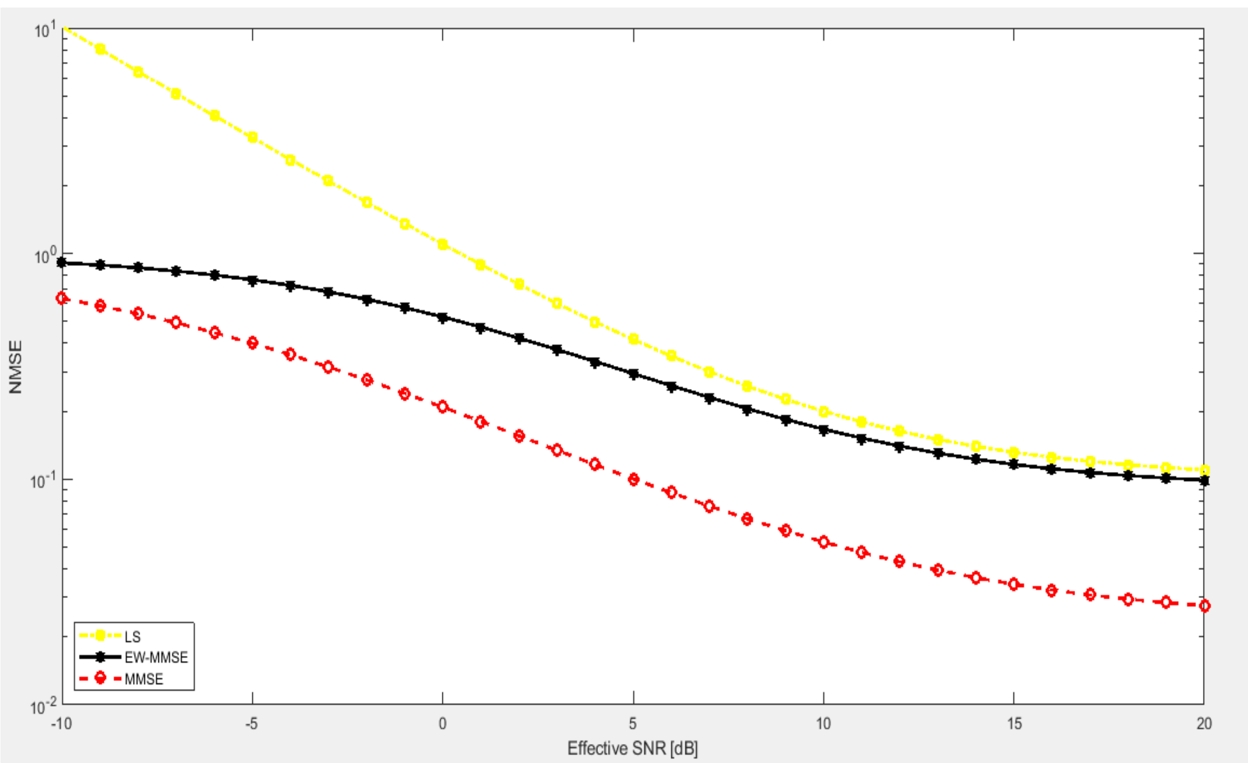

Figure 4. 7 : different estimators, the NMSE in the estimation of a spatially coupled channel based on the local scattering model with Gaussian angular distribution

The local scattering model is used with a Gaussian angular distribution and ASD'= 10, and the results are averaged over several nominal angles ranging from 0 to 360 degrees. Figure 4.7 illustrates that the NMSEs provided by the three estimators are quite different. Because it completely uses spatial channel correlation, the MMSE estimator is systematically the best estimate. The EW-MMSE estimator performs rather well (equal to MMSE estimation of an uncorrelated channel), however there is a significant difference from the MMSE estimator—even at high SNR where the error floor (induced by pilot contamination) has a greater value. When the SNR is low and the NMSE is more than one, the LS estimator performs very poorly. At low SNR where the NMSE is above 1, while the trivial all-zero estimate $\hat{h}_{jk}^{j} = 0_{M_j}$ gives an NMSE of 1. At higher SNRs, the LS estimator is comparable to the EW-MMSE estimator, but their respective error floors are different (if there is pilot contamination). The LS estimator can provide decent estimates of the channel direction, $\hat{h}_{jk}^{j} / \|\hat{h}_{jk}^{j}\|$, while the lack of statistical information makes it harder to get the right scaling of the channel norm $\|\hat{h}_{jk}^{j}\|$.

4.5 Number of Complex Multiplications per coherence for (50 ≤M ≤150)

The Number of complex multiplications per coherence block with 10 UEs, when using differenent channel estimation schemes for by variying Number of Antennas 50 ≤M 150.Figure 4.8-4.10

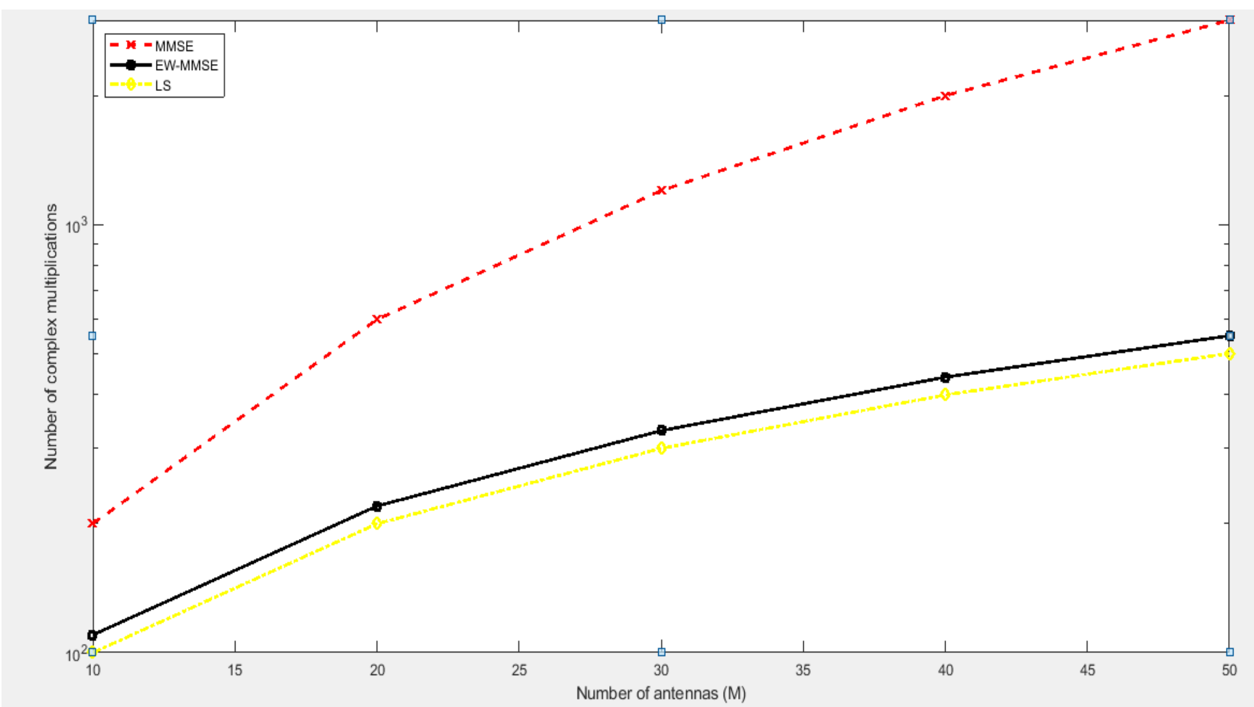

Figure 4. 8 :Number of complex multiplications per coherence block with 10 UEs, when using different channel estimation schemes, when M=50

shows the effect of increasing number of antennas in the system which leads increasing the Number of complex Multiplications per coherence block.

Under a scenario with K = 10 UEs in each cell, shows the number of complex multiplications per coherence block as a function of M. We ignored difficulty in pre computation of matrices that simply depend on channel statistics because they are often constant over a large number of coherence blocks. MMSE has the highest complexity, followed by EW-MMSE, which reduces complexity by 45–90% because the correlation between antennas is not included in the algorithm channel estimation. The complexity reduction of using LS instead of EW-MMSE is marginal: for M = 100 we only save an additional 1% by using LS.

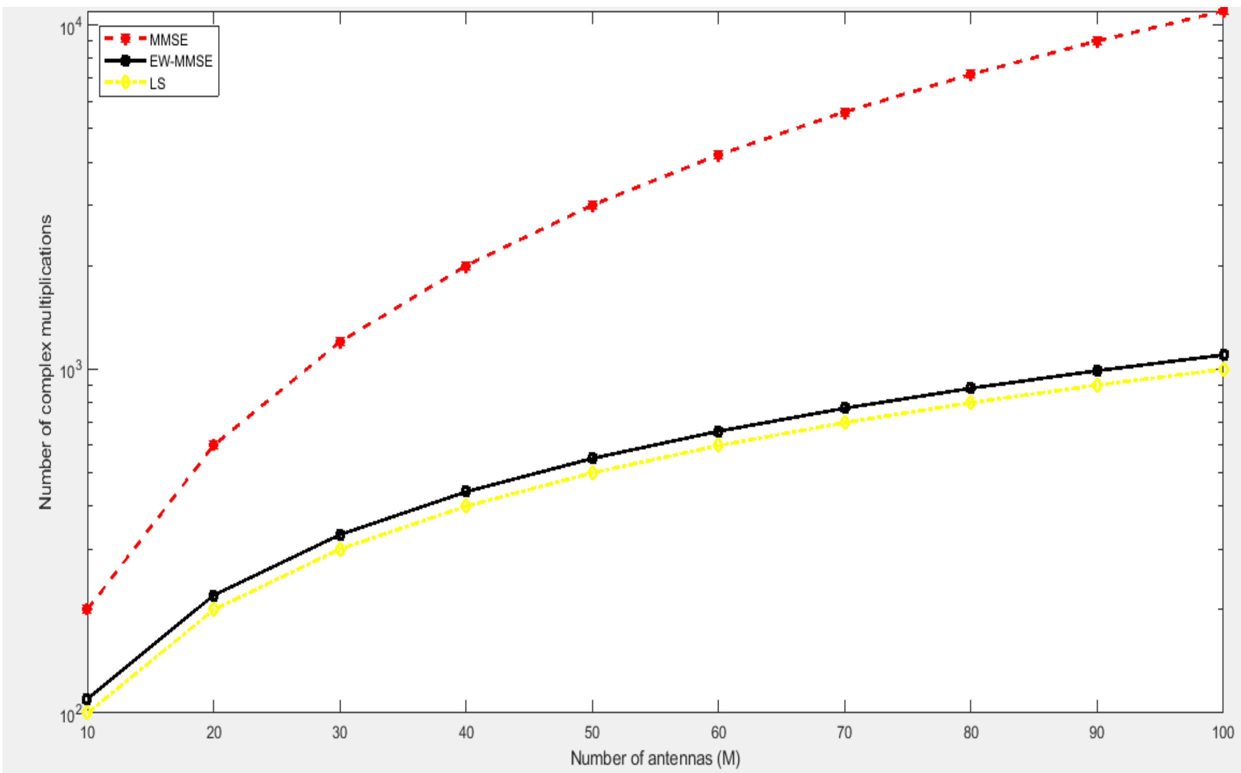

Figure 4. 9 :Number of complex multiplications per coherence block with 10 UEs, when using different channel estimation schemes, when M= 100

From the above figures we can clearly see that when the Number of antennas increases the number of complex multiplication of MMSE estimators increase around 5% of the other estimators. The

EW MMSE and LS estimator doesn’t show a significant increase and its around 1% increase in the number of complex multiplication.

The difference between the EW MMSE and LS is quite marginal and it’s around 1%. From this we can say that the MMSE estimator having the highest complexity followed by the EW MMSE and LS estimators. Also the complexity of the MMSE estimator increase while the Number of antennas in the system increases.

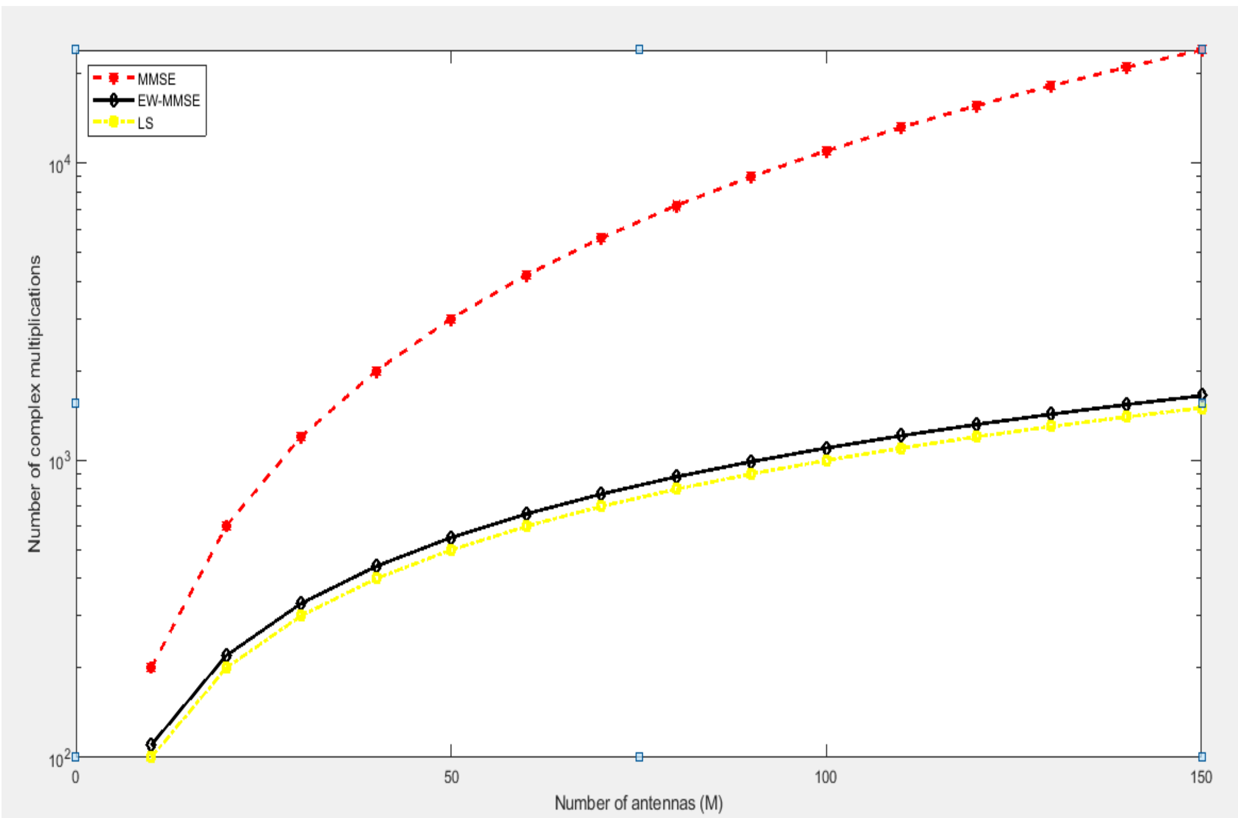

Figure 4. 10 :Number of complex multiplications per coherence block with 10 UEs, when using different channel estimation schemes, when M=150

4.6 Number of Complex Multiplications per coherence when (100 ≤k ≤200)

Another factor that increase complex multiplication in a given coherence block for a channel estimator is the increasing of the number users in the system. From figure 4.11-4.13 shows the effect of increasing the number of users per coherence block100≤k ≤200. The first figure shows the number of users is 100. And MMSE estimator is have to make 20000 complex multiplication. EW MMSE and LS are only 10000 complex multiplication per coherence block. The MMSE estimator is twice more complex than EW MMSE and LS estimators.

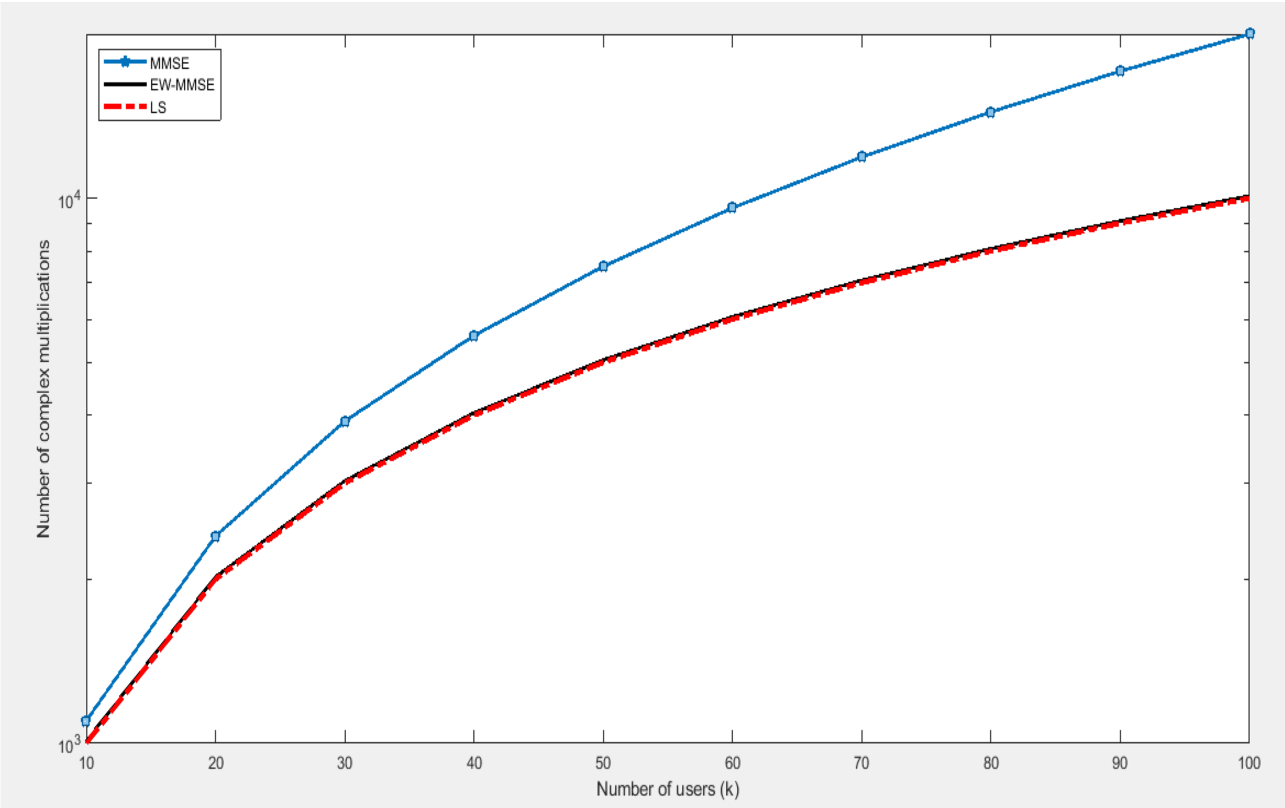

Figure 4.11: Number of complex multiplications per coherence block with, when number of users(K)= 100 when using different channel estimation schemes .

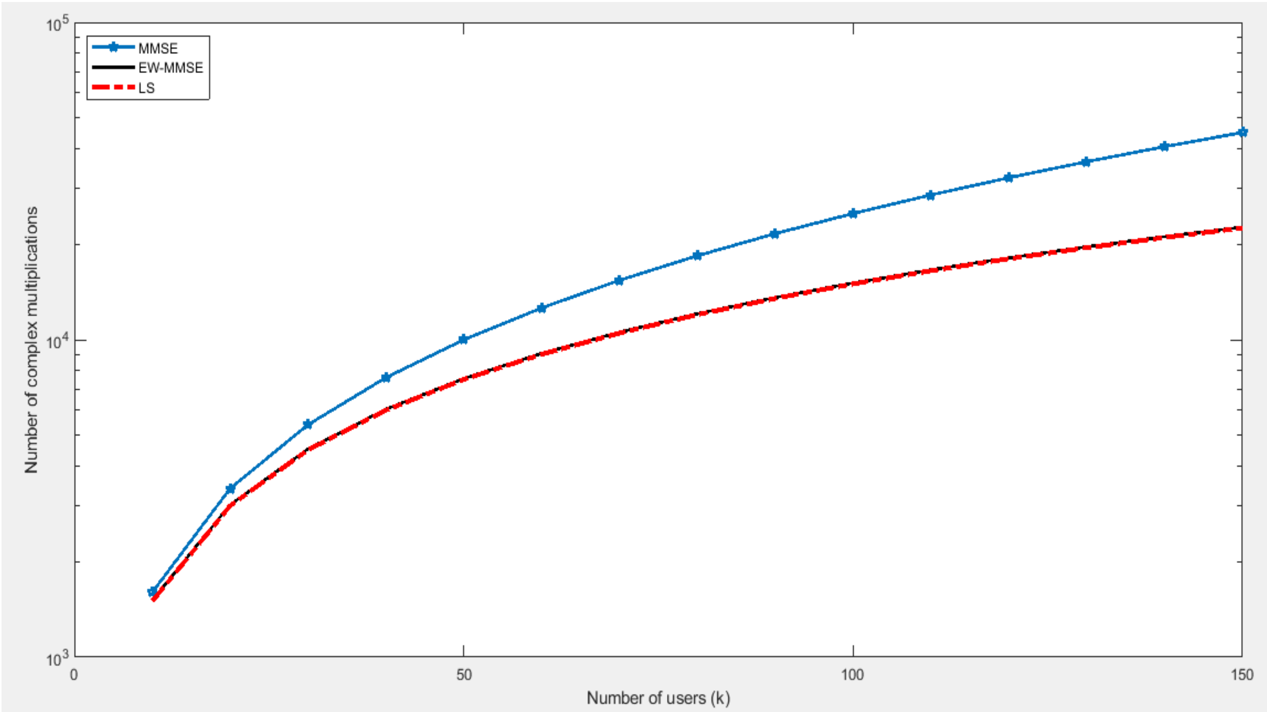

Figure 4. 12: Number of complex multiplications per coherence block with, when number of users(K)= 150 when using different channel estimation schemes.

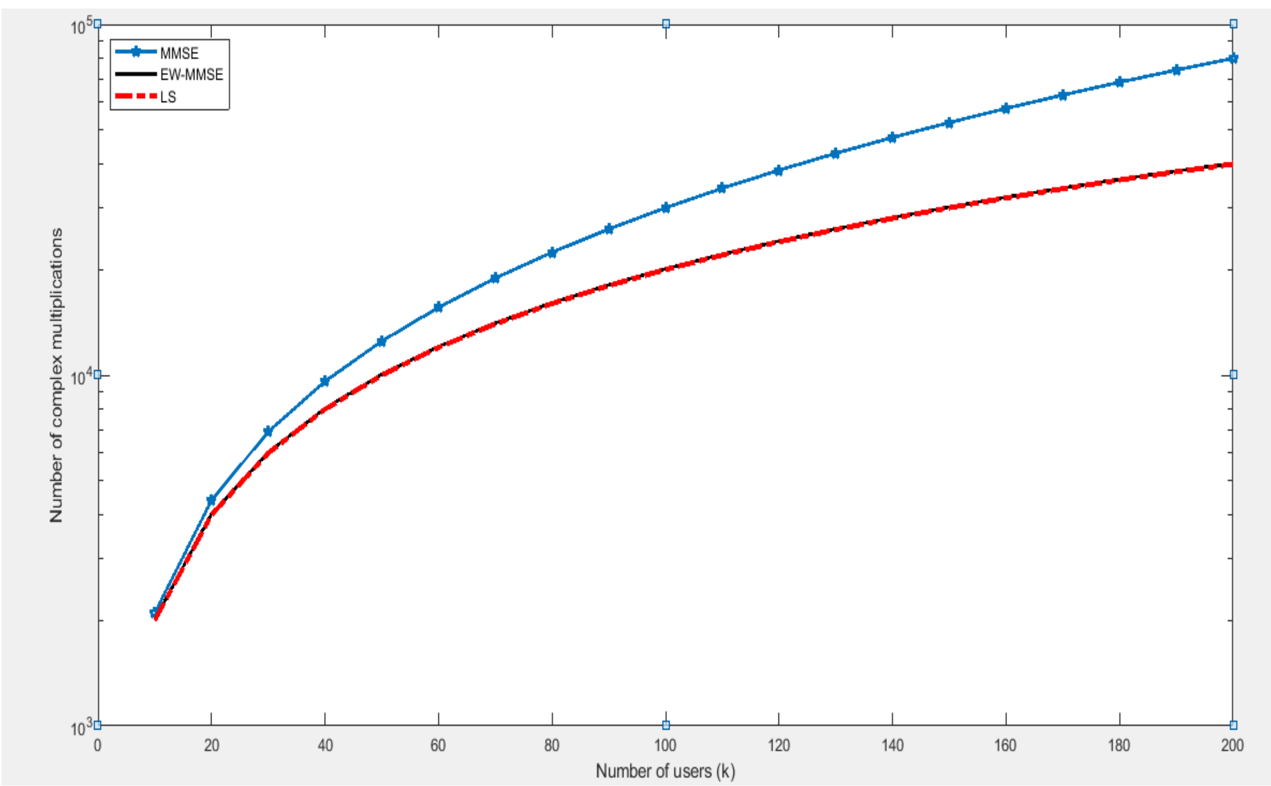

Figure 4. 13: Number of complex multiplications per coherence block with , when number of users(K)= 200 when using different channel estimation schemes.

Table 4. 4: Number of Complex Multiplications per coherence when (100 ≤k ≤200)

Number of Complex Multiplication per coherence block	**Number of user K**		
	K=100	**K=150**	**K=200**
MMSE	20000	450000	80000
EW MMSE	10000	22500	40000
LS	10000	22500	40000

Figure 4.12 shows for 150 users the number of complex multiplication is 45000 for that of MMSE estimator. And EW MMSE and LS estimator have almost the same complex multiplication which is 22500. Figure 4.13 shows for 200 users the number of complex multiplication is 80000 for that of MMSE estimator. And EW MMSE and LS estimator have almost the same complex multiplication which is 40000. From table 4.4 we can conclude that increasing the Number of users can in increase the number of complex multiplication in a given system. From this the MMSE estimator is twice complex than the EW MMSE and LS estimator. EW MMSE and LS estimator have the same complexity. Even though the complexity of Both of these estimator increase with respect to number of users, they are twice less complex than that of MMSE estimator.

CHAPTER FIVE

5 CONCLUSIONS AND FUTURE WORKS

5.1 CONCLUSION

Channel estimate at the base station is critical for realizing the full potential of Massive MIMO. This is often performed through the use of UL pilot transmission. This thesis investigated the UL and DL performance of a Multi massive MIMO system in terms of SE, complexity, and SNR with different fading reliability channels. The estimators LS, EW MMSE, and MMSE are used. When applying the MR combining technique, we generated the terms EW MMSE, MMSE, and LS estimation. Then, using these mathematical formulations, we generate simulations to compare these estimations. Figure 4.1-4.6 shows the spectral efficiency of those estimators under different fading realization.

The MMSE estimator exploits the statistical characteristics to obtain good estimates. Spatial correlation makes it easier to estimate channels to large antenna arrays. The gains are robust to imperfect knowledge of the statistics in which result produce a higher spectral efficiency for both the uplink and downlink transmission. While EM MMSE produce a considerable amount of Spectral efficiency. But LS estimator produce a low SE compare to the others. This because of states that the loss in SE incurred by using the LS estimator under Rican fading can be quite large depending on the dominance of LoS paths. The performance difference could be even large because the estimator improves the one link only but when the links between the BS and UE became many the performance is multiplied by the number of links.

The MMSE estimator's computing complexity climbs quadratically with the number of antennas. By ignoring the spatial connection between antennas, the alternative EW-MMSE estimator can considerably reduce complexity. The LS estimator can be used instead if the channel statistics are unknown.

The EW-MMSE estimator performs rather well (equal to MMSE estimation of an uncorrelated channel), however there is a significant difference from the MMSE estimator—even at high SNR where the error floor (induced by pilot contamination) has a greater value. When the SNR is low and the NMSE is more than one, the LS estimator performs very poor.

5.2 FUTURE WORKS

There are numerous study avenues that could be pursued in relation to this topic. One relevant research topic is to compare the per cell performance of a single cell system versus a Multicell system. Specifically, the goal is to observe the effect of increasing the number of cells on the performance of each cell.

Another possible future research related to this paper is to see the effect of increasing the number of users on the difference between the LS, EW MMSE and MMSE estimation techniques in the presence of pilot contamination. The same research could be done on the effect of increase in the number of antennas on the difference between the LS, EW MMSEand MMSE estimation techniques in the presence of pilot contamination. All of the work in this study is based on large MIMO systems operating in TDD mode. As a result of all of the experiments and simulations performed on this thesis for FDD huge MIMO systems, we can conclude that another new topic of research exists. Another area of research related to this topic is to estimate the performance these estimators using machine learning and Artificial intelligence.

REFERENCES

[1] W. Xiang, K. Zheng, and X. S. Shen, *5G mobile communications*. Springer, 2016.

[2] I. D. D. P. Alli, "Channel estimation in mobile wireless systems," 2012.

[3] X. Gao, *Doctoral thesis: Massive MIMO in real propagation environments*. Lund University, 2016.

[4] K. L. Lueth, "IoT market analysis: Sizing the opportunity," *IoT Anal. Report, March*, 2015.

[5] E. Björnson, J. Hoydis, and L. Sanguinetti, "Massive MIMO networks: Spectral, energy, and hardware efficiency," *Found. Trends Signal Process.*, vol. 11, no. 3–4, pp. 154–655, 2017, doi: 10.1561/2000000093.

[6] D. Neumann, M. Joham, and W. Utschick, "Channel estimation in massive MIMO systems," *arXiv Prepr. arXiv1503.08691*, 2015.

[7] O. Ozdogan, E. Bjornson, and E. G. Larsson, "Massive MIMO with Spatially Correlated Rician Fading Channels," *IEEE Trans. Commun.*, vol. 67, no. 5, pp. 3234–3250, 2019, doi: 10.1109/TCOMM.2019.2893221.

[8] Q. Cheng, "Novel channel estimation methods under pilot contamination in Massive MIMO," 2016.

[9] D. Neumann, T. Wiese, and W. Utschick, "Learning the MMSE Channel Estimator," *IEEE Trans. Signal Process.*, vol. 66, no. 11, pp. 2905–2917, 2018, doi: 10.1109/TSP.2018.2799164.

[10] A. A. Kwabena, "Multiple input multiple output (MIMO) operation principles," *Helsinki Metrop. Univ. Appl. Sci.*, 2013.

[11] D. Chandramouli, R. Liebhart, and J. Pirskanen, *5G for the Connected World*. John Wiley & Sons, 2019.

[12] S. B. In and E. T. Al, *Massive MIMO in 5G Networks : Selected Applications*. .

[13] E. G. Larsson, D. Danev, M. Olofsson, and S. Sorman, "Teaching the Principles of

Massive MIMO: Exploring reciprocity-based multiuser MIMO beamforming using acoustic waves,” *IEEE Signal Process. Mag.*, vol. 34, no. 1, pp. 40–47, 2017.

[14] H. Q. Ngo, “Massive MIMO: Fundamentals and System Designs, vol. 1642. Linköping, Sweden: Linköping Univ.” Electronic Press, 2015.

[15] E. G. Larsson, O. Edfors, F. Tufvesson, and T. L. Marzetta, “Massive MIMO for next generation wireless systems,” *IEEE Commun. Mag.*, vol. 52, no. 2, pp. 186–195, 2014.

[16] J. Mundy and K. Thomas, “What is massive MIMO technology?,” *5g. co. uk*, vol. 1, 2019.

[17] C.-X. Wang, S. Wu, L. Bai, X. You, J. Wang, and I. Chih-Lin, “Recent advances and future challenges for massive MIMO channel measurements and models,” *Sci. China Inf. Sci.*, vol. 59, no. 2, pp. 1–16, 2016.

[18] R. Chataut and R. Akl, “Massive MIMO systems for 5G and beyond networks—overview, recent trends, challenges, and future research direction,” *Sensors*, vol. 20, no. 10, p. 2753, 2020.

[19] J. Flordelis, F. Rusek, F. Tufvesson, E. G. Larsson, and O. Edfors, “Massive MIMO performance—TDD versus FDD: What do measurements say?,” *IEEE Trans. Wirel. Commun.*, vol. 17, no. 4, pp. 2247–2261, 2018.

[20] X. Zhu, Z. Wang, L. Dai, and C. Qian, “Smart pilot assignment for massive MIMO,” *IEEE Commun. Lett.*, vol. 19, p. 1, Jul. 2015, doi: 10.1109/LCOMM.2015.2409176.

[21] D. Mi, M. Dianati, L. Zhang, S. Muhaidat, and R. Tafazolli, “Massive MIMO performance with imperfect channel reciprocity and channel estimation error,” *IEEE Trans. Commun.*, vol. 65, no. 9, pp. 3734–3749, 2017.

[22] P. al Orten, “High Throughput Packet Radio using Sequential Decoding and Tailbiting,” 2002.

[23] M. Alam, C. C. Patra, C. Patra, and M. A. Sobhan, “A novel technique for transmission of M-ary signal through wireless fading channel using Wavelet denoising,” *J. Comput. Networks Commun.*, vol. 2011, 2011.

[24] E. Björnson, L. Sanguinetti, J. Hoydis, and M. Debbah, “Optimal design of energy-

efficient multi-user MIMO systems: Is massive MIMO the answer?," *IEEE Trans. Wirel. Commun.*, vol. 14, no. 6, pp. 3059–3075, 2015.

[25] S. Coleri, M. Ergen, A. Puri, and A. Bahai, "Channel estimation techniques based on pilot arrangement in OFDM systems," *IEEE Trans. Broadcast.*, vol. 48, no. 3, pp. 223–229, 2002.

[26] A. Khlifi and R. Bouallegue, "Comparison between Performances of Channel estimation Techniques for CP-LTE and ZP-LTE Downlink Systems," *arXiv Prepr. arXiv1208.2060*, 2012.

[27] L. Panchal, M. Upadhyay, N. Shah, and A. Amin, "Significant Implementation of LS and MMSE Channel Estimation for OFDM Technique," *Int. J. Eng. Res. Appl.*, vol. 4, no. 3, pp. 38–41, 2014.

[28] A. A. Agarwal, "Pilot based channel estimation for 3GPP LTE downlink," 2012.

[29] I. A. Rumyancev and A. S. Korotkov, "Survey on beamforming techniques and integrated circuits for 5G systems," in *2019 IEEE International Conference on Electrical Engineering and Photonics (EExPolytech)*, 2019, pp. 76–80.

[30] M. Schimpl *et al.*, "Association between walking speed and age in healthy, free-living individuals using mobile accelerometry—a cross-sectional study," *PLoS One*, vol. 6, no. 8, p. e23299, 2011.

[31] S. Farahani, "RF propagation, antennas, and regulatory requirements," *Zigbee Wirel. Networks Transceivers*, vol. 1, pp. 171–206, 2008.

[32] S. Sun, T. A. Thomas, T. S. Rappaport, H. Nguyen, I. Z. Kovacs, and I. Rodriguez, "Path loss, shadow fading, and line-of-sight probability models for 5G urban macro-cellular scenarios," in *2015 IEEE Globecom Workshops (GC Wkshps)*, 2015, pp. 1–7.

[33] H. Siljak, K. Psara, and A. Philippou, "Distributed antenna selection for massive MIMO using reversing Petri nets," *IEEE Wirel. Commun. Lett.*, vol. 8, no. 5, pp. 1427–1430, 2019.

[34] H. Q. Ngo, *Massive MIMO: Fundamentals and System Designs*, no. 1642. 2015.

APPENDEIX

UP LINK

```
close all;
clear;
clc
%Number of BSs
L = 16;
%Number of UEs per BS
K = 10;
%Define the range of BS antennas
Mrange = 10:10:100;
%Extract maximum number of BS antennas
Mmax = max(Mrange);
%Define the range of pilot reuse factors
fRange = 1;
%Select the number of setups with random UE locations
nbrOfSetups = 1;
%Select the number of channel realizations per setup
nbrOfRealizations = 100;
%Communication bandwidth
B = 20e6;
%Total uplink transmit power per UE (W)
p = 0.1;
%Noise figure at the BS (in dB)
noiseFigure = 7;
%Compute noise power
noiseVariancedBm = -174 + 10*log10(B) + noiseFigure;
sigma2=db2pow(noiseVariancedBm-30); %W
%Select length of coherence block
tau_c = 200;
%Angular standard deviation per path in the local scattering model (in
degrees)
ASDdeg = 5;
%Power control parameter delta
deltadB=10;
%Pilot Reuse parameter
f=1;
%Pilot Length
tau_p=K;
%Prelog factor assuming only UL transmission

prelogFactor=(tau_c -tau_p)/tau_c;
%Prepare to save simulation results for Theoretical and Monte-Carlo
sumSE_MonteCarlo_MMSE = zeros(length(Mrange),nbrOfSetups);
sumSE_MonteCarlo_EWMMSE = zeros(length(Mrange),nbrOfSetups);
sumSE_MonteCarlo_LS = zeros(length(Mrange),nbrOfSetups);
sumSE_Theoretical_MMSE = zeros(length(Mrange),nbrOfSetups);
sumSE_Theoretical_EWMMSE = zeros(length(Mrange),nbrOfSetups);
sumSE_Theoretical_LS = zeros(length(Mrange),nbrOfSetups);
sumSE_MonteCarlo_MMSE_Rayleigh = zeros(length(Mrange),nbrOfSetups);
sumSE_MonteCarlo_EWMMSE_Rayleigh = zeros(length(Mrange),nbrOfSetups);
sumSE_MonteCarlo_LS_Rayleigh = zeros(length(Mrange),nbrOfSetups);
sumSE_Theoretical_MMSE_Rayleigh = zeros(length(Mrange),nbrOfSetups);
sumSE_Theoretical_EWMMSE_Rayleigh = zeros(length(Mrange),nbrOfSetups);
sumSE_Theoretical_LS_Rayleigh = zeros(length(Mrange),nbrOfSetups);
%Preallocate matrices for storing the covariance matrices and mean vectors
```

```
RNormalized=zeros(Mmax,Mmax,K,L,L);
HMeanNormalized=zeros(Mmax,K,L,L);
%% Go through all setups
for n = 1:nbrOfSetups
%R and HMean is normalized i.e., norm(HMeanNormalized(:,k,l,j))^2=Mmax
[RNormalized,HMeanNormalized,channelGaindB,ricianFactor,probLOS] =
functionExampleSetup(L,K,Mmax,ASDdeg,0);
%Controlled UL channel gain over noise
channelGainUL= functionPowerControl(
channelGaindB,noiseVariancedBm,deltadB,L);
for m=1:length(Mrange)
[R_UL,HMean_UL,H_UL,H_UL_Rayleigh] = functionChannelGeneration(
RNormalized(1:Mrange(m),1:Mrange(m),:,:,:)...
,HMeanNormalized(1:Mrange(m),:,:,:),channelGainUL,ricianFactor,probLOS,K,L,Mr
ange(m),nbrOfRealizations);
HMeanZero=zeros(Mrange(m),K,L,L);
%The UL SE with MMSE for Rician fading
%Generate the MMSE channel estimates
Hhat_MMSE_UL =
functionChannelEstimateMMSE(R_UL,HMean_UL,H_UL,nbrOfRealizations,Mrange(m),K,
L,p,f,tau_p);
%Compute UL SE using use and then forget bound in (19) with MMSE

SE_MonteCarlo_MMSE =
functionMonteCarloSE_UL(Hhat_MMSE_UL,H_UL,prelogFactor,nbrOfRealizations,Mran
ge(m),K,L,p);
%Compute UL SE using Theorem 1
SE_Theoretical_MMSE = functionTheoreticalSE_UL_MMSE(
R_UL,HMean_UL,Mrange(m),K,L,p,tau_p,prelogFactor);
%Save average sum SE per cell
sumSE_MonteCarlo_MMSE(m,n) = mean(sum(SE_MonteCarlo_MMSE,1));
sumSE_Theoretical_MMSE(m,n) = mean(sum(SE_Theoretical_MMSE,1))
%The UL SE with MMSE for Rayleigh fading
%Generate the MMSE channel estimates
Hhat_MMSE_UL_Rayleigh =
functionChannelEstimateMMSE(R_UL,HMeanZero,H_UL_Rayleigh,nbrOfRealizations,Mr
ange(m),K,L,p,f,tau_p);
%Compute UL SE using use and then forget bound in (19) with MMSE
SE_MonteCarlo_MMSE_Rayleigh =
functionMonteCarloSE_UL(Hhat_MMSE_UL_Rayleigh,H_UL_Rayleigh,prelogFactor,nbrO
fRealizations,Mrange(m),K,L,p);
%Compute UL SE using Theorem 1 while all the mean vectors are zero
SE_Theoretical_MMSE_Rayleigh = functionTheoreticalSE_UL_MMSE(
R_UL,HMeanZero,Mrange(m),K,L,p,tau_p,prelogFactor);
%Save average sum SE per cell
sumSE_MonteCarlo_MMSE_Rayleigh(m,n) = mean(sum(SE_MonteCarlo_MMSE_Rayleigh
,1));
sumSE_Theoretical_MMSE_Rayleigh(m,n) = mean(sum(SE_Theoretical_MMSE_Rayleigh
,1));
%The UL SE with EW-MMSE for Rician fading
%Generate the EWMMSE channel estimates
Hhat_EWMMSE =
functionChannelEstimateEWMMSE(R_UL,HMean_UL,H_UL,nbrOfRealizations,Mrange(m),
K,L,p,f,tau_p);
%Compute UL SE using use and then forget bound in (19) with EWMMSE
```

```
SE_MonteCarlo_EWMMSE=
functionMonteCarloSE_UL(Hhat_EWMMSE,H_UL,prelogFactor,nbrOfRealizations,Mrang
e(m),K,L,p);
%Compute UL SE using Theorem 2
SE_Theoretical_EWMMSE = functionTheoreticalSE_UL_EWMMSE(
R_UL,HMean_UL,Mrange(m),K,L,p,tau_p,prelogFactor);
%Save average sum SE per cell
sumSE_MonteCarlo_EWMMSE(m,n) = mean(sum(SE_MonteCarlo_EWMMSE,1));
sumSE_Theoretical_EWMMSE(m,n) = mean(sum(SE_Theoretical_EWMMSE,1));
%The UL SE with EWMMSE for Rayleigh fading
%Generate the EWMMSE channel estimates
Hhat_EWMMSE_Rayleigh =
functionChannelEstimateEWMMSE(R_UL,HMeanZero,H_UL_Rayleigh,nbrOfRealizations,
Mrange(m),K,L,p,f,tau_p);
%Compute UL SE using use and then forget bound in (19) with EWMMSE
SE_MonteCarlo_EWMMSE_Rayleigh =
functionMonteCarloSE_UL(Hhat_EWMMSE_Rayleigh,H_UL_Rayleigh,prelogFactor,nbrOf
Realizations,Mrange(m),K,L,p);
%Compute UL SE using Theorem 2 while all the mean vectors are zero

SE_Theoretical_EWMMSE_Rayleigh = functionTheoreticalSE_UL_EWMMSE(
R_UL,HMeanZero,Mrange(m),K,L,p,tau_p,prelogFactor);
%Save average sum SE per cell
sumSE_MonteCarlo_EWMMSE_Rayleigh(m,n) =
mean(sum(SE_MonteCarlo_EWMMSE_Rayleigh,1));
sumSE_Theoretical_EWMMSE_Rayleigh(m,n) =
mean(sum(SE_Theoretical_EWMMSE_Rayleigh,1))
%The UL SE with LS for Rician fading
%Generate the LS channel estimates
Hhat_LS =
functionChannelEstimateLS(H_UL,nbrOfRealizations,Mrange(m),K,L,p,f,tau_p);
%Compute UL SE using use and then forget bound in (19) with LS
SE_MonteCarlo_LS =
functionMonteCarloSE_UL(Hhat_LS,H_UL,prelogFactor,nbrOfRealizations,Mrange(m)
,K,L,p);
%Compute UL SE using Theorem 3
SE_Theoretical_LS = functionTheoreticalSE_UL_LS(
R_UL,HMean_UL,Mrange(m),K,L,p,tau_p,prelogFactor);
%Save average sum SE per cell
sumSE_MonteCarlo_LS(m,n) = mean(sum(SE_MonteCarlo_LS,1));%average of all
cells and users
sumSE_Theoretical_LS(m,n) = mean(sum(SE_Theoretical_LS,1));%average of all
cells and users
%The UL SE with LS for Rayleigh fading
%Generate the LS channel estimates
Hhat_LS_Rayleigh =
functionChannelEstimateLS(H_UL_Rayleigh,nbrOfRealizations,Mrange(m),K,L,p,f,t
au_p);
%Compute UL SE using use and then forget bound in (19) with LS
SE_MonteCarlo_LS_Rayleigh =
functionMonteCarloSE_UL(Hhat_LS_Rayleigh,H_UL_Rayleigh,prelogFactor,nbrOfReal
izations,Mrange(m),K,L,p);
%Compute UL SE using Theorem 3 while all mean vectors are zero
SE_Theoretical_LS_Rayleigh = functionTheoreticalSE_UL_LS(
R_UL,HMeanZero,Mrange(m),K,L,p,tau_p,prelogFactor);
%Save average sum SE per cell
sumSE_MonteCarlo_LS_Rayleigh(m,n) = mean(sum(SE_MonteCarlo_LS_Rayleigh,1));
```

```
sumSE_Theoretical_LS_Rayleigh(m,n) = mean(sum(SE_Theoretical_LS_Rayleigh,1
%Output simulation progress
disp([num2str(Mrange(m)) ' antennas of ' num2str(Mmax)]);
clear R_UL HMean_UL
end
%Output simulation progress
disp([num2str(n) ' setups out of ' num2str(nbrOfSetups)]);
clear RNormalized HMeanNormalized

end
```

Plot the figure

```
figure;
c1=plot(Mrange,mean(sumSE_MonteCarlo_MMSE,2),'ks','MarkerSize',7);
hold on
m1=plot(Mrange,mean(sumSE_Theoretical_MMSE,2),'r-+','LineWidth',1);
hold on
c2=plot(Mrange,mean(sumSE_MonteCarlo_EWMMSE,2),'ks','MarkerSize',7);
hold on
m2=plot(Mrange,mean(sumSE_Theoretical_EWMMSE,2),'b-x','LineWidth',1);
hold on
c3=plot(Mrange,mean(sumSE_MonteCarlo_LS,2),'ks','MarkerSize',7);
hold on
m3=plot(Mrange,mean(sumSE_Theoretical_LS,2),'k.-','LineWidth',1);
hold on
xlabel('Number of antennas (M)');
ylabel('Average sum SE [bit/s/Hz/cell]');
legend([m1 m2 m3 ],'MMSE with Rician fading',' EW-MMSE with Rician
fading','LS with Rician fading','Location','NorthWest');
```

DOWN LINK

```
close all;
clear;
clc
%Number of BSs
L = 16;
%Number of UEs per BS
K = 10;
%Define the range of BS antennas
Mrange = 10:10:100;
%Extract maximum number of BS antennas
Mmax = max(Mrange);
%Define the range of pilot reuse factors
fRange = 1;
%Select the number of setups with random UE locations
nbrOfSetups = 1;
%Select the number of channel realizations per setup
nbrOfRealizations = 10;
%Communication bandwidth
B = 20e6;
%Total uplink pilot power per UE (W)
p = 0.1;
%Downlink pilot power per UE (W)

rho=0.1;

%Noise figure at the BS (in dB)
```

```
noiseFigure = 7;
%Compute noise power
noiseVariancedBm = -174 + 10*log10(B) + noiseFigure;
%sigma2=db2pow(noiseVariancedBm-30); %W
%Select length of coherence block
tau_c = 200;
%Angular standard deviation per path in the local scattering model (in
degrees)
ASDdeg = 5;
%Power control parameter delta
deltadB=10;
%Pilot Reuse parameter
f=1;
%Pilot Length
tau_p=f*K;
%Compute the prelog factor assuming only downlink transmission
prelogFactor=(tau_c -tau_p)/tau_c;
%Prepare to save simulation results for Theoretical and Monte-Carlo
sumSE_MonteCarlo_MMSE = zeros(length(Mrange),nbrOfSetups);
sumSE_MonteCarlo_EWMMSE = zeros(length(Mrange),nbrOfSetups);
sumSE_MonteCarlo_LS = zeros(length(Mrange),nbrOfSetups);
sumSE_Theoretical_MMSE = zeros(length(Mrange),nbrOfSetups);
sumSE_Theoretical_EWMMSE = zeros(length(Mrange),nbrOfSetups);
sumSE_Theoretical_LS = zeros(length(Mrange),nbrOfSetups);
sumSE_MonteCarlo_MMSE_Rayleigh = zeros(length(Mrange),nbrOfSetups);
sumSE_MonteCarlo_EWMMSE_Rayleigh = zeros(length(Mrange),nbrOfSetups);
sumSE_MonteCarlo_LS_Rayleigh = zeros(length(Mrange),nbrOfSetups);
sumSE_Theoretical_MMSE_Rayleigh = zeros(length(Mrange),nbrOfSetups);
sumSE_Theoretical_EWMMSE_Rayleigh = zeros(length(Mrange),nbrOfSetups);
sumSE_Theoretical_LS_Rayleigh = zeros(length(Mrange),nbrOfSetups);
%Preallocate matrices for storing the covariance matrices and mean vectors
RNormalized=zeros(Mmax,Mmax,K,L,L);
HMeanNormalized=zeros(Mmax,K,L,L);
%% Go through all setups
for n = 1:nbrOfSetups
%R and HMean is normalized i.e., norm(HMeanNormalized(:,k,l,j))^2=Mmax
[RNormalized,HMeanNormalized,channelGaindB,ricianFactor,probLOS] =
functionExampleSetup(L,K,Mmax,ASDdeg,0);
%Controlled DL channel gain over noise
channelGainDL= functionPowerControl(
channelGaindB,noiseVariancedBm,deltadB,L);

%If all UEs have same power
% channelGainOverNoise=channelGaindB-noiseVariancedBm;
for m=1:length(Mrange)
%Generate the channel realizations and scale the normalized R and HMean
[R_DL,HMean_DL,H_DL,H_DL_Rayleigh] = functionChannelGeneration(
RNormalized(1:Mrange(m),1:Mrange(m),:,:,:)...
,HMeanNormalized(1:Mrange(m),:,:,:),channelGainDL,ricianFactor,probLOS,K,L,Mr
ange(m),nbrOfRealizations);
%Creating zero mean vectors for Rayleigh fading i.e., blocking all the LoS
paths
HMeanZero=zeros(Mrange(m),K,L,L);
%The DL SE with MMSE for Rician fading
%Generate the MMSE channel estimates
```

```
Hhat_MMSE_DL =
functionChannelEstimateMMSE(R_DL,HMean_DL,H_DL,nbrOfRealizations,Mrange(m),K,
L,p,f,tau_p);
%Compute DL SE using use and then forget bound in (40) with MMSE
SE_MonteCarlo_MMSE =
functionMonteCarloSE_DL(Hhat_MMSE_DL,H_DL,prelogFactor,nbrOfRealizations,K,L,
rho);
%Compute DL SE using Theorem 4
SE_Theoretical_MMSE = functionTheoreticalSE_DL_MMSE(
R_DL,HMean_DL,Mrange(m),K,L,p,tau_p,prelogFactor,rho);
%Save average sum SE per cell
sumSE_MonteCarlo_MMSE(m,n) = mean(sum(SE_MonteCarlo_MMSE,1));
sumSE_Theoretical_MMSE(m,n) = mean(sum(SE_Theoretical_MMSE,1));
%The DL SE with MMSE for Rayleigh fading
%Generate the MMSE channel estimates
Hhat_MMSE_DL_Rayleigh =
functionChannelEstimateMMSE(R_DL,HMeanZero,H_DL_Rayleigh,nbrOfRealizations,Mr
ange(m),K,L,p,f,tau_p);
%Compute DL SE using use and then forget bound in (40) with MMSE
SE_MonteCarlo_MMSE_Rayleigh =
functionMonteCarloSE_DL(Hhat_MMSE_DL_Rayleigh,H_DL_Rayleigh,prelogFactor,nbrO
fRealizations,K,L,rho);
%Compute DL SE using Theorem 4
SE_Theoretical_MMSE_Rayleigh = functionTheoreticalSE_DL_MMSE(
R_DL,HMeanZero,Mrange(m),K,L,p,tau_p,prelogFactor,rho);
%Save average sum SE per cell
sumSE_MonteCarlo_MMSE_Rayleigh(m,n) =
mean(sum(SE_MonteCarlo_MMSE_Rayleigh,1));
sumSE_Theoretical_MMSE_Rayleigh(m,n) =
mean(sum(SE_Theoretical_MMSE_Rayleigh,1);
%The DL SE with EW-MMSE for Rician fading

%Generate the EWMMSE channel estimates
Hhat_EWMMSE =
functionChannelEstimateEWMMSE(R_DL,HMean_DL,H_DL,nbrOfRealizations,Mrange(m),
K,L,p,f,tau_p);
%Compute DL SE using use and then forget bound in (40) with EW-MMSE
SE_MonteCarlo_EWMMSE =
functionMonteCarloSE_DL(Hhat_EWMMSE,H_DL,prelogFactor,nbrOfRealizations,K,L,r
ho);
%Compute DL SE using Theorem 5
SE_Theoretical_EWMMSE = functionTheoreticalSE_DL_EWMMSE(
R_DL,HMean_DL,Mrange(m),K,L,p,tau_p,prelogFactor,rho);
%Save average sum SE per cell
sumSE_MonteCarlo_EWMMSE(m,n) = mean(sum(SE_MonteCarlo_EWMMSE,1));
sumSE_Theoretical_EWMMSE(m,n) = mean(sum(SE_Theoretical_EWMMSE,1));
%The DL SE with EW-MMSE for Rayleigh fading
%Generate the EWMMSE channel estimates
Hhat_EWMMSE_Rayleigh =
functionChannelEstimateEWMMSE(R_DL,HMeanZero,H_DL_Rayleigh,nbrOfRealizations,
Mrange(m),K,L,p,f,tau_p);
%Compute DL SE using use and then forget bound in (40) with EW-MMSE
SE_MonteCarlo_EWMMSE_Rayleigh =
functionMonteCarloSE_DL(Hhat_EWMMSE_Rayleigh,H_DL_Rayleigh,prelogFactor,nbrOf
Realizations,K,L,rho);
%Compute DL SE using Theorem 5
```

```
SE_Theoretical_EWMMSE_Rayleigh = functionTheoreticalSE_DL_EWMMSE(
R_DL,HMeanZero,Mrange(m),K,L,p,tau_p,prelogFactor,rho);
%Save average sum SE per cell
sumSE_MonteCarlo_EWMMSE_Rayleigh(m,n) =
mean(sum(SE_MonteCarlo_EWMMSE_Rayleigh,1));
sumSE_Theoretical_EWMMSE_Rayleigh(m,n) =
mean(sum(SE_Theoretical_EWMMSE_Rayleigh,1));
%The DL SE with LS for Rician fading
%Generate the LS channel estimates
Hhat_LS =
functionChannelEstimateLS(H_DL,nbrOfRealizations,Mrange(m),K,L,p,f,tau_p);
%Compute DL SE using use and then forget bound in (40) with LS
SE_MonteCarlo_LS =
functionMonteCarloSE_DL(Hhat_LS,H_DL,prelogFactor,nbrOfRealizations,K,L,rho);
%Compute DL SE using Theorem 6
SE_Theoretical_LS = functionTheoreticalSE_DL_LS(
R_DL,HMean_DL,Mrange(m),K,L,p,tau_p,prelogFactor,rho);
%Save average sum SE per cell
sumSE_MonteCarlo_LS(m,n) = mean(sum(SE_MonteCarlo_LS,1));
sumSE_Theoretical_LS(m,n) = mean(sum(SE_Theoretical_LS,1));
%The DL SE with LS for Rayleigh fading
%Generate the LS channel estimates

Hhat_LS_Rayleigh =
functionChannelEstimateLS(H_DL_Rayleigh,nbrOfRealizations,Mrange(m),K,L,p,f,t
au_p);
%Compute DL SE using use and then forget bound in (40) with LS
SE_MonteCarlo_LS_Rayleigh =
functionMonteCarloSE_DL(Hhat_LS_Rayleigh,H_DL_Rayleigh,prelogFactor,nbrOfReal
izations,K,L,rho);
%Compute DL SE using Theorem 6
SE_Theoretical_LS_Rayleigh = functionTheoreticalSE_DL_LS(
R_DL,HMeanZero,Mrange(m),K,L,p,tau_p,prelogFactor,rho);
%Save average sum SE per cell
sumSE_MonteCarlo_LS_Rayleigh(m,n) = mean(sum(SE_MonteCarlo_LS_Rayleigh,1));
sumSE_Theoretical_LS_Rayleigh(m,n) = mean(sum(SE_Theoretical_LS_Rayleigh,1))
%Output simulation progress
disp([num2str(Mrange(m)) ' antennas of ' num2str(Mmax)]);
end
%Output simulation progress
disp([num2str(n) ' setups out of ' num2str(nbrOfSetups)]);
clear RNormalized HMeanNormalized
end
%% Plot the figure
figure;
c3=plot(Mrange,mean(sumSE_MonteCarlo_LS,2),'ks','MarkerSize',7);
hold on
m3=plot(Mrange,mean(sumSE_Theoretical_LS,2),'k.-','LineWidth',1);
hold on
c1r=plot(Mrange,mean(sumSE_MonteCarlo_MMSE_Rayleigh,2),'ks','MarkerSize',7);
hold on
m1r=plot(Mrange,mean(sumSE_Theoretical_MMSE_Rayleigh,2),'r+:','LineWidth',1);
hold on
c2r=plot(Mrange,mean(sumSE_MonteCarlo_EWMMSE_Rayleigh,2),'ks','MarkerSize',7)
;
hold on
```

```
m2r=plot(Mrange,mean(sumSE_Theoretical_EWMMSE_Rayleigh,2),'bx:','LineWidth',1
);
hold on
c3r=plot(Mrange,mean(sumSE_MonteCarlo_LS_Rayleigh,2),'ks','MarkerSize',7);
hold on
m3r=plot(Mrange,mean(sumSE_Theoretical_LS_Rayleigh,2),'k.:','LineWidth',1);
xlabel('Number of antennas (M)');
ylabel('Average sum SE [bit/s/Hz/cell]');
legend([ m3 m1r m3r ],'MMSE With Rayleigh','EW-MMSE with Rayleigh fading',
'LS with Rayleigh','Location','Northwest');
```

NMSE Vs SNR

```
close all;
clear;
%Number of BS antennas
M = 100;
%Angular standard deviation in the local scattering model (in degrees)
ASDdeg = 73;
%Range of nominal angles of the desired UE
varphiDesiredDegrees = linspace(-180,180,73);
varphiDesiredRadians = varphiDesiredDegrees*(pi/180);
%Range of nominal angles of the interfering UE
varphiInterfererDegrees = linspace(-180,180,73);
varphiInterfererRadians = varphiInterfererDegrees*(pi/180);
%Define the antenna spacing (in number of wavelengths)
antennaSpacing = 1/2; %Half wavelength distance
%Define the range of the effective SNR in (3.13) for the desired UE
SNR1dB = -10:1:20;
SNR1 = 10.^(SNR1dB/10);
%Define the range of the effective SNR in (3.13) for the interfering UE
SNR2dB = SNR1dB-10;
SNR2 = 10.^(SNR2dB/10);
%Preallocate matrices for storing the simulation results
NMSE_MMSE =
zeros(length(SNR1dB),length(varphiInterfererRadians),length(varphiDesiredRadi
ans),length(M));
NMSE_EWMMSE =
zeros(length(SNR1dB),length(varphiInterfererRadians),length(varphiDesiredRadi
ans),length(M));
NMSE_LS =
zeros(length(SNR1dB),length(varphiInterfererRadians),length(varphiDesiredRadi
ans),length(M));
%% Go through all angles of desired UE
for n1 = 1:length(varphiDesiredRadians)
%Output simulation progress
disp([num2str(n1) ' angles out of ' num2str(length(varphiDesiredRadians))]);
%Compute the spatial correlation matrix of the desired UE
R1 =
functionRlocalscattering(max(M),varphiDesiredRadians(n1),ASDdeg,antennaSpacin
g);
%Go through all angles of interfering UE
for n2 = 1:length(varphiInterfererRadians)
%Compute the spatial correlation matrix of the interfering UE
R2 =
functionRlocalscattering(M,varphiInterfererRadians(n2),ASDdeg,antennaSpacing)
;
%Go through all number of antennas
```

```
for s = 1:length(SNR1dB)
%Compute the NMSE in (3.20) with the MMSE estimator
NMSE_MMSE(s,n1,n2) = real(trace(R1 -
SNR1(s)*R1*((SNR1(s)*R1+SNR2(s)*R2+eye(M))\R1)))/trace(R1);
%Compute the matrix in (3.33) that the received pilot signal is
%multiplied with in the EW-MMSE estimator
A_EWMMSE = (sqrt(SNR1(s))/(SNR1(s)+SNR2(s)+1))*eye(M);
%Compute the NMSE in (3.20) with the EW-MMSE estimator
NMSE_EWMMSE(s,n1,n2) = (trace(R1) +
trace(A_EWMMSE*(SNR1(s)*R1+SNR2(s)*R2+eye(M))*A_EWMMSE') -
2*real(trace(A_EWMMSE'*R1))*sqrt(SNR1(s)))/trace(R1);
%Compute the matrix in (3.36) that the received pilot signal is
%multiplied with in the LS estimator
A_LS = eye(M)/sqrt(SNR1(s));
%Compute the NMSE in (3.20) with the LS estimator
NMSE_LS(s,n1,n2) = (trace(R1) +
trace(A_LS*(SNR1(s)*R1+SNR2(s)*R2+eye(M))*A_LS') -
2*real(trace(A_LS'*R1))*sqrt(SNR1(s)))/trace(R1);
end
end
end
%% Plot the simulation results
figure;
hold on; box on;
plot(SNR1dB,mean(mean(NMSE_LS,2),3),'b-.','LineWidth',1);
plot(SNR1dB,mean(mean(NMSE_EWMMSE,2),3),'k-','LineWidth',1);
plot(SNR1dB,mean(mean(NMSE_MMSE,2),3),'r--','LineWidth',1);
xlabel('Effective SNR [dB]');
ylabel('NMSE');
set(gca,'YScale','log');
ylim([1e-2 1e1]);
legend('LS','EW-MMSE','MMSE','Location','SouthWest');
```

complexity

```
close all;
clear;
K = 100;
Mrange = 10:10:100;
tau_p = K;
complexity_MMSE = Mrange*tau_p + Mrange.^2;
complexity_EW_MMSE = Mrange*(tau_p + 1);
complexity_LS = Mrange*tau_p;
figure;
hold on; box on;
plot(Mrange,complexity_MMSE,'p','LineWidth',2);
plot(Mrange,complexity_EW_MMSE,'k','LineWidth',2);
plot(Mrange,complexity_LS,'r-.','LineWidth',3);
xlabel('Number of users (k)');
ylabel('Number of complex multiplications');
set(gca,'YScale','log');
legend('MMSE','EW-MMSE','LS','Location','NorthWest');
```